BIOSYNTHESIS AND MATURATION OF 'NEW WORLD' HANTAVIRUS GLYCOPROTEINS

By
Lisa Marie Fernando

A Thesis
Submitted to the Faculty of Graduate Studies
in Partial Fulfillment of the Requirements
for the Degree of

Master of Science

Department of Medical Microbiology and Infectious Diseases
Faculty of Medicine
University of Manitoba
Winnipeg, Manitoba
Canada

THE UNIVERSITY OF MANITOBA

FACULTY OF GRADUATE STUDIES

*****

COPYRIGHT PERMISSION PAGE

Biosynthesis and Maturation of 'New World' Hantavirus Glycoproteins

BY

Lisa Marie Fernando

A Thesis/Practicum submitted to the Faculty of Graduate Studies of The University of Manitoba in partial fulfillment of the requirements of the degree of

MASTER OF SCIENCE

TABLE OF CONTENTS

ACKNOWLEDGEMENTS

This study would not have been possible without the assistance of a great many people.

My sincere gratitude is extended to the members of my committee for their support over the past two years and their constructive criticism of this thesis. They include Drs. Michael Drebot, Mary Lynn Duckworth and Keith Fowke.

I would like to thank Dr. Ramon Flick for his untiring assistance with cloning strategies and his perspective as a bunyavirus scientist. I am very appreciative of his encouragement and sense of humour during my studies.

In addition, I would like to thank Michael Garbutt and Daryl Dick (Special Pathogens Program, Health Canada) for their invalulable technical assistance and John Rutherford (Department of Medical Microbiology, University of Manitoba) for training on the confocal microscope.

I would like to acknowledge the DNA core facility at the Canadian Science Center for Human and Animal Health for aid with primer synthesis and DNA sequencing.

Furthermore, I would like to recognize and thank the University of Manitoba, Department of Medical Microbiology for their financial assistance.

Lastly, but most importantly, I would like to express my gratitude to my supervisor Dr. Heinz Feldmann. His patience, encouragement and guidance have been greatly appreciated during my time in his lab. Heinz has shown me the true meaning of research and working with him has been an invaluable experience.

LIST OF FIGURES

LIST OF TABLES

LIST OF APPENDICES

LIST OF ABBREVIATIONS

aa	amino acids
Amp	ampicillin
BCCV	Black Creek Canal virus
BHK	baby hamster kidney
cDNA	complementary deoxyribonucleic acid
CMV	Cytomegalovirus
CPE	cytopathic effect
DMEM	Dulbecco's modified Eagle's medium
DMSO	dimethyl sulfoxide
dNTP	deoxynucleoside triphosphate
DTT	dithiothreitol
DNA	deoxyribonucleic acid
ECL	enhanced chemiluminescence
EDTA	ethylenediamine-tetraacetic acid
ELISA	enzyme-linked immunosorbent assay
ER	endoplasmic reticulum
FBS	fetal bovine serum
FITC	fluorescein isothiocyanate
GFP	green fluorescent protein
GMEM	Glasgow Minimum Essential medium
GPC	glycoprotein precursor
HA	hemagglutinin (influenza A virus)
His	histidine
HCl	hydrochloric acid
HFRS	Hemorrhagic fever with renal syndrome
HPS	Hantavirus pulmonary syndrome
HTNV	Hantaan virus
HRP	horse radish peroxidase
IFA	immunofluorescence assay
Ig	immunoglobulin
INFV	influenza virus
LB medium	Luria-Bertani medium
M.O.I.	multiplicity of infection
mRNA	messenger ribonucleic acid
NaCl	sodium chloride
NW	New World
OD	optical density
OW	Old World
PBS	phosphate buffered saline
PCR	polymerase chain reaction
pSFV	Semliki Forest virus expression plasmid
PVDF	polyvinylidene difluoride

RNA	ribonucleic acid
RNase	ribonuclease
rNTP	ribonucleoside triphosphate
RT-PCR	reverse-transcription polymerase chain reaction
SDS	sodium dodecyl sulfate
SDS-PAGE	sodium dodecyl sulphate polyacrylamide gel electrophoresis
SFV	Semliki Forest virus
SNV	Sin Nombre virus
SP	signal peptide
TD	transmembrane domain
UV	ultraviolet
v/v	volume per volume
w/v	weight per volume

ABSTRACT

Members of the *Bunyaviridae* family are known to mature and bud at the Golgi complex which is pre-determined by the location of the viral glycoproteins. While this dogma has been well accepted for Old World (OW) hantaviruses, it has been challenged with respect to New World (NW) hantaviruses (Ravkov *et al.*, 1997). The present study addresses the localization of the glycoproteins of Black Creek Canal virus (BCCV), a NW hantavirus, by using recombinant expression systems.

Individual expression of BCCV G1 resulted in Golgi localization whereas individual expression of BCCV G2 localized in the ER. Furthermore, both G1 and G2 glycoproteins were not detected on the plasma membrane. To further understand the mechanism of Golgi targeting by BCCV G1, GFP-hantaviral glycoprotein fusion proteins were constructed. When the cytoplasmic tail of BCCV G1 was fused to GFP and expressed, a Golgi pattern was observed, suggesting that the cytoplasmic tail of BCCV harboured a Golgi targeting signal. Removal of the hydrophobic carboxyl-terminal amino acids [which makes up the BCCV G2 signal peptide (SP)] resulted in a substantial reduction in Golgi targeting, suggesting that the G2 SP is the primary Golgi targeting signal which may work in conjunction with a weaker secondary signal located in the remainder of the BCCV G1 cytoplasmic tail. To investigate the nature of the signal, the G2 SP was replaced with an influenza virus (INFV) SP. Following expression, this fusion protein was located in the Golgi, signifying that the Golgi targeting signal of BCCV was not sequence specific; rather, the hydrophobicity of BCCV was essential.

In conclusion, the results from this study indicate that NW hantaviruses have a similar glycoprotein processing pathway as OW hantaviruses. Thus, it appears that as with all other bunyaviruses, the maturation of NW hantaviruses occurs mainly at the Golgi membranes.

1 INTRODUCTION

1.1 History and Geographic Distribution

Hantaviruses are known to cause worldwide human illness. The first documented cases occurred during the Korean War (1950-1953) where approximately 3000 UN soldiers were affected and the mortality rate was 7-10% (Hart & Bennett, 1994; McCaughey & Hart, 2000; Johnson, 2001). At the same time, a similar disease was occurring in Scandinavia and USSR called *nephropathia epidemica* (Hart & Bennett, 1994; Johnson, 2001). The first hantavirus was isolated from the striped field mouse *Apodemus agrarius* in 1978 (Lee *et al.*, 1978; McCaughey & Hart, 2000). Hantaan virus (HTNV) was deemed the sole agent (and prototype) responsible for the disease during the Korean War, now called Hemorrhagic Fever with Renal Syndrome (HFRS) (Mertz *et al.*, 1997; Lee *et al.*, 1978). Since the discovery of HTNV, several other HFRS causing agents have been discovered such as Seoul virus, Dobrava virus and Puumula virus; collectively, these viruses are termed Old World (OW) hantaviruses which cause HFRS. Today, OW hantaviruses cause between 150 000 to 200 000 hospitalized cases of HFRS annually and the mortality rate hovers between 1-15% (Simmons & Riley, 2002). The majority of cases reported are from China, although a significant but unknown number are diagnosed in Korea, Russia, the Balkans, Western Europe and Scandinavia (Simmons and Riley, 2002) (Table 1).

Table 1: Officially recognized members of the genus *Hantavirus*, family *Bunyaviridae*

Species	Disease	Reservoir	Distribution
Old World Hantaviruses			
Hantaan virus (HTNV)	**HFRS**	***Apodemus agrarius***	**China, Russia, Korea**
Saaremaa virus (SAAV)	**HFRS**	***Apodemus agrarius***	**Estonia, Balkans**
Dobrava virus (DOBV)	**HFRS**	***Apodemus flavicolis***	**Balkans**
Seoul virus (SEOV)	**HFRS**	***Rattus norvegicus, Rattus rattus***	**Worldwide**
Puumula virus (PUUV)	**HFRS**	***Clethrionomys glareolus***	**Europe, Scandinavia, Russia**
New World Hantaviruses			
Sin Nombre virus (SNV)	**HPS**	***Peromyscus maniculatis***	**U.S., Canada, Mexico**
New York virus (NYV)	**HPS**	***Peromyscus leucopus***	**U.S.**
Andes Virus (ANDV)	**HPS**	***Oligoryzomys longicaudatus***	**South America**
Bayou virus (BAYV)	**HPS**	***Oryzomys palustris***	**U.S.**
Black Creek Canal (BCCV)	**HPS**	***Sigmodon hispidus***	**U.S.**
Laguna Negra virus (LANV)	**HPS**	***Calomys laucha***	**Paraguay, Bolivia**

(modified and with permission from Simmons & Riley, 2002; Nemirov *et al.*, 1999; Sjolander *et al.*, 2002)

HFRS, hemorrhagic fever with renal syndrome; HPS, hantavirus pulmonary syndrome

Despite the "eastern" localization of HFRS, human hantavirus disease has found its way to the New World in the form of another distinct clinical disease: hantavirus pulmonary syndrome (HPS) (Nichol *et al.*, 1993; Simmons and Riley, 2002). The virus which causes HPS was first recognized in May of 1993 in the Four Corners area of New Mexico, Utah, Arizona and Colorado, after a cluster of deaths occurred (Nichol *et al.*, 1993; Duchin *et al.*, 1994; McCaughey & Hart, 2000; Johnson, 2001). Hantavirus infection was suspected and was confirmed when the etiologic agent of this new disease was isolated from the rodent reservoir *Peromyscus maniculatis* (Johnson, 2001). Sin Nombre virus (SNV) was deemed responsible for HPS and was recognized as the prototype of New World (NW) hantaviruses (Nichol *et al.*, 1993; Johnson, 2001). Since the discovery of SNV in 1993, approximately 400 cases of HPS have been reported in North America (http://www.cdc.gov/ncidod/diseases/hanta/hps/noframes/caseinfo.htm) and the mortality rate has been approximately 40% (Simmons and Riley, 2002). Following the identification of SNV, many other NW hantaviruses have been discovered throughout North and South America such as Black Creek Canal virus (BCCV), Bayou virus and Andes virus (Meyer & Schmaljohn, 2000) (Table 1).

With respect to Canada, according to Drebot *et al.*, (2000), the ubiquitous deer mouse, *Peromyscus maniculatis* is the primary reservoir for SNV. The first case of HPS in Canada was recognized in 1994 originating from British Columbia and to date there have been 41 cases of HPS plus one case which was imported from Argentina (Drebot, personal communication).

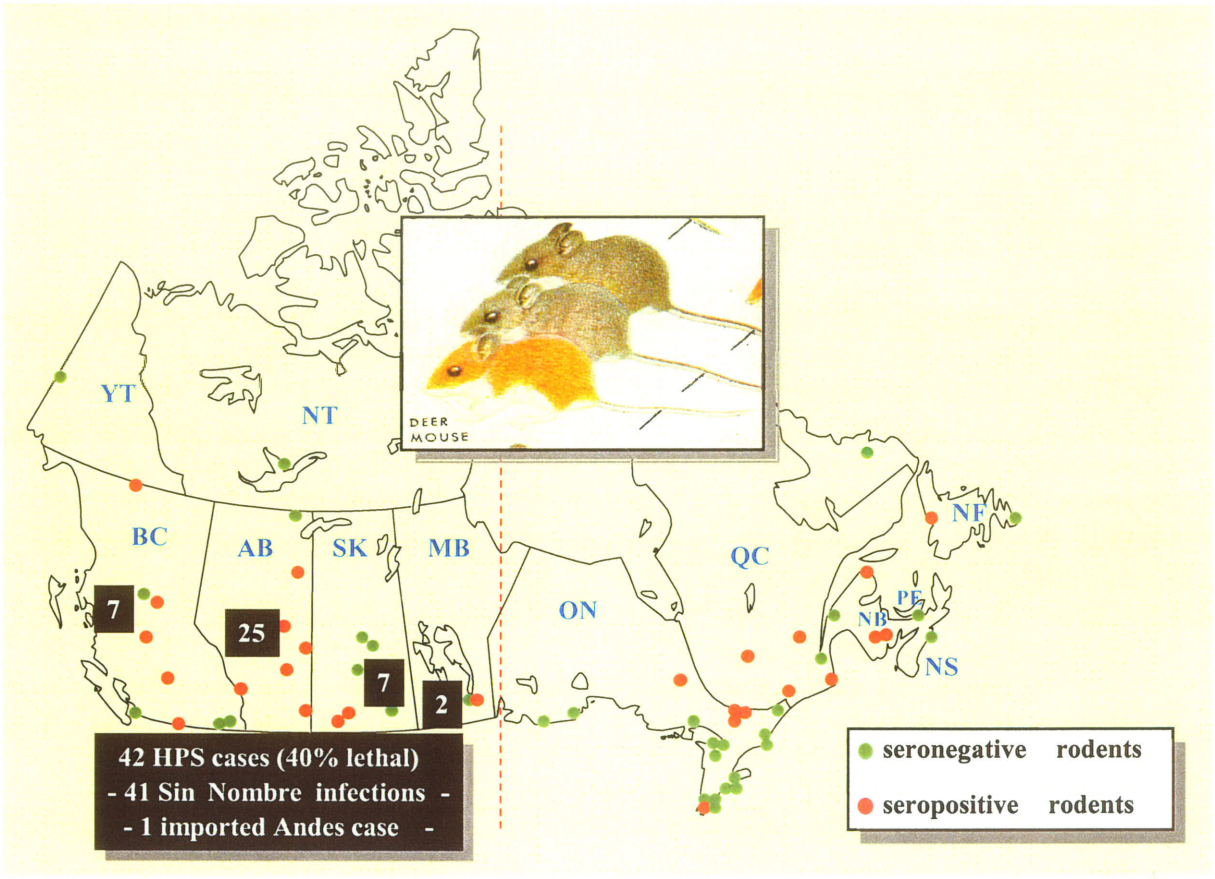

Figure 1: Prevalence of SNV and HPS cases in Canada. All HPS cases to date (41) have been caused by Sin Nombre with 1 imported case from Argentina (Andes virus). Cases have only occurred in western Canada despite the presence of seropositive rodents (*Peromyscus maniculatis*) throughout Canada (with permission from Drebot *et al.*, manuscript in preparation).

All of the HPS cases reported have originated from the western provinces and the majority were male patients who had acquired the virus through domestic and farming activities. Since 1994, the number of HPS cases has fluctuated which may be a reflection of the increased numbers of infected rodents due to the mild winters and increased breeding capacity. Although HPS cases have only been documented in the western provinces, seropositive rodents have been found in all provinces except for Prince Edward Island and Nova Scotia (Drebot *et al.,* 2000; Drebot *et al.*, 2001) (Figure 1).

1.2 Transmission of Hantaviruses

Unlike the other bunyaviruses, hantaviruses are carried by rodents and are spread to humans by aerosolized contaminated rodent excreta (Schmaljohn & Hooper, 2001; Simmons & Riley, 2002) (Figure 2). Rodents become infected through close contact with an infected animal and by aggressive behavior such as fighting and biting (Figure 2). Infected rodents can shed virus in their saliva, feces and urine for as long as one year or more after infection (Beaty & Calisher, 1991; Simmons & Riley, 2002). Although considerable amounts of viral antigen can be detected in organs, the rodents remain asymptomatic (Beaty & Calisher, 1991). Humans are usually dead end hosts when they inhale aerosolized virus from rodent excreta (Figure 2), however cases of human-to-human transmission were documented in Argentina with the Andes virus (Lopez *et al.*, 1996; Lopez *et al.*, 1997).

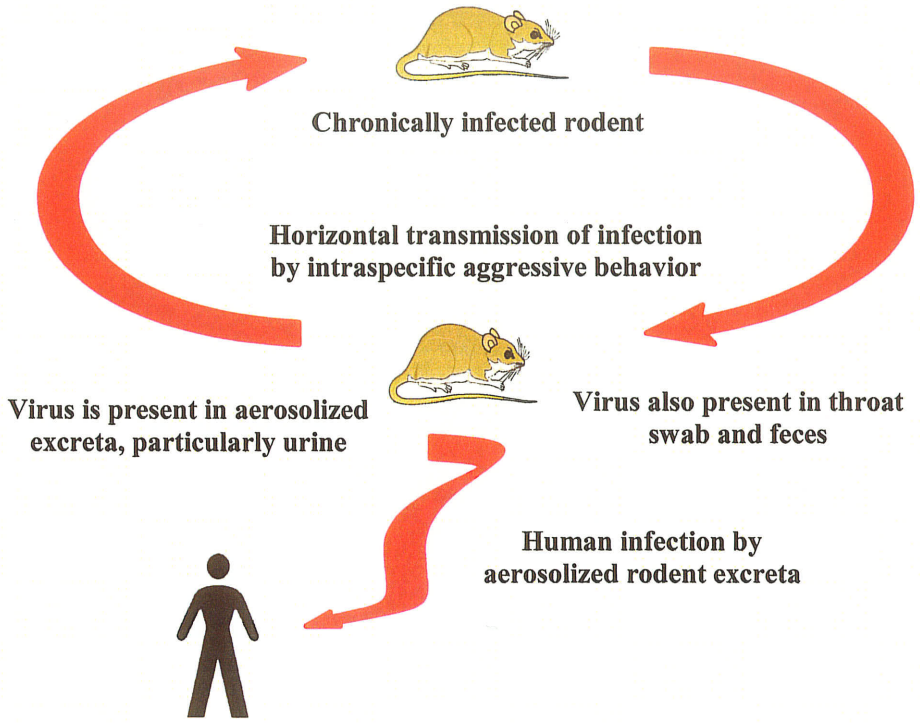

Figure 2: Transmission of hantaviruses. Chronically infected rodents shed virus in urine, feces and saliva. Humans acquire the virus by inhaling aerosolized rodent excreta (http://www.cdc.gov/ncidod/diseases/hanta/hps).

There is a general consensus that the genetic relationship among hantaviruses resembles their primary rodent reservoirs (Drebot *et al.*, 2001; Plyusnin & Morzunov, 2001). Thus, the worldwide appearance of HFRS and HPS reflects the geographic distribution of the rodent reservoirs (Pilaski *et al.*, 1994; Feldmann, 2000).

1.3 Diseases associated with Hantaviruses

In addition to the different locations of disease occurance, OW and NW hantaviruses cause very different and distinct diseases. After an incubation period of 4-42 days, HFRS is characterized by a sudden onset of "flu-like" symptoms followed by renal complications and hemorrhagic manifestations (Mertz *et al.*, 1997) (Table 2). The first signs of hemorrhaging may occur as a flushing of the face, injection of conjunctiva and mucous membranes which can rapidly develop into visceral hemorrhage. One-third of deaths occur in this stage due to vascular leakage and acute shock (Feldmann, 2000).

In comparison, HPS is characterized by "flu-like" symptoms following an incubation period of 10-21 days, leading to pulmonary leakage and cardiovascular collapse (Young *et al.*, 1998). Normally death occurs from cardiogenic shock rather than from respiratory failure even with adequate tissue oxygenation. Although renal failure is uncommon in HPS, certain HPS causing viruses produce renal complications (Feldmann, 2000; Simmons and Riley, 2002) (Table 2).

Table 2: Clinical features of HFRS and HPS. *Distinguishing features are reported in terms of minimum/maximum occurrences of the characteristic signs.
- rarely reported; + infrequently or mild; ++/+++/++++ more frequent to severe manifestation.
(modified and with permission from Schmaljohn and Hjelle, 1997)

Distinguishing Features*	**HFRS (mod to severe) HTN, SEO, DOB**	**HFRS (mild) PUU**	**HPS (prototype) SN, NY**	**HPS (renal variant) BAY, BCC, AND**
Hemorrhage	+++	+	+	+
Renal Damage	+++/++++	+/++++	+	++/+++
Pulmonary Leakage	+/++	-/+	++++	+++/++++
Mortality (%)	1-15	<1	40	40

1.4 Pathogenesis

In both animals and humans, hantavirus replication occurs predominantly in endothelial cells and macrophages (Mackow & Gavrilovskaya, 2001). According to Peters and Khan (2002), human disease begins with the inhalation of virus particles which settle in the terminal respiratory bronchiole or alveolus. Cellular entry of susceptible cells is via β3-integrins (receptor for human pathogenic hantaviruses) which are critical adhesive receptors on endothelial cells and platelets that regulate vascular permeability and platelet activation and adhesion. Consequently, hantavirus-associated diseases (HFRS, HPS) primarily affect blood vessels and involve variable degrees of generalized capillary dilation and edema. A hallmark in hantavirus pathogenesis is an increased vascular permeability that appears to be due to endothelial dysfunction (Feldmann, 2000).

In terms of HFRS, the onset of disease is associated with the activation of complement and by triggering mediator release from platelets and immune effector cells. Consequently, immune complexes may be involved in vascular injury. The most dramatic microscopic lesions in HFRS involve the kidneys. Severe HFRS is characterized by abundant protein-rich gelatinous retroperitoneal edema fluid and hemorrhagic necrosis. In addition, vascular disturbances give rise to hypotension and shock and also appear to account for renal failure (Feldmann, 2000).

With respect to HPS, it is believed that alveolar macrophages or other susceptible cells are infected creating a viremia that results in infected pulmonary capillary endothelium and infection to lesser degrees, of other organs in the body. The host's

immune response to infection includes the secretion of soluble mediators such as TNF-α , nitric oxide and IFN-α, which have effects on capillary endothelial permeability; this results in pulmonary edema in the case of HPS (Peters & Khan, 2002).

Although HFRS and HPS differ with respect to pulmonary and renal/hemorrhagic manifestations, they both result in increased vascular permeability and acute thrombocytopenia (Mackow & Gavrilovskaya, 2001). The means by which some hantaviruses cause hemorrhage or pulmonary edema may be related to virus-specific differences in terms of receptor interaction, alterations in intracellular signaling, the specific induction of cytokines or the differential regulation of additional platelet or endothelial cell receptors (Mackow & Gavrilovskaya, 2001).

1.5 Diagnosis and Case Management

The diagnosis of hantavirus infections is primarily based on clinical observations and the detection of a host specific humoral immune response. The test of choice is the IgM capture ELISA due to its high sensitivity and specificity. Elevated IgM titers are usually detected with the onset of clinical symptoms and persist for several weeks before they decline over the next 3-6 months (Feldmann, 2000). Additionally, a direct ELISA is used to detect IgG antibodies that appear concurrently or slightly later than IgM. IgG titers rapidly increase and can remain for many years.

Other detection assays include: 1) RT-PCR for detection of virus-specific RNA in urine and blood samples, 2) in situ hybridization and 3) immunohistochemistry, both used to detect viral antigen or viral RNA in human or rodent tissues (Feldmann, 2000).

Currently, there is no specific effective therapy for hantavirus infections and treatment is mainly supportive (fluid management and ventilatory support). Ribavirin has been shown to have an *in vitro* antiviral effect on hantaviruses. The efficacy of ribavirin (a common antiviral drug) in the treatment of HPS is unclear whereas success has been reported for HFRS patients (Enria *et al.*, 2001).

1.6 Biology of Hantaviruses

1.6.1 Morphology

Hantaviruses form their own genus within the family *Bunyaviridae* (van Regenmortel, 2000). An electron micrograph of hantaviruses shows pleomorphic enveloped virions, 80-120 nm in diameter (Figure 3B) (Schmaljohn & Hooper, 2001; Simmons & Riley, 2002). Surface glycoproteins, G1 and G2, are type I transmembrane proteins that project from the lipid bilayered envelope and surround three single-stranded negative sense genome segments denoted large, medium and small (Schmaljohn & Hooper, 2001; Simmons & Riley, 2002) (Figure 3A). The large (L) segment encodes the RNA-dependent RNA polymerase which is responsible for RNA replication and transcription. Several copies of the virus polymerase protein are believed to be packaged within each virion and are associated with the virus ribonucleocapsids through non-covalent interactions (Simmons & Riley, 2002). The medium (M) segment encodes a glycoprotein precursor (GPC) which is co-translationally cleaved to yield two envelope glycoproteins (G1 and G2).

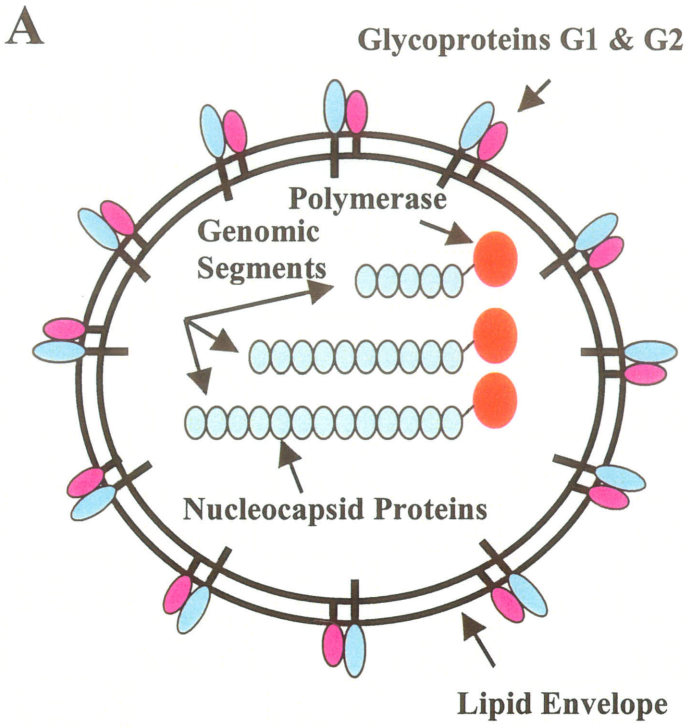

Figure 3: (A) Schematic diagram depicting the putative hantavirus virion structure. Note the glycoproteins G1 and G2 protruding from the lipid envelope, the nucleocapsid proteins associated with the small (S), medium (M) and large (L) genomic segments, and the virus polymerase associated with the genomic segments (modified and with permission from Simmons and Riley, 2002). (B) Electron micrograph of Sin Nombre hantavirus particles (http://www.cdc.gov/ncidod/diseases/hanta/hps).

The glycoprotein heterodimer of hantaviruses plays a key role in virus entry (attachment to the cellular receptor and fusion), a crucial role in maturation and budding of the virus and as a target for neutralizing antibodies in the host (Simmons & Riley, 2002).

The small (S) segment encodes the nucleocapsid protein which encapsidates the RNA genome segments (Schmaljohn & Hooper, 2001; Plyusnin, 2002; Simmons & Riley, 2002).

1.6.2 Replication

Hantaviruses replicate exclusively in the cytoplasm of infected cells (Schmaljohn & Hooper, 2001) (Figure 4). It has been determined that the glycoprotein heterodimer of human pathogenic hantaviruses binds to β3-integrin (β1-integrin is the receptor for non-pathogenic hantaviruses), which is a cellular receptor found on susceptible cells, such as endothelial cells, macrophages and platelets (Gavrilovskaya *et al.*, 1998). Following attachment, receptor mediated endocytosis and uncoating occurs. Primary transcription is started by the L protein which uses the encapsidated RNA as template to produce positive sense viral mRNA, which are then translated by cellular ribosomes. The L protein then switches from primary transcription to replication, producing full-length viral complementary RNA (viral cRNA) (Schmaljohn & Hooper, 2001). The positive sense intermediate is then used as template for synthesis of negative sense full-length viral genomic RNA (vRNA).

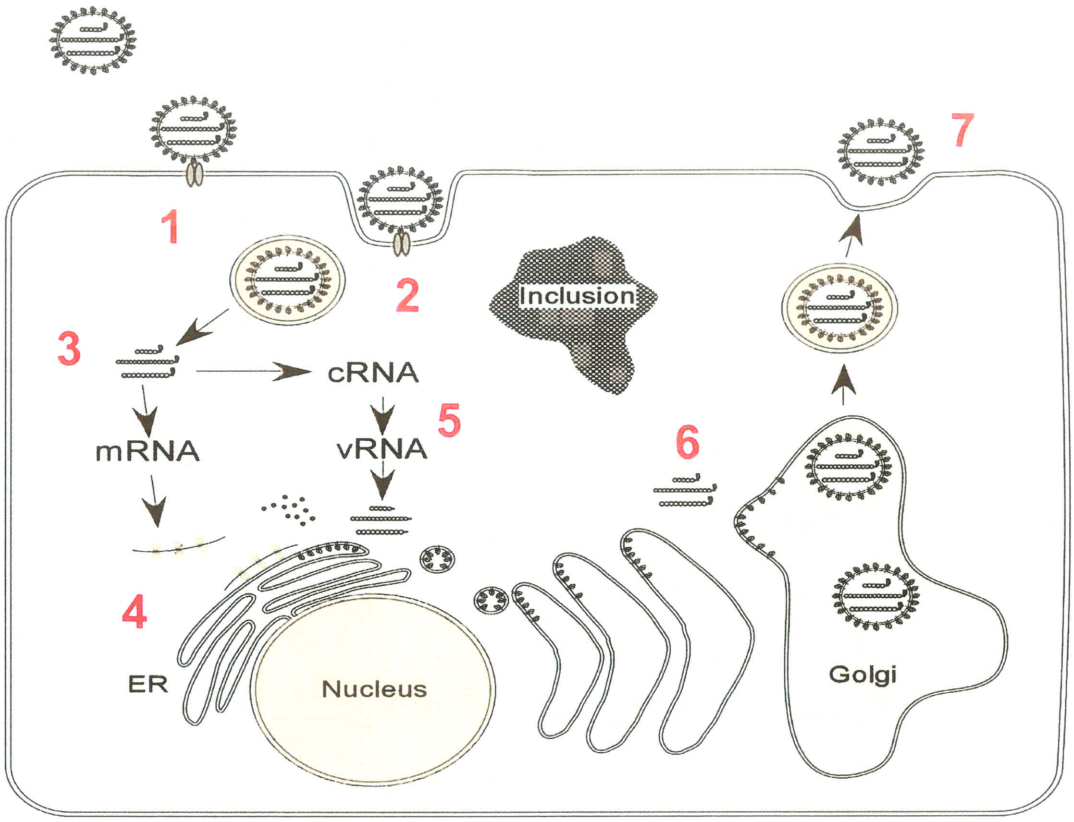

Figure 4: Hantavirus replication cycle. Steps in the replication cycle are as follows: 1. virion attachment to cell surface receptors; 2. receptor mediated endocytosis and virus uncoating; 3. primary transcription; 4. translation of virus proteins; 5. replication of virus genomic RNA through an intermediate virus cRNA; 6. assembly of virions at the Golgi apparatus; 7. virus release by exocytosis. Note the intracytoplasmic nucleocapsid inclusion body that is commonly seen in many of the hantaviruses (with permission from Simmons & Riley, 2002).

In general, it is believed that the glycoproteins are transported from the ER to the Golgi apparatus where they accumulate. Maturation of viral particles is believed to occur at Golgi membranes by the interaction between the glycoproteins and the N protein, the major component of the ribonucleocapsids. Virus particles bud into the Golgi cisternae and are then released at the plasma membrane by exocytosis (Schmaljohn & Hooper, 2001).

1.6.3 Protein Processing

The glycoproteins G1 and G2 are the only products of the M segment and are produced when the glycoprotein precursor is cleaved by a signal peptidase. G1 and G2 are type I transmembrane proteins, thus they are anchored in the membrane by carboxyterminal hydrophobic domains. Both glycoproteins are N-glycosylated with mainly endoglycosidase H sensitive carbohydrates of the high mannose type (Antic *et al.*, 1992; Pensiero & Hay, 1992; Plyusnin & Morzunov, 2001). Typically, one would expect that the carbohydrates would change to complex once in the Golgi rendering them no longer endoglycosidase H sensitive, but this is not the case (Schmaljohn, *et al.*, 1986; Antic *et al.*, 1992).

In general, the hantavirus G1 glycoprotein possesses a hydrophobic signal peptide (16 -23 aa) at the amino-terminal end (Plyusnin *et al.*, 1996). It is well known that the hydrophobic signal peptide is responsible for mediating translocation of the protein into the ER and is then cleaved off (Doms *et al.*, 1993) (Figure 5).

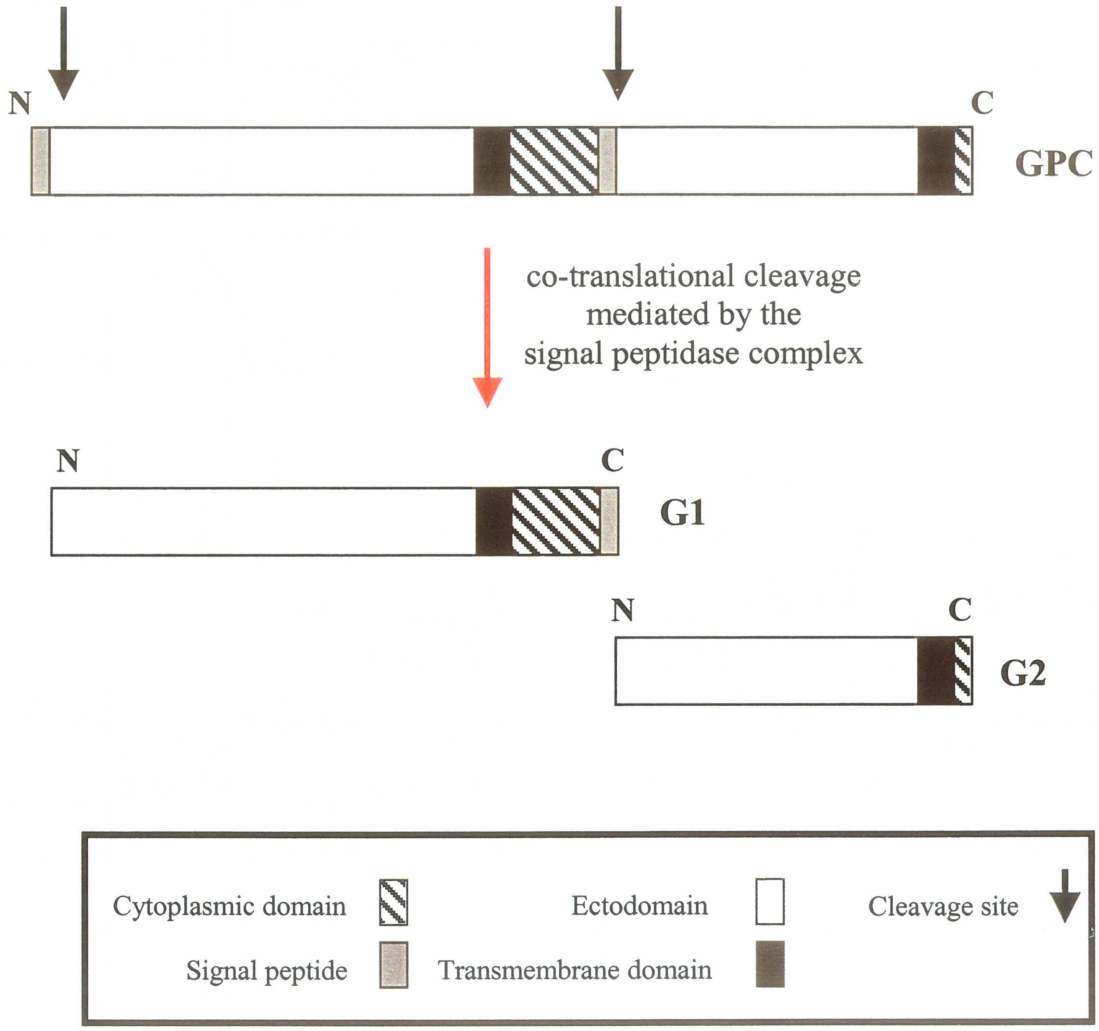

Figure 5: Schematic representation of the hantavirus glycoproteins. The glycoprotein precursor (GPC) is co-translationally cleaved by a signal peptidase producing G1 and G2.

The ectodomain of G1 is approximately 450 aa in length followed by a 75 aa hydrophobic membrane-associated domain in which the exact topology through the lipid bilayer is unknown; this is followed by a cytoplasmic loop (approximately 130 aa) and a second 23 aa hydrophobic signal peptide which serves as a signal sequence for G2 (Lober *et al.*, 2001) (Figure 5). The highly conserved WAASA motif is at the C-terminus of G1, after which cleavage occurs. G1 has an unusually long cytoplasmic tail, approximately 131 aa and it may function as the matrix protein thus interacting with the nucleocapsid protein or with the virion RNA (Spiropoulou *et al.*, 1994; Plyusnin *et al.*, 1996). In comparison, the ectodomain of G2 is approximately 450 aa, followed by 30 aa hydrophobic region and a short but highly charged cytoplasmic tail (9 aa) (Spiropoulou *et al.*, 1994; Plyusnin *et al.*, 1996) (Figure 5).

1.7 Intracellular Budding of Old World and New World Hantaviruses

An essential step in the life cycle of hantaviruses, and for that matter, all enveloped viruses, includes acquiring a lipoprotein coat by budding though one of the cellular membranes (Pettersson & Melin, 1996). Enveloped viruses have elucidated many different ways of carrying out this crucial step. For example, rota- and flaviviruses mature at the endoplasmic reticulum while rhabdo-, paramyxo- and retroviruses mature at the cytoplasmic membrane. In comparison, bunya-, corona- and rubella viruses bud from the Golgi apparatus (Pettersson & Melin, 1996). It is believed that the site of budding and maturation is dependent on the accumulation of one of the envelope proteins in the budding compartment (Pettersson & Melin, 1996). Amino acid sequence motifs on proteins are responsible for determining localization of membrane proteins (Stanley,

1996). These are called targeting or signaling motifs which may act as binding sites for other proteins which confer these properties (Stanley, 1996).

It is accepted for HTNV, the prototype OW hantavirus, that the heterodimeric glycoproteins are targeted to the Golgi complex from where virus assembly and maturation occurs (Pensiero & Hay, 1992; Ruusala *et al.*, 1992; Shi & Elliott, 2002; Anheier *et al.,* submitted). While the fate of the heterodimeric glycoproteins is established, the intracellular localization of the individually expressed HTNV glycoproteins is not well understood. For example, Pensiero and Hay (1992) and Anheier *et al.*, (submitted) demonstrated that when HTNV G1 is expressed alone, it is retained in the Golgi, while HTNV G2, expressed individually, is retained in the ER. In contrast, Ruusala *et al.*, (1992) and Shi and Elliott (2002) showed that both HTNV G1 and G2 when expressed alone are retained in the ER.

Anheier *et al.*, (submitted) demonstrated that Golgi localization of the Hantaan virus G1 was dependent on the cytoplasmic domain and independent of heterodimerization with G2. Furthermore, ER localization of Hantaan virus G2 was independent of its transmembrane and cytoplasmic domains and export of G2 was dependent on heterodimerization with G1. Likewise, glycoproteins of other members of the *Bunyaviridae* family demonstrate Golgi targeting. For example, a short region within the cytoplasmic tail of the G1 glycoprotein for Uukuniemi virus (Genus *Phlebovirus*) was responsible for mediating Golgi targeting (Andersson & Pettersson, 1998).

1.8 Objectives and Hypothesis

In 1997, Ravkov and colleagues showed that infection of Vero E6 cells with BCCV resulted in BCCV assembly at the plasma membrane, BCCV glycoprotein expression at the plasma membrane and BCCV release from the apical side of polarized Vero cells. This study provided the first set of data to suggest a new mechanism of virus maturation for NW hantaviruses. If NW hantaviruses possess a different means of budding, the glycoproteins should be targeted to different subcellular compartments.

The present study was established to study expression and targeting of NW hantavirus glycoproteins. BCCV was chosen for this study since it was the virus that was shown to bud at the plasma membrane by Ravkov *et al.*, (1997). By choosing the same virus, this would allow for direct comparison. BCCV, named after the geographic landmark near to the rodent's capture site, was isolated in 1995 from the rodent *Sigmodon hispidus* and was deemed responsible for a HPS case in Florida in 1994 (Rollin *et al.*, 1995). It is hypothesized that BCCV glycoproteins will be targeted to the plasma membrane to facilitate maturation of virus particles at this particular compartment. To test this hypothesis, the BCCV glycoproteins will be expressed in eukaryotic cells by transfection of plasmid DNA. The subcellular targeting of the glycoproteins will be analyzed by immunofluorescence, double immunofluorescence, cell fractionation in combination with immunoblotting and carbohydrate analysis using specific endoglycosidases.

Our group previously demonstrated (Anheier *et al.*, submitted) the importance of the cytoplasmic tail of G1 and G2 for subcellular targeting of HTNV, the prototype OW

hantavirus. In an alternate strategy, fusion proteins will be generated between the green fluorescent protein (GFP) and specific domains of the BCCV glycoproteins. The subcellular localization of these fusion proteins will be analyzed as described above.

GFP originates from the jellyfish *Aequorea victoria* and is naturally fluorescent (Stearns, 1995; Sacchetti *et al.*, 2000). GFP is chosen as a fluorescent tag since it possesses several useful properties: its fluorescence is not species-specific, it does not require any unusual cofactors, the protein is relatively small (28 kD), it does not form multimers that might interfere with the function of the protein to which it is fused (Stearns, 1995), and most importantly, GFP tagging permits protein movement to be followed in living cells (Chalfie, 1995; Sacchetti *et al.*, 2000).

It is well known that hantavirus glycoproteins are difficult to express (Spiropoulou, 2001; Anheier, personal communication). As an alternative approach to studying BCCV glycoprotein expression and localization, the Semliki Forest virus expression system will be used. SFV is a member of the *Alphavirus* genus within the family *Togaviridae* (van Regenmortel, 2000; Schlesinger & Schlesinger, 2001). It was originally isolated from mosquitoes and is spread by mosquitoes to rodents and birds. SFV is classified as a mild human pathogen and is considered a biosafety level 2 agent (Liljestrom & Garoff, technical manual 2nd edition). Several features of the SFV expression system make it an ideal cDNA expression system. First, the SFV RNA genome is infectious due to its positive sense polarity thus it functions directly as mRNA. Secondly, SFV can infect a wide variety of cell types. In addition, SFV replication occurs in the cell cytoplasm, which eliminates problems which may arise with nuclear

replication such as mRNA splicing. Lastly, the RNA replication is efficient and leads to a high expression of the viral proteins (Liljestrom and Garoff, 1991).

1.9 Significance of the Study

An unusual method of plasma membrane budding has been suggested for hantaviruses (Ravkov *et al.*, 1997). The present study will enable us to test this hypothesis using a recombinant expression system.

The implications of these studies are immense as they will provide new knowledge about the viral life cycle, specifically pertaining to the glycoprotein processing and virus maturation. Detailed knowledge about virus maturation may lead to new concepts for therapeutic interventions. It may even offer an explanation for the different clinical signs and symptoms which are observed between OW and NW hantavirus infections.

2 MATERIALS AND METHODS

2.1 Cells and Viruses

Vero E6 (green monkey kidney) cells were cultured in Dulbecco's modified Eagle's medium (DMEM, Sigma) with 10% heat inactivated fetal bovine serum (FBS) and 1% penicillin/streptomycin.

BHK-T7 (baby hamster kidney) cells were kindly provided by Klaus Conzelmann (Max-von-Pettenkofer Institute, University of Munich, Germany). Cells were cultured in Glasgow Minimum Essential medium (GMEM, Invitrogen) supplemented with 10% heat inactivated Newborn calf serum, geneticin (1 mg/ml, added fresh), tryptose-phosphate (1X), MEM Amino Acid solution without glutamine (2X), 1% glutamine and 1% penicillin/streptomycin. BHK-T7 cells constitutively express the T7 polymerase.

BHK-21 (baby hamster kidney) cells were cultured in Glasgow Minimum Essential medium (Invitrogen) supplemented with 10% heat inactivated FBS and 1% penicillin/streptomycin.

293T (human embryonic kidney) cells were cultured in DMEM (Sigma) with 10% heat inactivated FBS and 1% penicillin/streptomycin. Tissue culture dishes and sterile coverslips were coated with poly-D-Lysine (1 mg/ml, Sigma) for 30 minutes at 37°C to minimize cell detachment, prior to seeding of cells. Following incubation with poly-D-lysine, dishes were washed 3 times with sterile water, prior to seeding of cells. The 293T cell line is a derivative of 293, into which the gene for the temperature

sensitive simian virus 40 T antigen has been inserted. This line produces replication-competent T antigen in large amounts at 37°C (American Type Culture Collection).

All cell lines were incubated in the presence of 5% CO_2 at 37°C. Cells seeded for transfections, were cultured in medium without antibiotics.

Escherichia coli Top 10 chemically competent cells were purchased from Invitrogen. *E. coli* XL1-Blue competent cells were made in house by growing 0.5 ml of *E. coli* XL1-Blue overnight culture in 50 ml of LB broth at 37°C with shaking until the OD_{660} was within 0.5-0.8. Cells were then incubated for 20 minutes on ice followed by centrifuging at 2500 rpm for 10 minutes at 4°C. Pellet was resuspended in 5 ml of TSS buffer (85% LB broth, 10% polyethylene glycol, 5% DMSO and 50 mM $MgCl_2$), aliquoted and stored at -80°C.

BCCV was obtained from the Centers for Disease Control and Prevention (Atlanta, Georgia). HTNV was obtained from the Institute of Virology (Marburg, Germany). For BCCV and HTNV stock preparations, Vero E6 cells were seeded into two T-162cm^2 flasks and inoculated with virus at a 1:100 dilution, in 10 ml. Virus was allowed to adsorb for one hour, then 40 ml of DMEM supplemented with 2% FBS, 1% penicillin/streptomycin and 1% glutamine was added. When the first signs of CPE were visible, flasks were frozen at –80°C, thawed and centrifuged at low speed to pellet out cell debris. Supernatants were pooled and aliquoted and virus stocks were stored in liquid nitrogen. All handling of infectious BCCV and HTNV was performed under appropriate biocontainment conditions as outlined in the Health Canada Laboratory

Biosafety Guidelines (http://www.hc-sc.gc.ca/pphb-dgspsp/publicat/lbg-ldmbl-96/index.html).

2.2 Antibodies and Primers

See Table 3 for a list of primary and secondary antibodies used.

See Appendix I for a list of primers used. Primers for BCCV and HTNV are based on Genbank sequences L39950 and Y00386, respectively. See Appendix II for nucleotide sequence of BCCV M segment.

2.3 RNA Extraction

RNA extraction was performed to generate RNA template for RT-PCR. Vero E6 cells were infected with BCCV or HTNV at a M.O.I. of 0.01. Cells were harvested at 10 days post infection using Trizol LS (Invitrogen). Total RNA was extracted using the TRIZOL LS protocol (Invitrogen). Briefly, isolation of RNA was performed in the following manner: 1) homogenization of infected cells in Trizol LS; 2) separation of RNA from protein and DNA (phase separation) with the addition of chloroform; 3) RNA precipitation with isopropyl alcohol; 4) RNA wash with 75% ethanol and 5) redissolving RNA in Rnase-free water.

2.4 Polymerase Chain Reaction (PCR)

PCR was performed using *Pfu Turbo* DNA polymerase (Stratagene) in a Perkin Elmer GeneAmp PCR System 2400 thermocycler. *Pfu Turbo* DNA polymerase was chosen since it has been shown to significantly increase PCR product yields and exhibits a low error rate due to its proofreading activity. PCR was performed on pDisplay BCCV

Table 3: Summary of primary and secondary antibodies

Antibody	Company	Source	Method	Dilution
Primary Antibodies				
Anti-HA	Sigma	rabbit	IFA	1:50
			Western Blot	1:2000
FITC-Conjugated Anti-HA High Affinity	Roche	Rat	Double IFA	1:50
Anti-GFP	Oncogene	Rabbit	Western Blot	1:2000
Anti-Giantin	Covance	Rabbit	Single/Double IFA	1:1000
Secondary Antibodies				
Anti-Rabbit FITC	Sigma	Goat	IFA	1:100
Anti-Rabbit Cy3	Rockland	Goat	IFA	1:100
Anti-Rabbit HRP	Sigma	Goat	Western Blot	1:30 000

G1 clone to generate BCCV G1 cytoplasmic tail and BCCV G1 truncated cytoplasmic tail for the GFP-hantaviral glycoprotein fusion protein constructs.

A typical 100 µl reaction consisted of: 70 µl of sterile water, 10 µl of 10x PCR buffer, 4.0 µl of dNTP (10 mm each), 6.0 µl of 10 µM forward primer, 6.0 µl of 10 µM reverse primer, 2.0 µl of DNA (1:1000 dilution) and 2.0 µl (5 units) of *Pfu Turbo* DNA polymerase. All reactions were set up on ice.

A typical thermocycling protocol for PCR included:

Cycles	Temperature and Time
1x	Initial denaturation 95°C for 2 min
35-50x	-Denaturation at 94°C for 30 s -Annealing temperature dependent on melting temperature of primers, 30s -Elongation at 72°C for 1 min (dependent on PCR fragment length)
1x	Prolonged elongation time 72°C for 7 min
∞	4°C

2.4.1 Reverse Transcription-Polymerase Chain Reaction (RT-PCR)

RT-PCR was conducted using Titan One Tube RT-PCR kit (Roche) and performed in a Perkin Elmer GeneAmp PCR System 2400 thermocycler. See Appendix I for a list of inserts which were generated by RT-PCR. Two mastermixes were set up (total volume of 25 µl each), then combined. Mastermix 1: 12.5 µl of sterile water, 4 µl of 0.2 mM (each) dNTP mix, 2.5 µl 5 mM DTT solution, 1 µl (5 units) Rnase inhibitor, 2.0 µl of 10 µM forward primer, 2.0 µl of 10 µM reverse primer and 1.0 µl of RNA (1 ug – 1 pg total RNA, BCCV or HTNV). Mastermix 2: 14 µl of water, 10 µl of 5x RT-PCR buffer and 1 µl of enzyme mix. All reactions were set up on ice.

A typical thermocycling protocol for RT-PCR included:

Cycles	Temperature and Time
1x	Reverse transcription at 50°C for 30 min
1x	Initial denaturation 94°C for 2 min
35-50x	-Denaturation at 94°C for 30 s -Annealing temperature dependent on melting temperature of primers, 30s -Elongation at 68°C for 45sec-2 min (dependent on PCR fragment length)
1x	Prolonged elongation time 68°C for 7 min
∞	4°C

2.4.2 Product Analysis

All amplicons were verified for size and quality by 0.8% agarose gel electrophoresis, run in Tris/acetate/EDTA electrophoresis buffer. Agarose gels were stained with ethidium bromide, which was added to the melted agarose when it was cast, run at 120 volts for 30 minutes and DNA was visualized with a MacroVue UV-25 Hoefer transilluminator.

2.5 Cloning

Using sequence specific primers, inserts were generated either by PCR or RT-PCR and verified by 0.8% agarose gel electrophoresis. Amplicons were PCR purified (QIAquick PCR purification kit, Qiagen) or gel extracted (QIAquick gel extraction kit, Qiagen) and digested in parallel with the appropriate vector with restriction enzymes (New England Biolabs). Following the digestion, the cut vector and insert were PCR purified (QIAquick PCR purification kit, Qiagen) and ligated using 1unit/μl of T4 DNA ligase [Roche, a typical ligation reaction consisted of x μl of water, 2.0 μl of 10x buffer, 1.0 μl vector, 3.0 – 10.0 μl of insert and 1.0 μl of T4 DNA ligase (for a total

volume of 20.0 µl)] and incubated overnight at 16°C. *E. coli* Top 10 chemically competent cells (Invitrogen) or *E. coli* XL-1 Blue competent cells were transformed by thawing cells on ice then adding the entire ligation reaction (20 ul) to the competent cells, followed by incubation on ice for 10 minutes. Cells were heat shocked at 42°C for 30 sec, then placed on ice and ice cold SOC medium was added. The reaction was incubated at 37°C with shaking for 1 hour, then was plated on LB+Amp (100µg/ml) plates and incubated for 16 hours at 37°C. Colonies were screened by miniprep analysis (QIAprep Spin Miniprep Kit, Qiagen) and restriction enzyme digestion. All constructs were fully sequenced through the entire insert region using the dideoxy technique based on Sanger *et al.*, (1977). The amplicons were analyzed using an ABI 3100 Genetic Analyzer.

2.5.1 pDisplay constructs

BCCV RNA was used to amplify the G1 (nucleotides 106-2013) and G2 (nucleotides 2014-3477) open reading frames by RT-PCR using sequence specific primers containing *Xma*I and *Pst*I restriction sites (Appendix IA). Inserts were cloned into pDisplay (Invitrogen), a mammalian expression vector. pDisplay (Figure 6A) allows the protein of interest to be processed in mammalian cells, thus the recombinant protein more closely resembles its native form. pDisplay also offers a T7 promoter/priming site for *in vitro* transcription of sense RNA and for sequencing of inserts, an ampicillin selection marker and a HA epitope which allows for protein detection using an anti-HA antibody.

2.5.2 pSFV1 leader constructs

BCCV RNA was used to amplify the G1 (nucleotides 106-2013) and G2 (nucleotides 2014-3477) open reading frames by RT-PCR using sequence specific primers containing *Bam*HI and *Xma*I restriction sites (Appendix IB). BCCV G1 and BCCV G2 were individually cloned into the pSFV1 expression plasmid (Figure 6C). The pSFV1 expression plasmid and pSFV-Helper 1 plasmid (Figure 6C) were kindly provided by Liljestrom and Garoff (Sweden). The pSFV1 expression plasmid contains the four genes encoding the SFV replicase (nsP1-4).

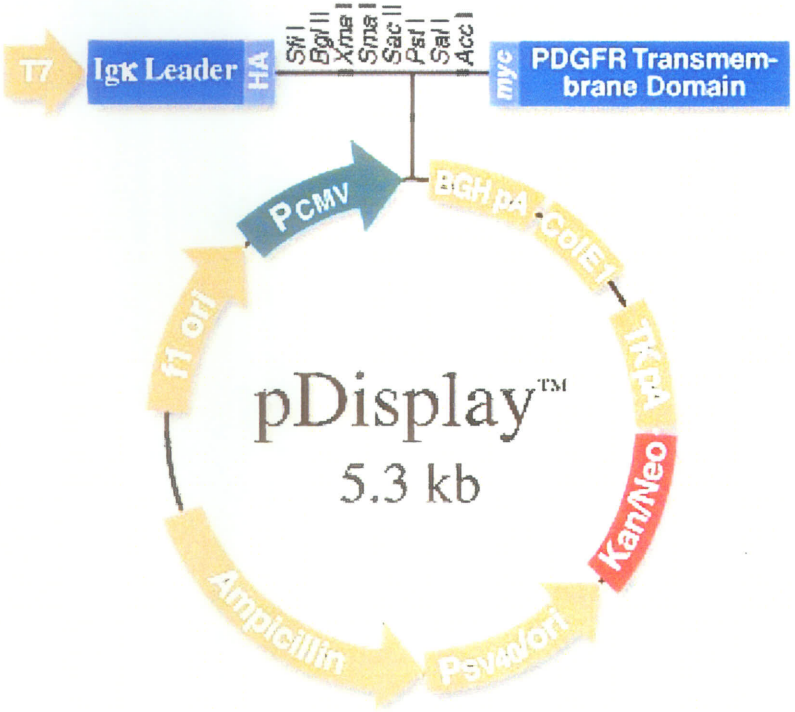

A

Figure 6A: Vector map of pDisplay (Invitrogen)

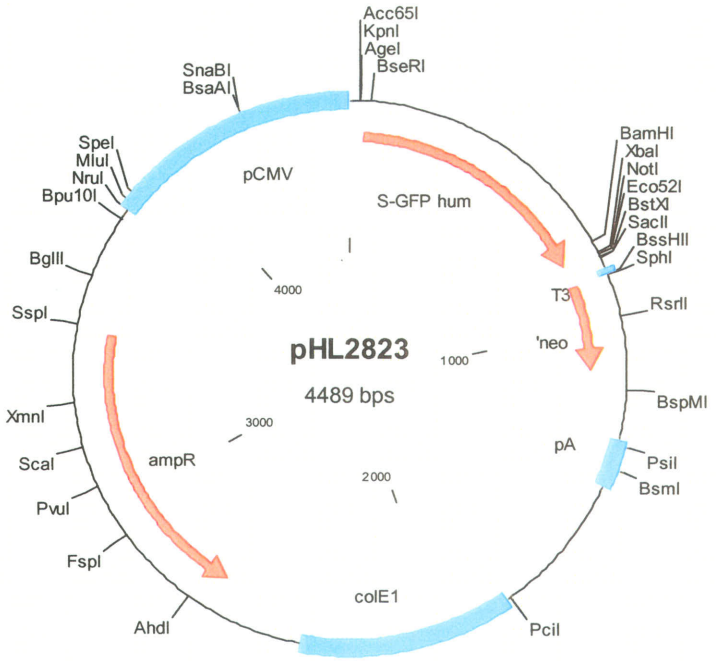

B

Figure 6B: Vector map of pHL2823
(Flick & Hobom, unpublished)

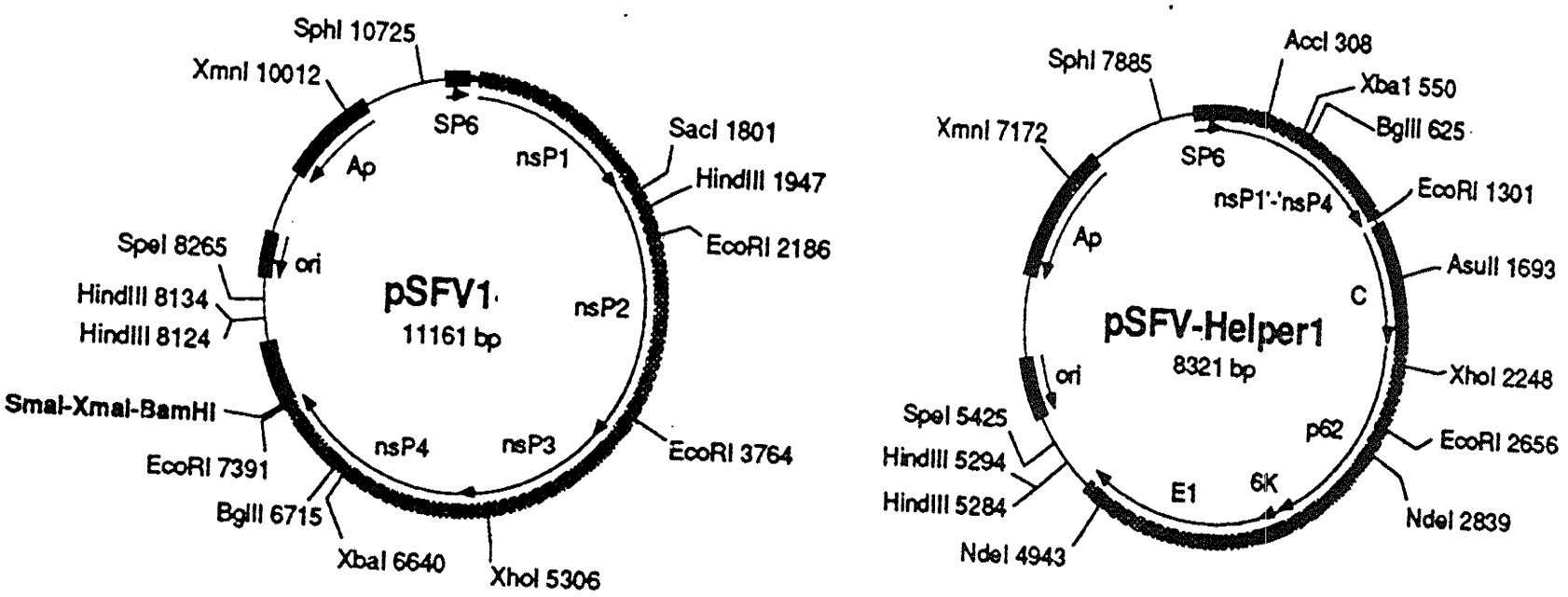

Figure 6C: Vector maps of pSFV1 and pSFV-Helper1 (Liljestrom & Garoff, 1991)

The coding region for the subgenomic 26S RNA, encoding the structural proteins of the virus, was deleted and replaced with a *Bam*HI – *XmaI*/*Sma*I polylinker sequence. The polylinker is followed by a cassette of translational stop codons in all three reading frames located downstream from the 26S promoter site (Liljestrom and Garoff, 1991). pSFV1 has a SP6 promoter for *in vitro* transcription and an ampicillin resistance marker for bacterial selection. pSFV-Helper1 has a similar backbone, however it lacks the nsP genes but carries the structural genes (Liljestrom and Garoff, 1991).

The leader sequence (derived from immunoglobulin kappa) from pDisplay (Invitrogen) was cloned into the polylinker site of the pSFV1 expression plasmid by Sebastian Haferkamp (Special Pathogens Program). Since pSFV1 leader contains a signal peptide, expressed proteins using the recombinant SFV system can be directed through the ER/Golgi secretory pathway.

2.5.3 SFV Expression System

The SFV expression vectors are based on a cDNA clone of the full-length SFV genome under the control of a SP6 RNA polymerase promoter. The gene of interest can be cloned into a polylinker site which has replaced the SFV structural genes. The recombinant vector DNA can be introduced into an *in vitro* transcription kit. By using the SP6 RNA polymerase, recombinant mRNAs are generated and can be transfected into cells by electroporation or lipofection. In the cytoplasm of the transfected cell, the recombinant SFV vector RNA is replicated by the virus-encoded replicase and translated into protein (Liljestrom and Garoff, 1991; Liljestrom & Garoff, technical manual 2nd edition).

The SFV recombinant RNA molecule can also be packaged into infectious SFV particles *in vivo* by co-transfection with both recombinant RNA and a helper RNA. The helper RNA contains the genes encoding the structural proteins but lacks the packaging signal and the replicase gene. The recombinant-RNA-encoded replicase amplifies both RNA species but the capsid protein only packages recombinant RNA molecules into nucleocapsids due to the presence of the packaging signal. Assembly and budding of new recombinant SFV virions occurs at the cell surface through an interaction between cytoplasmically preformed nucleocapsids and the viral spike membrane proteins embedded in the plasma membrane. The nucleocapsids bud out from the plasma membrane to form new infectious SFV particles which provide a one-step virus stock since the viruses are replication deficient (Figure 7) (Liljestrom and Garoff, 1991; Liljestrom & Garoff, technical manual 2nd edition).

2.5.4 *In vitro* transcription of pSFV1 leader constructs

To generate mRNA transcripts of pSFV1 leader constructs for transfection into BHK-21 cells, recombinant and helper mRNAs were synthesized by *in vitro* transcription as described in Liljestrom & Garoff (technical manual 2nd edition and Liljestrom and Garoff, 1991). *In vitro* transcription is possible due to the presence of a SP6 RNA polymerase promoter in the SFV expression vectors.

Five μg of pSFV-Helper 1 plasmid DNA was digested with *Spe*I (to linearize plasmid) in a total volume of 20 μl at 37°C for 1 hour. Following digestion, helper plasmid DNA was purified using the QIAquick PCR purification kit (Qiagen) and was eluted in 15 μl of sterile water.

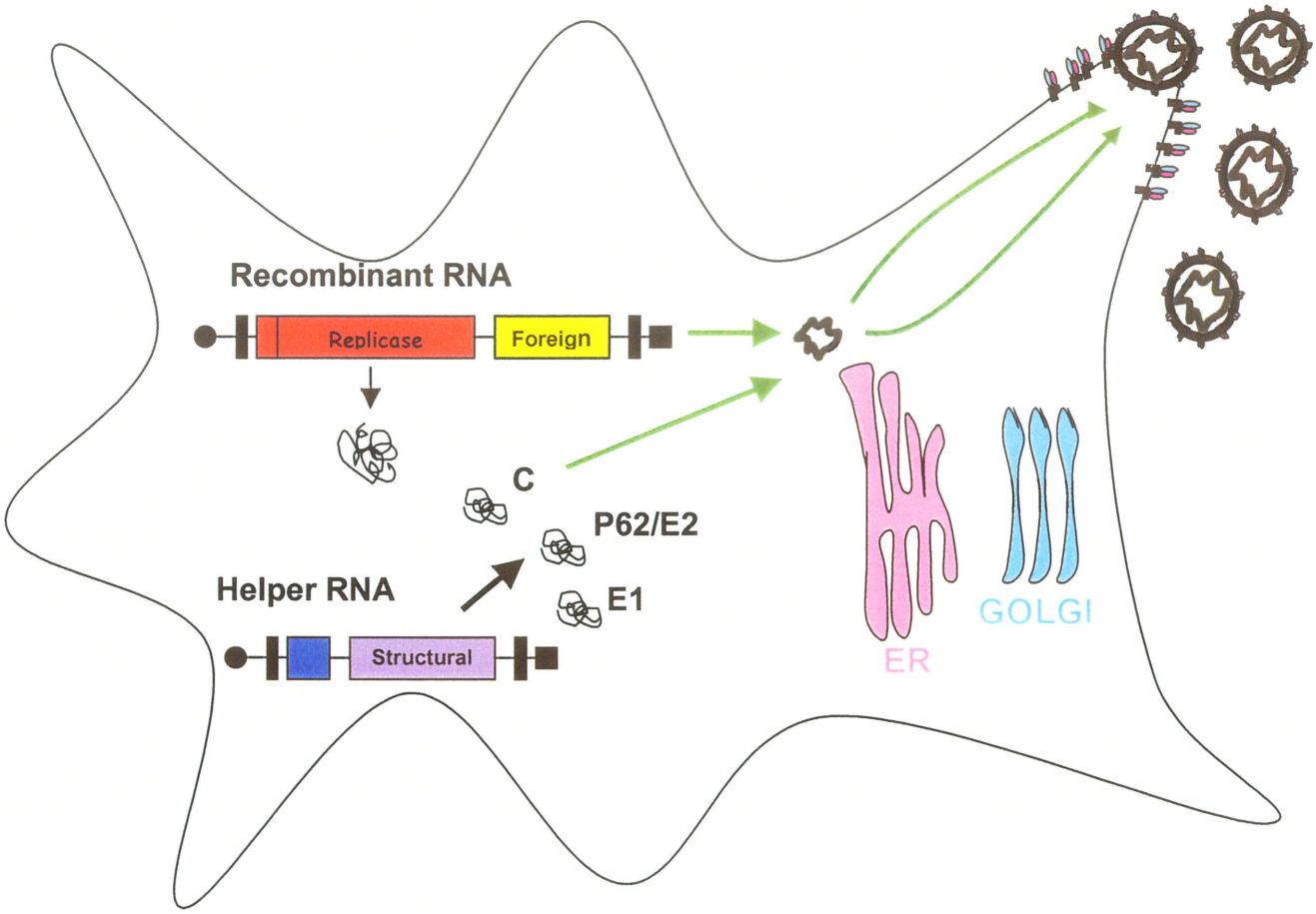

Figure 7: Schematic presentation of *in vivo* packaging of recombinant RNA into SFV particles. Recombinant and Helper RNAs are co-transfected into BHK cells where the recombinant-RNA-encoded replicase amplifies both RNA species. The capsid protein (C) only packages recombinant RNA molecules into nucleocapsids, since the Helper RNAs lack a packaging signal (residing in the *ns*P1 gene). Assembly and budding of new recombinant SFV virions occurs at the cell surface through an interaction between cytoplasmically preformed nucleocapsids and the viral spike membrane proteins p62 and E1 (modified from Liljestrom and Garoff, 1991).

The following reaction was set up for the helper plasmid cut DNA, pSFV1 leader BCCV G1 and pSFV1 leader BCCV G2 and incubated at 40°C for 1 hour: 1.5 µg DNA, 5.0 µl 10x SP6 buffer, 5.0 µl of 10 mM m7G(5')ppp(5')G, 5.0 µl 50 µM DTT, 5.0 µl rNTP mix, 1.5 µl of Rnase inhibitor, 0.5 µl SP6 RNA polymerase and 28.0 µl of sterile water. Following incubation, 5 µl was run on a 0.8% agarose gel containing ethidium bromide to verify RNA production. RNA was confirmed by obtaining a band of appropriate size on the agarose gel. mRNA was stored at –80°C.

2.5.5 GFP-hantaviral glycoprotein fusion protein constructs

All GFP-hantaviral glycoprotein fusion protein constructs were expressed under CMV control using pHL2823 as a vector plasmid, which was kindly provided by Flick and Hobom (Sweden, unpublished) (Figure 6B). The GFP used contains a His tag and utilizes human codon usage for better expression in human cell lines. In addition, GFP is under CMV control, the vector backbone of pHL2823 is pcDNA3 (Invitrogen), it contains ampicillin and neomycin resistances and has a polyadenylation site. The sequences of the oligonucleotides, restriction sites used and the cloning strategy for generating the GFP-hantaviral glycoprotein fusion protein constructs are listed in Appendix IC. BCCV G1 full length and truncated cytoplasmic tails were generated by PCR from the BCCV G1 pDisplay clone. HTNV G1 and HTNV G1 truncated cytoplasmic tails were generated using sequence specific primers by RT-PCR. In the case of BCCV and HTNV G1, an unique restriction enzyme, *Bsm*BI was used for direct insertion into pHL2823. Subsequent digestion with *Bsm*BI resulted in cleavage adjacent to the *Bsm*BI restriction site, thus generating *Bam*HI and *Xba*I compatible ends. BCCV

G2 and HTNV G2 cytoplasmic tails were generated using hybridized oligolinkers (see 2.5.6). BCCV G2 SP for the N and C-terminus of GFP along with BCCV G2 SP inverted were also generated by insertion of oligolinkers. BCCV G2 SP inverted consists of the SP rotated, so that the amino acids at the N terminus are now at the C terminus and vice versa. Site directed mutagenesis was performed on pHL2823 using QuickChange Site-Directed Mutagenesis kit (Stratagene) to synthesize a *Bcl*I restriction site to facilitate the cloning at the N terminus of pHL2823.

Influenza (INFV) hemagglutinin (HA) transmembrane (TD) or HA signal peptide (SP) oligolinkers were designed based on the influenza Aichi strain, A/Aichi/2/68 (H3N2) (M55059, Armstrong *et al.*, 2000). The oligolinkers were cloned at the C-terminus of GFP or at the C-terminus of GFP-BCCV G1 truncated cytoplasmic tail [GFP-BCCV $G1_{650\text{-}648}$ (truncated)].

2.5.6 Hybridization of oligolinkers for GFP-hantaviral glycoprotein fusion protein constructs

Since many of the inserts for the GFP-hantaviral glycoprotein fusion protein constructs were very short in length (30-80 bps), synthesis of the inserts in the form of an oligolinker was preferred over generating the inserts by PCR or RT-PCR (see Appendix IC for a list of inserts which were generated by oligolinkers). Forward and reverse oligolinkers which spanned the entire length of the insert and contained the appropriate restriction sites were synthesized and then hybridized together to form a double-stranded DNA insert. Hybridization was performed by combining 20 µl of the two complementary primers (100 µM each), 10 µl of 10X hybridization buffer (1M NaCl, 1M

Tris HCl) and 50 µl of water. Incubation parameters: 70°C for 10 min, 32°C for 2 hours and 4°C for 12 hours.

2.6 *In vitro* transcription and translation

This system provides a convenient method that couples transcription and translation and is ideal for the verification of the expression of a protein. *In vitro* transcription and translation was performed on pDisplay BCCV G1 and pDisplay BCCV G2 constructs using TnT Quick Coupled Transcription/Translation System (Promega) as described in the instruction manual. In brief, the TnT Quick Coupled Transcription/Translation System involved mixing circular plasmid DNA with a Mastermix containing the RNA polymerase, nucleotides, salts and a reticulocyte lysate (rich in translational machinery). Mixture was incubated at 30°C for 90 minutes and then the synthesized proteins were analyzed by SDS-PAGE and autoradiography.

2.7 Transfections

2.7.1 Transfection of pDisplay BCCV G1 construct and pDisplay BCCV G2 construct into BHK-T7 cells

BHK-T7 cells were transfected at 60-70% confluency (24 well dish) using Lipofectamine 2000 (Invitrogen). One µg of plasmid MaxiPrep DNA (QIAfilter Plasmid Maxi kit, Qiagen) was mixed with 20 µl of Opti-MEM (Invitrogen) and 25 µl of Opti-MEM (Invitrogen) was mixed with 1.5 µl of Lipofectamine 2000. Both mixtures were incubated for five minutes at room temperature after which they were combined and incubated for fifteen minutes at room temperature. After incubation, 160 µl of fresh Opti-MEM was added to the mix (Lipofectamine + DNA). Medium was removed from

BHK-T7 cells and the DNA/Lipofectamine mix was added. Cells were incubated at 37°C with 5% CO_2 for 24-48 hours.

2.7.2 Transfection of pSFV1 leader BCCV G1 mRNA and pSFV1 leader BCCV G2 mRNA into BHK-21 cells

BHK-21 cells seeded in 10 cm dishes were transfected at 60-70% confluency. Seven hundred and fifty µl of Opti-MEM (Invitrogen) was combined with 15 µl of helper mRNA and 15 µl of BCCV G1 or G2 mRNA. In a separate tube, 750 µl of Opti-MEM was combined with 30 µl of Lipofectamine 2000 (Invitrogen). Both mixtures were incubated for five minutes at room temperature then combined and incubated further for 15 minutes at room temperature. Following incubation, 1.5 ml of Opti-MEM was added to this mixture and transferred to the cells whose medium had been removed. Transfected cells were incubated at 37°C with 5% CO_2. At 24 hours post transfection, 5.0 ml of GMEM supplemented with 10% FBS and 1% penicillin/streptomycin was added to the transfected cells. Cells were monitored until CPE presented. The supernatant (containing recombinant SFV virions) was collected and spun at 1000g for 2 minutes. Supernatants were pooled and aliquoted into 1.0 ml aliquots and stored at –80°C.

2.7.3 Transfection of GFP-hantaviral glycoprotein fusion protein constructs into 293T cells

293T cells were transfected at 60-70% confluency (24 well dish) using Lipofectamine 2000 (Invitrogen). 0.8 µg of plasmid MaxiPrep DNA (QIAfilter Plasmid Maxi kit, Qiagen) was mixed with 20 µl of Opti-MEM (Invitrogen) and 25 µl of Opti-MEM was mixed with 1.0 µl of Lipofectamine 2000, both mixtures were incubated for

five minutes at room temperature. Following, both mixes were combined and incubated for fifteen minutes at room temperature. After incubation, 160 µl of fresh Opti-MEM was transferred to mix (Lipofectamine + DNA). Media was removed from 293T cells and DNA/Lipofectamine mix was added. Cells were incubated at 37°C with 5% CO_2 for 24-48 hours.

2.8 Infection of BHK-21 cells with SFV BCCV G1 and SFV BCCV G2

BHK-21 cells were infected at 80-90% confluency in 10 cm tissue culture dishes. Five hundred µl (M.O.I. ~ 1) of pSFV1 leader BCCV G1 or BCCV G2 virus supernatant was mixed with 1.5 ml of GMEM (no supplements) and then added to cells whose media had been removed. Virus was allowed to adsorb for one hour at 37°C. Following incubation, 6.5 ml of GMEM supplemented with 10% FBS and 1% penicillin/streptomycin was added. Cells were incubated at 37°C with 5% CO_2 for 16-30 hours.

2.9 Light Microscopy

Transfected or infected cells were viewed in the tissue culture dish using a hund Wilovert S light microscope.

2.10 Harvesting of Cells

Transfected or infected cells were harvested using 1X SDS-gel loading buffer [62.5 mM 0.5 M Tris-Cl, pH 6.8, 2% (w/v) SDS, 10% (v/v) glycerol, 0.1% (w/v) bromophenol blue and 300 mM 2-mercaptoethanol] under reducing conditions. If supernatant was desired it was collected, if not, it was discarded. Tissue culture dishes were placed on ice and 1X SDS-gel loading buffer was added (50 µl per well of a 24 well

tissue culture dish, 250 µl per well of a 6 well tissue culture dish and 500 µl for a 10 cm tissue culture dish). SDS-gel loading buffer was incubated with the cells for 5 minutes on ice followed by collection using a cell scraper or pipette tip. Cell lysates were boiled for 5 minutes at 99°C, then stored at –20°C.

2.11 SDS-PAGE and Semi-dry transfer

Proteins were electrophoresed (200 volts for 45 minutes) on 10 cm (l) x 7.5 cm (h) (thickness 1.0 mm) 10% SDS mini-gels (15% for characterization of carbohydrates) using a discontinuous buffer system that incorporates SDS in the buffer (Laemmli, 1970). In this system, proteins are denatured by heating them in a buffer which contains sodium dodecyl sulphate (SDS) and a thiol reducing agent such as 2-mercaptoethanol. Proteins were then transferred from the SDS gel to PVDF transfer membrane (Amersham Pharmacia Biotech) using a Trans-blot SD semi-dry transfer apparatus (Bio-Rad).

Semi-dry transfer for a mini-gel was performed by wetting the surface of the trans-blot apparatus and placing a filter pad which was soaked in anode buffer (75 ml of 0.67M boric acid, 200 ml of methanol and 725 ml of sterilized water) was placed on the wet surface. PVDF transfer membrane was incubated in methanol for 5 minutes then wet in anode buffer before placement on the anode soaked filter pad. The stacking portion of the SDS-gel was removed and the resolving portion was soaked in anode buffer then placed on top of the PVDF. As each layer was added on, the air was rolled out by dragging a pipette across the surface. The remaining filter pad was soaked in cathode buffer (75 ml of 0.67M boric acid, 50 ml of methanol and 875 ml of sterilized water) and placed on top of the gel and air bubbles were rolled out. Transfer of a

mini-gel was run at 60 mA per gel, for 90 minutes.

2.12 Immunoblot

Following transfer, the membrane was blocked overnight in 5% skim milk + 0.1% Tween to reduce non-specific binding to the membrane. The following morning, the blot was washed three times with PBS/0.1% Tween then incubated with the primary antibody for 1 hour with rocking at room temperature. The blot was then washed three times with PBS/0.1% Tween and incubated with the secondary antibody for 1 hour with rocking at room temperature. The blot was again washed with PBS/0.1% Tween three times, followed by three washes with PBS. Proteins were visualized using the ECL +plus Western Blotting Detection system (Amersham Biosciences) as described in the instruction manual. Briefly, ECL +plus is a sensitive chemiluminescent system used for protein blotting where an antibody system coupled to horse radish peroxidase converts an ECL substrate into a light signal.

2.13 Characterization of Carbohydrates

To further confirm the intracellular location of the BCCV G2, the N-linked carbohydrates were characterized to determine if they were high-mannose (indicative of ER localization) or complex (indicative of Golgi localization). Endoglycosidase H removes N-glycans of high mannose type while N-glycosidase F cleaves all types of asparagine bound N-glycans (Figure 11A & B, respectively). Cell lysates were treated with endoglycosidase H (Roche) and N-glycosidase F (Roche) separately. 1µl of cell lysate was incubated with 10 units of enzyme (either endo H or N-glycosidase F) in PBS overnight at 37°C. The negative control included incubating the cell lysate only with

PBS, without enzyme. Following incubation, 4X SDS-gel loading buffer was added and samples were run on a 15% SDS gel. Detection of proteins was determined by immunoblot using anti-HA (Sigma).

2.14 Immunofluorescence Assay

2.14.1 Single Immunofluorescence

Transfected or infected cells, on coverslips, were fixed with 2% paraformaldehyde for 20 minutes at room temperature or at 4°C overnight. Following fixation, cells were washed three times with PBS then permeabilized using 0.1% Triton X-100 (in PBS) for 20-30 minutes at room temperature, followed by three PBS washes. Treatment with Triton X-100 was omitted for surface IFAs. Cells were incubated with the primary antibody at 37°C for 1 hour followed by three PBS washes. Cells were then incubated with the secondary antibody for 1 hour at 37°C, followed by three PBS washes. Coverslips were mounted on microscope slides using Gelmount (CedarLane) and viewed under UV illumination.

2.14.2 Double Immunofluorescence

To confirm the intracellular location of the BCCV glycoprotein G1, co-localization experiments were performed with giantin, a resident Golgi protein. If BCCV G1 was located in the same location as giantin, co-localization would be expected. Giantin is a membrane-inserted component of the cis and medial Golgi with a large rod-like cytoplasmic domain.

Infected BHK-21 cells were fixed with 2% paraformaldehyde. Following fixation, cells were washed three times with PBS then permeabilized with 0.1% Triton X-100 (in

PBS) for 20-30 minutes at room temperature, followed by three PBS washes. Cells were incubated with FITC-conjugated anti-HA for detection of BCCV G1 (1:50 dilution in PBS, Roche) and anti-giantin (1:1000 dilution in PBS, Covance) for one hour at 37°C, followed by three PBS washes. Cells were then incubated with the secondary antibody, goat anti-rabbit Cy3 (1:100 dilution in PBS, Rockland) for one hour at 37°C followed by three PBS washes. Coverslips were mounted on microscope slides using Gelmount (Cederlane). Co-localization was studied using confocal microscopy.

2.15 UV Microscopy

Transfected or infected cells were viewed in the tissue culture dish or coverslips were fixed with 2% paraformaldehyde for 20 minutes at room temperature or at 4°C, overnight, then viewed under UV illumination (Zeiss, Axiovert 100) 24-48 hours post transfection or infection. UV pictures were taken using Northern Eclipse software. Co-localization studies were performed using an Olympus IX70 confocal microscope and images were processed using Fluoview 2.1 software.

2.16 Membrane Fractionation of GFP-hantaviral glycoprotein fusion proteins

To determine if GFP-hantaviral glycoprotein fusion proteins were membrane associated or cytosolic, alkaline carbonate extraction was performed on 293T cells 46-72 hours post transfection (method obtained from current protocols online, http://www.mrw2.interscience.wiley.com/cponline). 293T cells were transfected with individual constructs (two wells of a 6 well plate per sample) as explained in section 2.7.3. At 46-72 hours post transfection, supernatant was removed and cells were washed three times with PBS, then once with 100 mL NaCl. Occasionally, the transfected cells

would detach from the plate thus, the nonadherent cells were isolated between washes by microcentrifugation (2 minutes at 1000g). Cells were then scraped (adherent) or resuspended (nonadherent) into 1 ml of ice-cold 100 mM sodium carbonate, pH 11.5 and homogenized (five strokes) in a 2 ml Dounce homogenizer. The homogenate was then incubated for 30 minutes on ice and 1.0 ml of sodium carbonate was added to attain the necessary volume for ultracentrifugation. The homogenate was then centrifuged for 60 minutes at 50 000 rpm using a TLS-55 rotor (Beckman) at 4 °C. Following centrifugation, the supernatant was transferred to a fresh tube and concentrated 3-5 times using a concentrator (Savant Speed Vac SC110). The pellet was resuspended in 250 µl of sodium carbonate. Pellet and supernatant fractions were then mixed with 4x SDS-PAGE sample buffer containing β-mercaptoethanol and run on SDS-PAGE (10% gel). Proteins were visualized by immunoblot using an anti-GFP antibody (Oncogene).

3 RESULTS

3.1 Expression of pDisplay BCCV G1 and G2 constructs

3.1.1 Confirmation of expression in BHK-T7 cells by immunoblot and IFA

BHK-T7 cells were transfected with either pDisplay BCCV G1 or pDisplay BCCV G2. In addition to a CMV promoter, pDisplay has a T7 promoter which allows for transcription by using the T7 polymerase which is constitutively expressed in BHK-T7 cells. At 26 hours post transfection, cells were harvested and run on a 10% SDS-PAGE. Using an anti-HA antibody (1:2000) followed by a HRP-conjugated goat anti-rabbit antibody (1:30 000), immunoblot analysis revealed a band at 54 kDa indicative of BCCV G2 (Figure 8, lane 3). Unfortunately, no product was detected for BCCV G1 (expected molecular weight of 72 kDa) (Figure 8, lane 2). pDisplay was transfected as a negative control to ensure that the detected proteins were not derived from the cell or the vector itself (Figure 8, lane 1). Transfection of pDisplay BCCV G1 was conducted in other cell lines (Hela and 293T) while using different amounts of DNA and Lipofectamine 2000 reagent. All attempts to express BCCV G1 have been unsuccessful to date.

Expression of pDisplay BCCV G2 was also confirmed by IFA. Transfected cells were fixed at 48 hours post transfection and probed with anti-HA (1:50) followed by Cy3-conjugated goat anti-rabbit (1:100). An intracellular stain was performed by treating the cells with Triton X-100 thus permeabilizing the plasma membrane, allowing entry of the antibody.

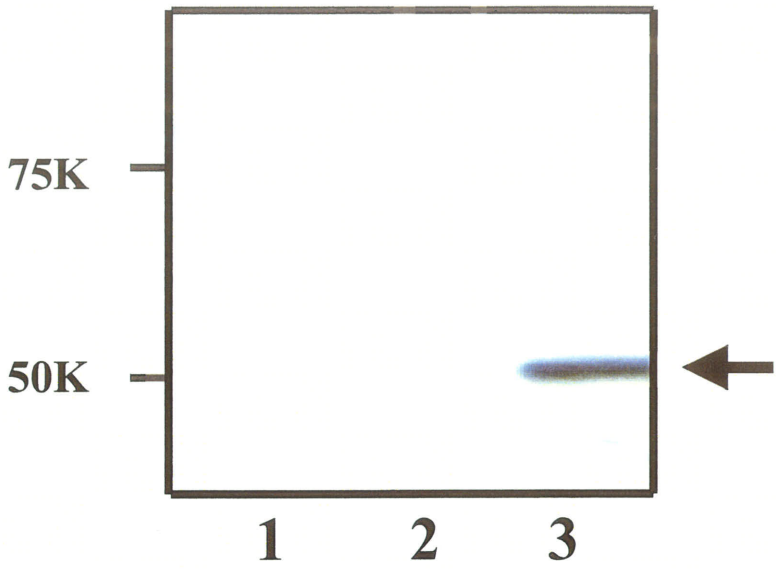

Figure 8: Expression of BCCV G2 confirmed by immunoblot. BHK-T7 cells were transfected with pDisplay (negative control), pDisplay BCCV G1 and pDisplay BCCV G2 and harvested at 26 hours post transfection. Proteins were detected with anti-HA (1:2000) followed by a HRP-conjugated goat anti-rabbit antibody (1:30 000). Lane 1: pDisplay, Lane 2: BCCV G1 (expected MW of 72 kDa) and Lane 3: BCCV G2 (54 kDa).

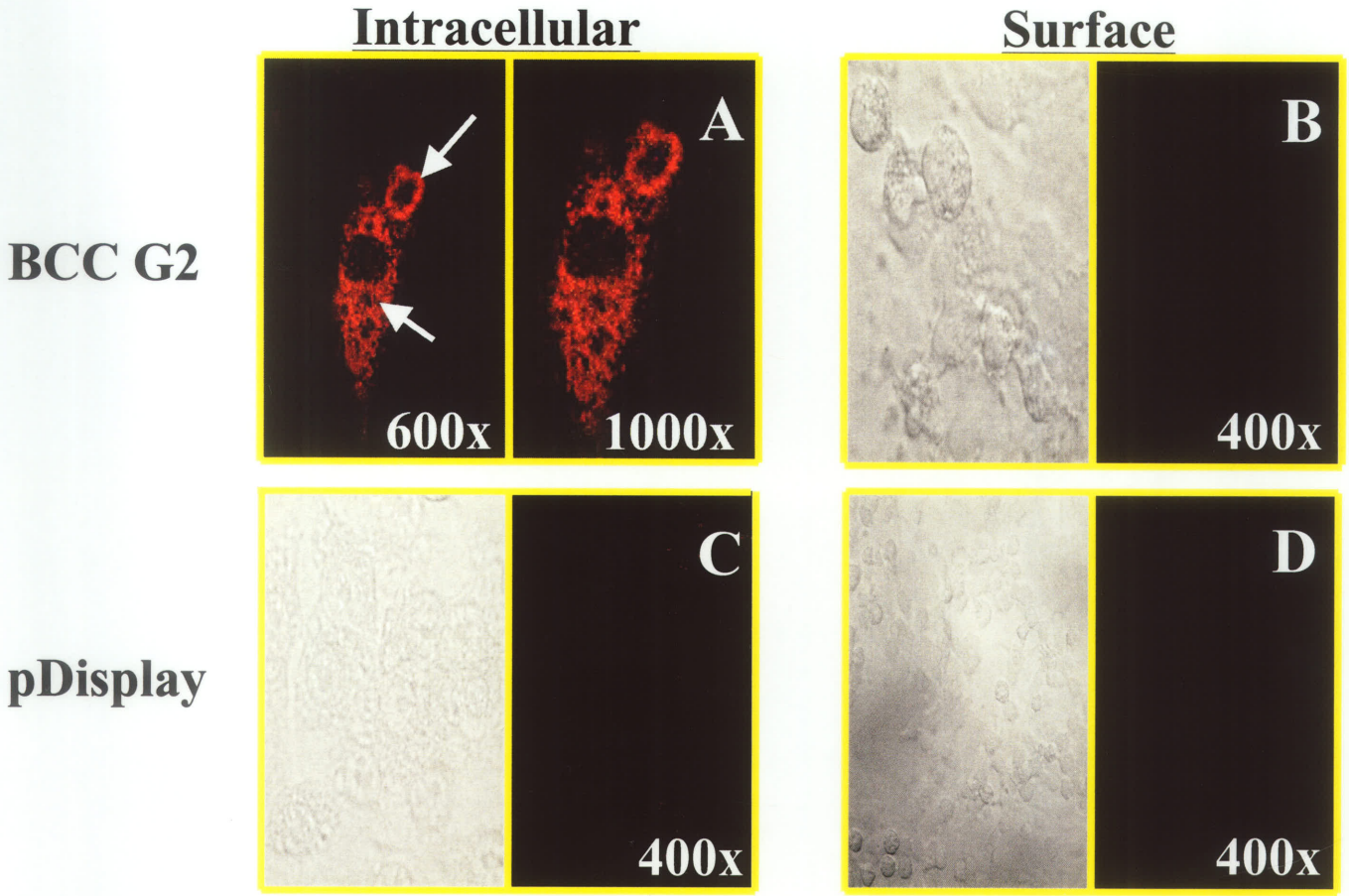

Figure 2: Intracellular expression of BCCV G2 confirmed by immunufluorescence. BHK-T7 cells were transfected with pDisplay BCCV G2 and fixed at 48 hrs post transfection. Cells were either permeabilized with Triton-X-100 to stain intracellular proteins or left non permeabilized to detect surface expression. BCCV G2 was detected with anti-HA (1:50), followed by Cy3-conjugated goat anti-rabbit antibody (1:100). Panel A: Intracellular detection of BCCV G2 in the ER (red stain surrounding the nucleus indicated by the arrows) at 600x and 1000x magnification (60x and 100x objective, 10x ocular), Panel B: BCCV G2 was not detected on the surface of BHK-T7 cells, Panels C and D: pDisplay was used as a negative control. Brightfield pictures have been included for cells which were negative under UV illumination.

Under UV illumination, BCCV G2 showed a typical ER pattern (staining around the nucleus) with the intracellular stain (Figure 9A). BCCV G2 was not found on the cell surface with a surface stain (Figure 9B). pDisplay was transfected as a negative control (Figure 9C & D). Brightfield pictures have been included to demonstrate that cells were present even though they were negative under UV illumination.

In contrast, pDisplay BCCV G1 could not be detected by IFA, thereby confirming the negative results obtained by immunoblot analysis.

3.1.2 Confirmation of expression by *in vitro* transcription and translation

Since detection of expression of BCCV G1 in mammalian cells (*in vivo*) could not be achieved by immunoblot or IFA, it was crucial to determine if expression of the protein was even possible *in vitro*. To determine if the construct had the potential to be transcribed and translated, the construct was introduced into an *in vitro* transcription and translation kit (Promega). Autoradiography detection revealed the presence of both BCCV G1 (72 kDa) and BCCV G2 (54 kDa) (Figure 10, lanes 1 and 2 respectively) indicating that the open reading frame had been correctly inserted. pDisplay was used as a negative control (Figure 10, lane 3).

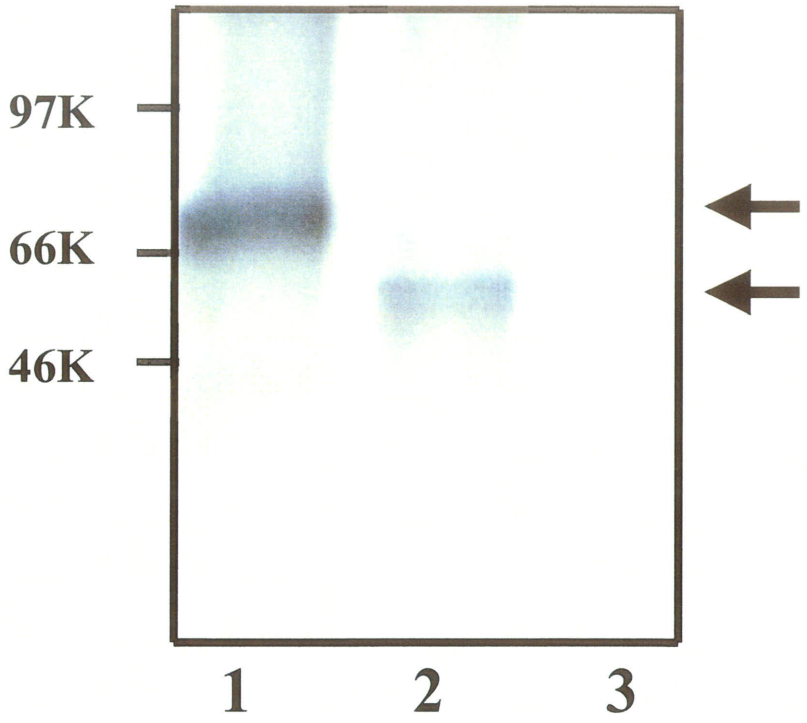

Figure 10: Expression of BCCV G1 and BCCV G2 confirmed by *in vitro* transcription and translation and detected by autoradiography. Lane 1: BCCV G1 (72 kDa), Lane 2: BCCV G2 (54 kDa) and Lane 3: pDisplay (negative control).

3.1.3 Characterization of BCCV G2 carbohydrates

IFA data suggested that BCCV G2 was located in the ER. To further confirm this subcellular location, cell lysates of BHK-T7 transfected cells were treated with endoglycosidase H and N-glycosidase F, then run on a 15% SDS-PAGE. Proteins were detected by immunoblot using an anti-HA antibody (1:2000) followed by a goat anti-rabbit HRP antibody (1:30 000). Treatment with endo H preferentially hydrolyzes N-glycans of the high mannose type; this type of glycosylation is normally found with ER localized glycoproteins (Figure 11A). In comparison, N-glycosidase F cleaves all types of asparagine bound N-glycans (complex type and high mannose type) (Figure 11B). The combined use of both endoglycosidases will allow to define the subcellular localization of a glycoprotein in either the ER or the Golgi complex. Treatment of BCCV G2 with endo H and N-glycosidase F demonstrated a shift of almost 3 kDa, which is the expected shift for the removal of one asparagine-linked sugar on G2 (Figure 11C and D). The sensitivity to endo H and N-glycosidase F indicated a high mannose type carbohydrate on BCCV G2 which is indicative of a protein located in the ER, which confirms the IFA data (Figure 9).

3.2 Expression of BCCV G1 and G2 using the SFV expression system

Since expression of BCCV G1 was not achieved using the pDisplay clones, the Semliki Forest virus expression system was used as an alternative route for expression to overcome this problem.

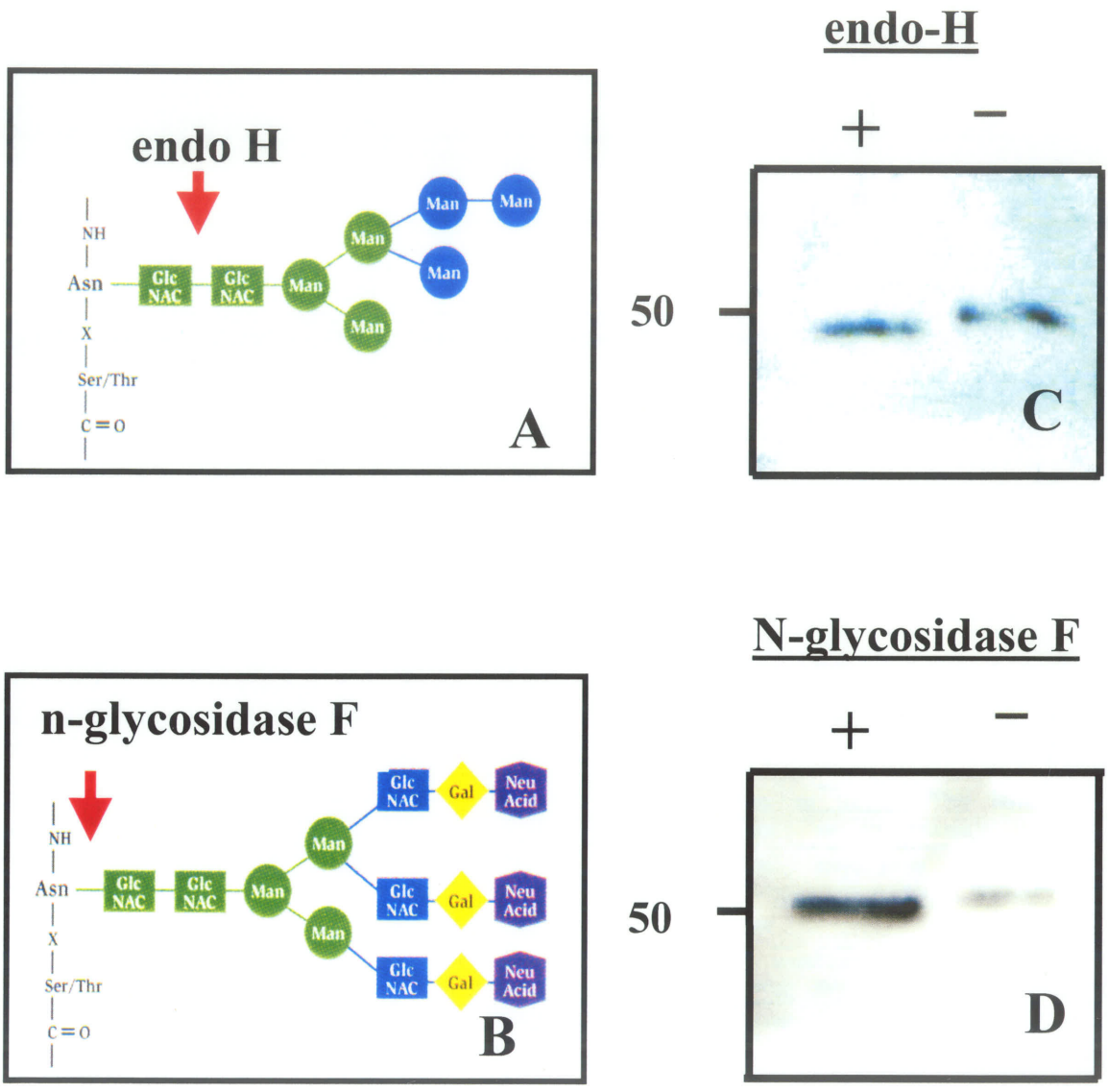

Figure 11: Characterization of BCCV G2 using endoglycosidase H and N-glycosidase F. Panels A and B demonstrate the cleavage site of both enzymes denoted by the arrows (Invitrogen). BHK-T7 cells were transfected with pDisplay BCCV G2 and harvested at 48 hours post transfection, then treated with endo H and N-glycosidase F. Proteins were run on 15% SDS-PAGE and detected by immunoblot using anti-HA (1:2000) followed by goat anti-rabbit HRP (1:30 000). Panel C: an expected shift (3 kDa) is seen for BCCV G2, demonstrating endo H sensitivity which is confirmed by N-glycosidase F treatment (Panel D).

3.2.1 Confirmation of infection of BHK-21 cells with SFV BCCV G1 and SFV BCCV G2 by immunoblot and IFA

BHK-21 cells were infected with either recombinant SFV BCCV G1 virus or recombinant SFV BCCV G2 virus. CPE was observed between 16 to 24 hours post infection. CPE was characterized by rounding of cells and detachment from the monolayer. Infected cells were treated with 50 μg/ml of cycloheximide for 5 hours then harvested at 24 hours post infection. The purpose of adding cycloheximide was to inhibit eukaryotic protein synthesis by preventing initiation and elongation on 80S ribosomes (Lackie *et al.*, 1999). It was hypothesized that the addition of cycloheximide would help generate a clearer result as to where the proteins were accumulating. Harvested cells were run on 10% SDS-PAGE followed by an immunoblot using anti-HA (1:2000) followed by a goat anti-rabbit HRP antibody (1: 30 000). Immunoblot results revealed the presence of BCCV G2 (54 kDa) but not BCCV G1 (Figure 12, lanes 3 and 1 respectively). The negative control included uninfected cells which had the same treatment as the other samples (Figure 12, lane 2). A positive control [recombinant SFV CCHF (Crimean Congo Hemorrhagic Fever) G2 virus] was included as a infection and immunoblot control which was successful (data not shown).

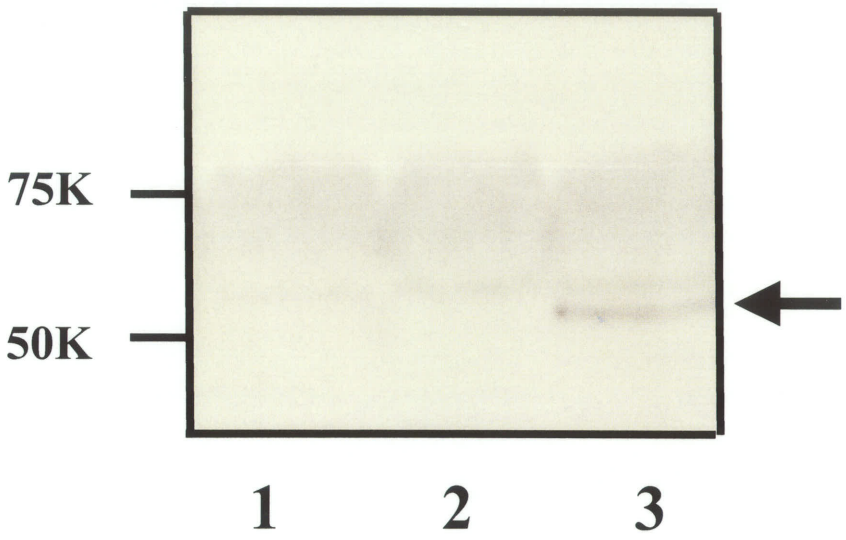

Figure 12: Immunoblot of BHK-21 cells infected with SFV BCCV G1 and SFV BCCV G2. Infected cells were treated with 50ug/ml of cycloheximide for 5 hours then harvested at 24 hours post infection. Recombinant proteins were detected with rabbit anti-HA antibody (1:1000) and goat-anti-rabbit HRP antibody (1:30 000). Lane 1: BCCV G1 (could not be detected at 72 kDa), Lane 2: Negative control (uninfected cells with same treatment) and Lane 3: BCCV G2 (detected at 54 kDa, arrow).

Further confirmation of expression was determined by IFA. Infected BHK-21 cells with SFV BCCV G1 or SFV BCCV G2 were positive using anti-HA (1:50) followed by a FITC-conjugated goat anti-rabbit antibody (1:100) in an intracellular IFA. Surprisingly, and in contrast to the immunoblot data, expression of BCCV G1 could be demonstrated. Staining of SFV BCCV G1, either with or without cycloheximide treatment appeared as a cap on the nucleus, suggestive of a Golgi stain (Figure 13A & B). In comparison, staining of SFV BCCV G2, either with or without cycloheximide appeared as either a ring around the nucleus or as clumps, which did not correlate with either an ER or Golgi pattern (Figure 13C & D). Thus, the subcellular localization of BCCV G2, expressed through a recombinant SFV remained unclear. The negative controls included uninfected cells with the same treatment (Figure 13E & F). The negative controls did show some fluorescence which can be attributed to either the secondary antibody binding non specifically to the cells or due to the auto-fluorescence of the cells under UV illumination.

3.2.2 Co-localization studies using double immunofluorescence

To confirm the subcellular location of SFV BCCV G1 and SFV BCCV G2 in infected BHK-21 cells, double immunofluorescence was performed. Infected cells were permeabilized with Triton X-100 and then incubated with FITC-conjugated anti-HA (1:50) in conjunction with either anti-giantin (for BCCV G1, 1:1000). Following the incubation with the primary antibody, a Cy3-conjugated goat anti-rabbit antibody (1:100) was added to detect anti-giantin.

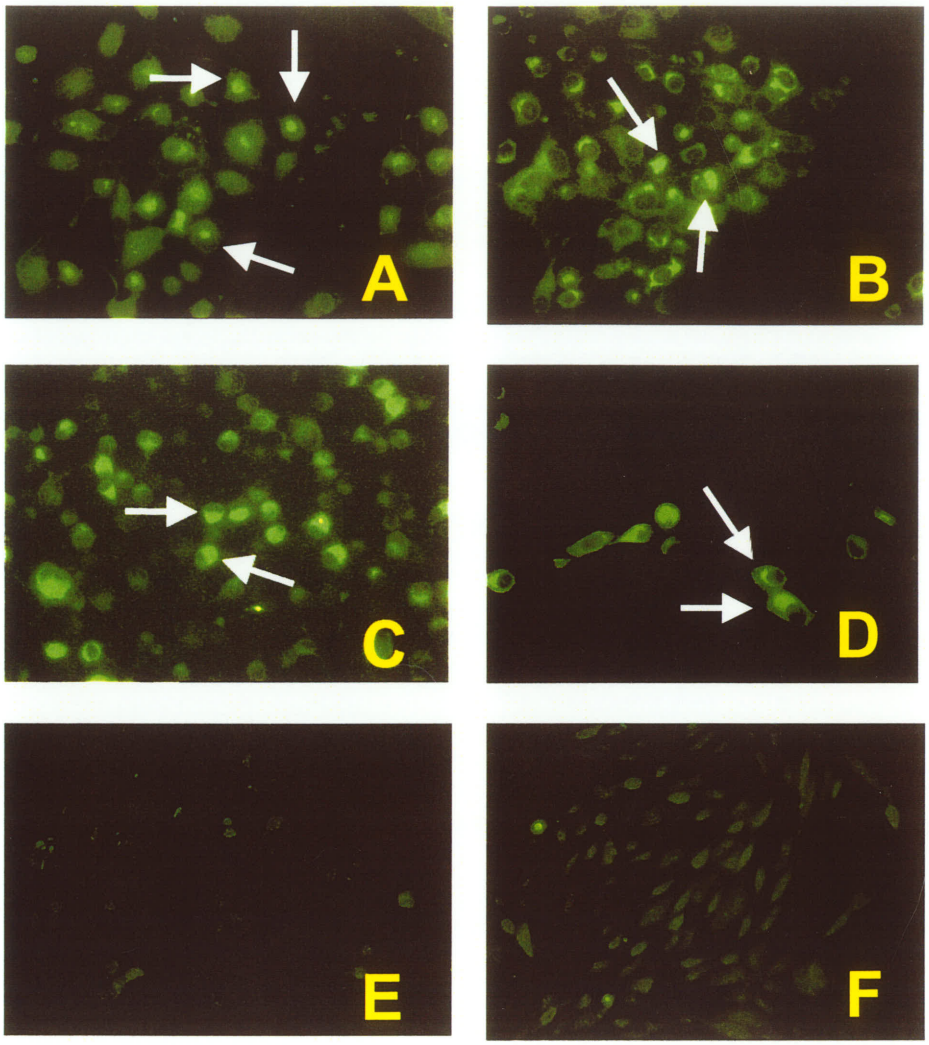

Figure 13: Infection of BHK-21 cells with recombinant SFV BCCV G1 and SFV BCCV G2 viruses. BHK-21 cells were infected with recombinant SFV BCCV G1 or G2 and at 24 hours post infection, cells were fixed with 2% paraformaldehyde. Fixed cells were permeabilized and treated with anti-HA (1:50) followed by a FITC-conjugated goat anti-rabbit antibody (1:100). (A) BCCV G1 expression without cycloheximide treatment showed a Golgi pattern (bright green clumps within the cells indicated by the arrows), (B) BCCV G1 expression with cycloheximide treatment. Cells were treated with 50 ug/ml of cycloheximide for 5 hours prior to fixation at 24 hours post infection, (C) BCCV G2 expression without cycloheximide (intracellular localization is unclear, arrows), (D) BCCV G2 expression with cycloheximide treatment. Cells were treated with 50ug/ml of cycloheximide for 5 hours prior to fixation at 24 hours post infection, (E) negative control (uninfected cells with same treatment as in A and C), (F) negative control with cycloheximide treatment. Note: please see figure 18 for presentation of a typical Golgi stain.

Co-localization of BCCV proteins with the Golgi or ER markers was determined by confocal microscopy. Giantin is a membrane-inserted component of the cis and medial Golgi with a large rod-like cytoplasmic domain.

Figure 14 demonstrates the co-localization studies of SFV BCCV G1 and giantin. Despite the presence of a similar pattern in the anti-HA and anti-giantin images, a clear merge image could only be achieved for some cells, suggesting that there is small amount of co-localization between SFV BCCV G1 and giantin. Despite many attempts at using different Golgi markers and dilutions, a more convincing co-localization was never demonstrated.

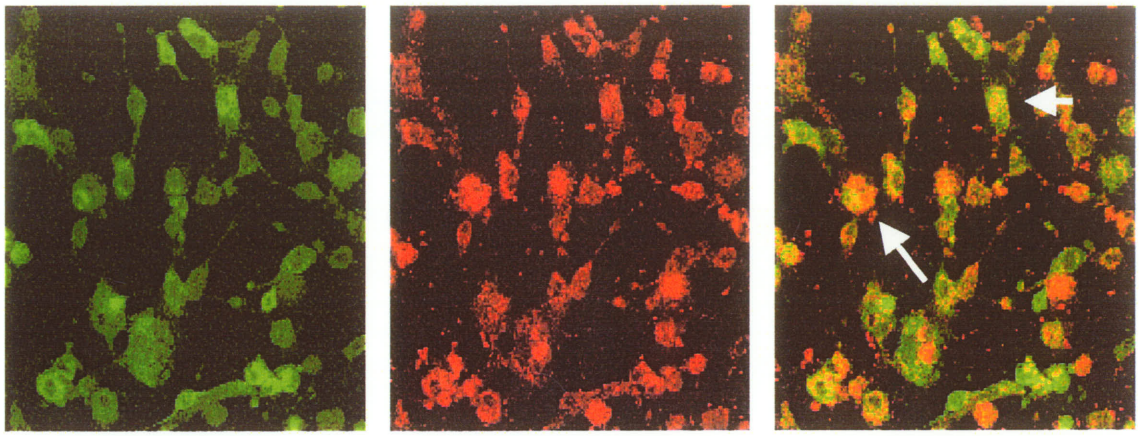

Figure 14: Co-localization studies of SFV BCCV G1 and giantin. BHK-21 cells infected with recombinant SFV BCCV G1 were fixed with 2% paraformaldehyde at 24 hours post infection, then permeabilized with Triton X-100. Cells were double-stained with FITC-conjugated anti-HA (1:50) and anti-giantin (1:1000). Anti-giantin was detected with goat-anti-rabbit Cy3 (1:100). Co-localization was determined using confocal microscopy (40x). Staining for BCCV G1 and giantin may not reflect a typical Golgi pattern (distinct round clumps within the cell) since SFV may alter cellular morphology. Areas of weak co-localization are shown with arrows in the merge image.

3.3 Expression of GFP-hantaviral glycoprotein fusion proteins

As expected, expression of the full-length BCCV glycoproteins appeared to be difficult. Since our previous studies on the HTNV glycoproteins suggested an important role for the G1 cytoplasmic tail in subcellular targeting, GFP fusion proteins with specific BCCV G1 domains was analyzed next.

3.3.1 Analysis of protein hydrophilicity for BCCV G1/G2, HTNV G1/G2 proteins and INFV hemagglutinin protein using Kyte and Doolittle Analysis

In order to more precisely define and confirm previous data on the different domains of hantavirus glycoproteins, hydrophobicity/hydrophilicity plots were performed. Predictions were calculated using methods derived from Kyte and Doolittle (Kyte & Doolittle, 1982) (Figures 15 and 16). Kyte and Doolittle values fall within a range of +4 to -4, with hydrophilic residues having a negative score and hydrophobic residues having a positive score (Kyte & Doolittle, 1982). Based on this calculation, the BCCV domains which were required for the construction of the GFP-fusion proteins were defined as follows:

G1 cytoplasmic domain:	aa 540-647
G2 signal peptide	aa 648-671
G2 cytoplasmic domain:	aa 1150-1159

Once the domains were defined, the different GFP-hantaviral glycoprotein fusion protein constructs were made (Figure 17) for expression and characterization of subcellular localization.

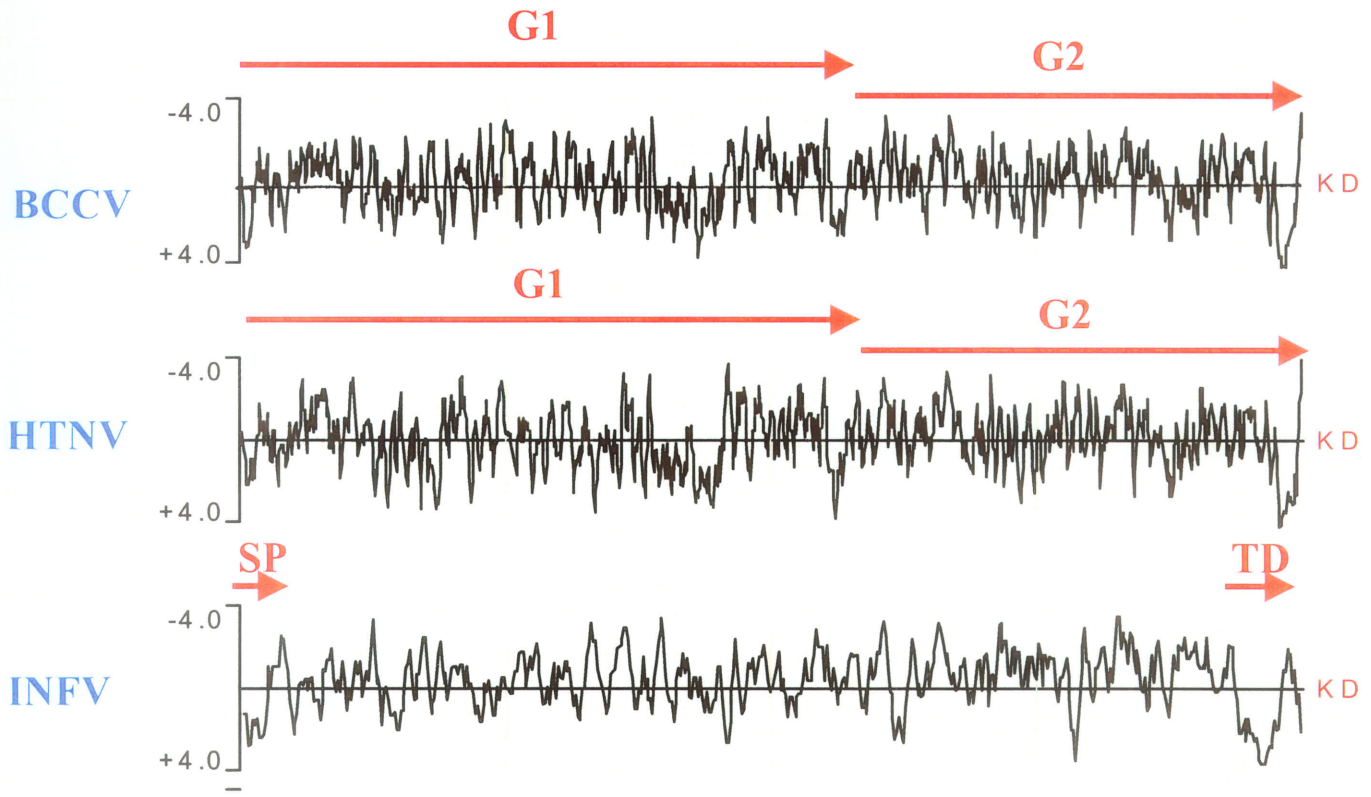

Figure 15: Kyte and Doolittle (KD) hydrophilicity plots comparing BCCV G1/G2, HTNV G1/G2 and INFV SP and TD. Values above the axis represent hydrophilic amino acids and values below the axis line represent hydrophobic amino acids. Amino acids corresponding to G1, G2, SP or TD regions have been illustrated above with an arrow.
SP: signal peptide, TD: transmembrane domain

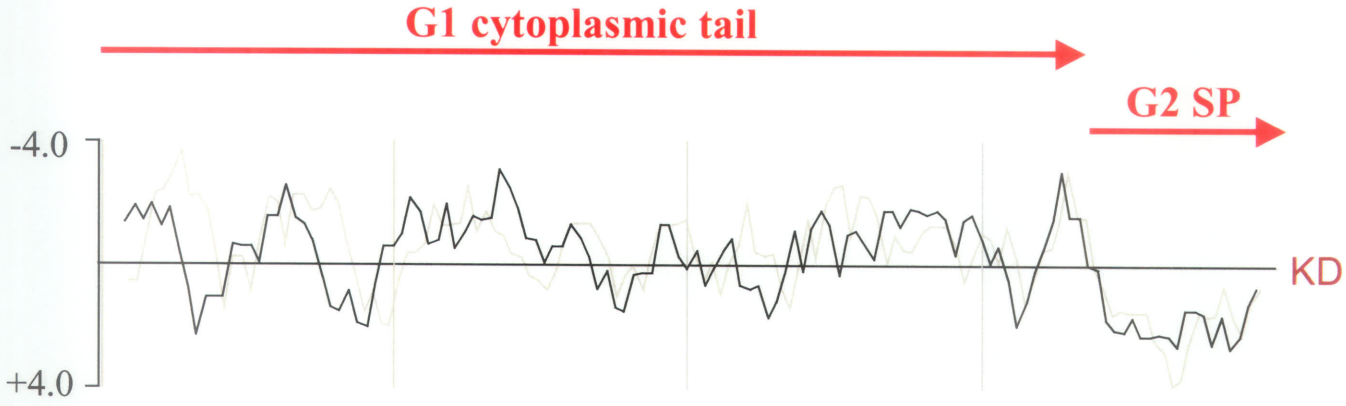

Figure 16: Kyte and Doolittle (KD) hydrophilicity plot comparing BCCV G1 cytoplasmic tail (black line) and HTNV G1 cytoplasmic tail (grey line). Located at the C terminus of the cytoplasmic tail is a G2 hydrophobic transmembrane domain which serves as a G2 signal peptide (Loeber *et al.*, 2001). Values above the axis represent hydrophilic amino acids and values below the axis line represent hydrophobic amino acids. Amino acids corresponding to the G1 cytoplasmic tail and G2 SP have been illustrated above with an arrow

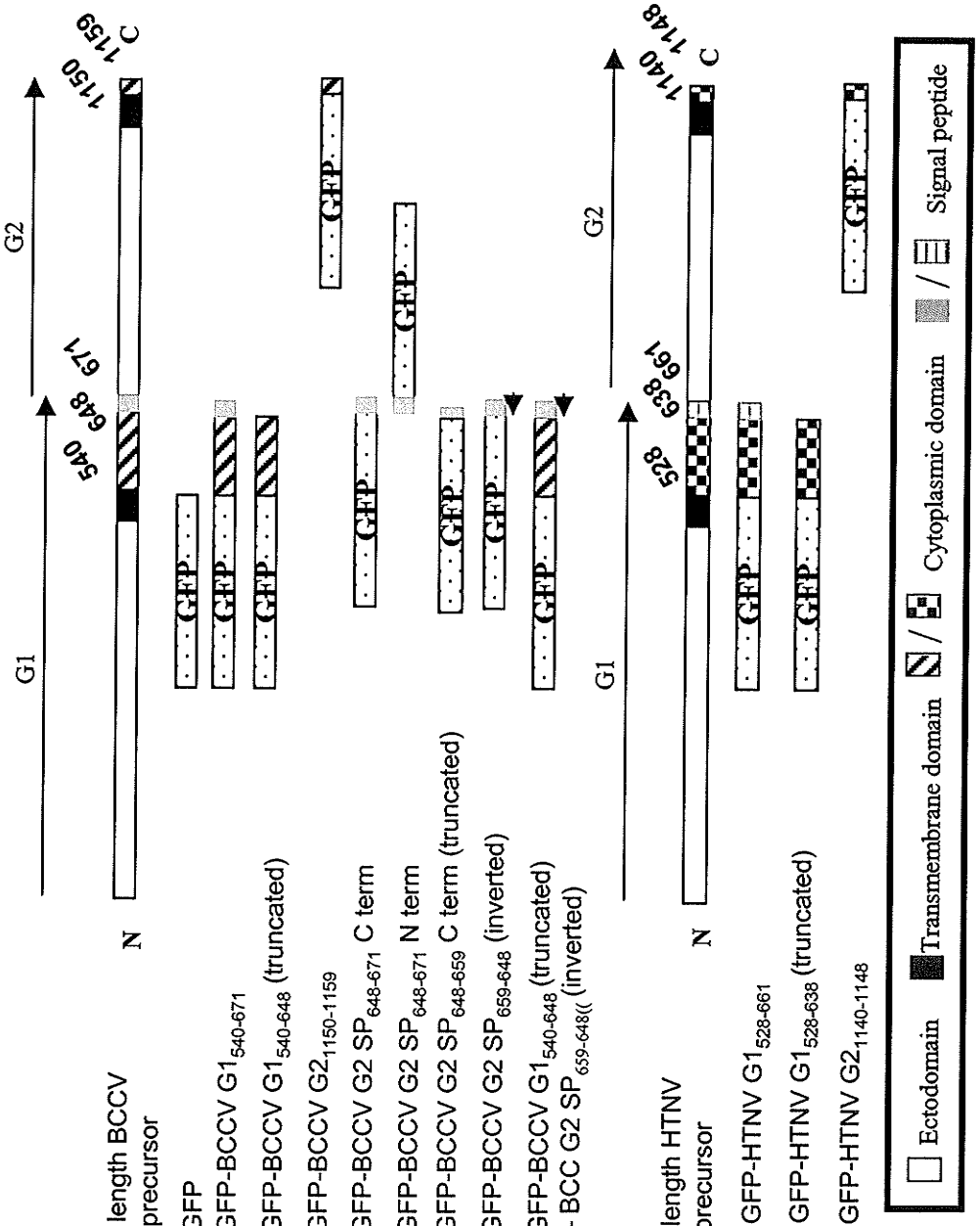
Full length BCCV precursor
1 GFP
2 GFP-BCCV G1540-671
3 GFP-BCCV G1540-648 (truncated)
4 GFP-BCCV G21150-1159
5 GFP-BCCV G2 SP648-671 C term
6 GFP-BCCV G2 SP648-671 N term
7 GFP-BCCV G2 SP648-659 C term (truncated)
8 GFP-BCCV G2 SP659-648 (inverted)
9 GFP-BCCV G1540-648 (truncated) – BCC G2 SP659-648(((inverted)
Full length HTNV precursor
10 GFP-HTNV G1528-661
11 GFP-HTNV G1528-638 (truncated)
12 GFP-HTNV G21140-1148
G1
G2
N
C
540
648
671
1150
1159
528
638
661
1140
1148
GFP
Ectodomain
Transmembrane domain
Cytoplasmic domain
Signal peptide

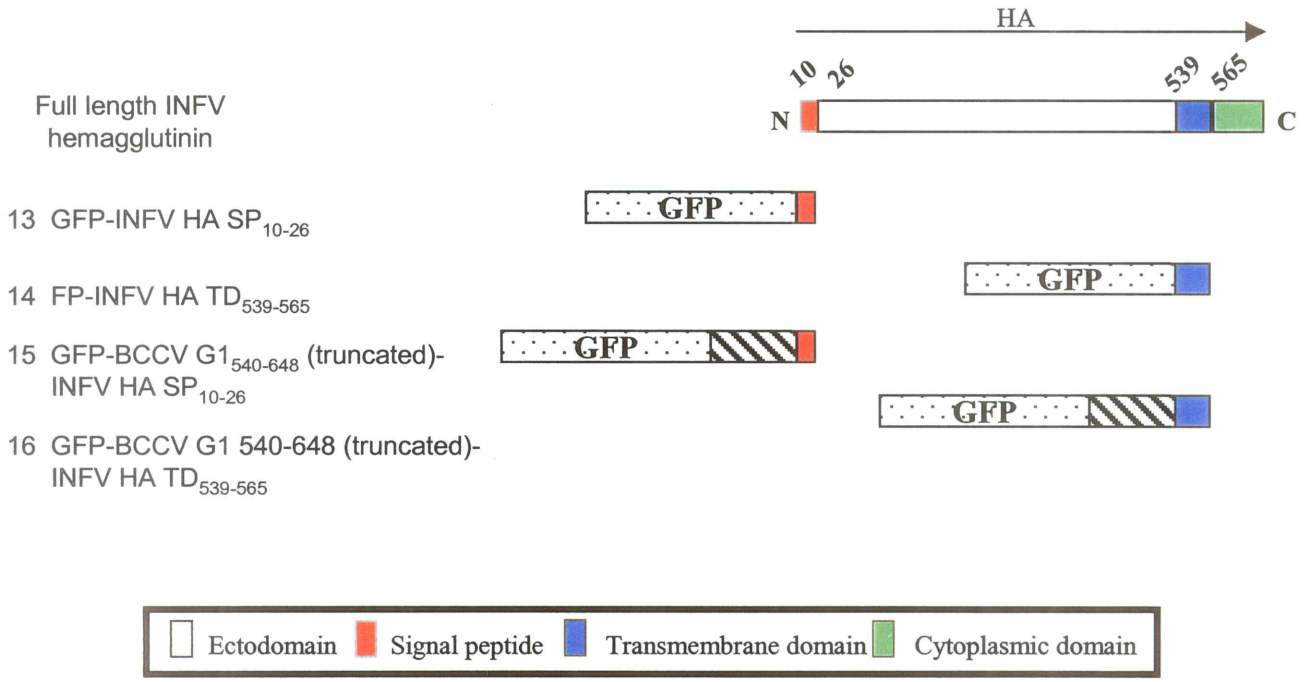

Figure 17: Construct summary of GFP-hantaviral glycoprotein fusion protein constructs. Construct numbers are on the left followed by the construct name (amino acids of the fused proteins are included) and schematic representation. The BCCV GPC and INFV HA numbering is in accordance with the aminoacid sequence deposited into Genbank (L39950 and M55059, respectively).

3.3.2 Characterization of GFP-hantaviral glycoprotein fusion proteins in 293T cells by UV microscopy and membrane fractionation

293T cells were transfected with GFP-BCCV $G1_{540-671}$ and within 24-48 hours post transfection, green clumps accumulated within the cell, characteristic of Golgi localization (Figure 18: construct 2A, the number below each figure represents the construct number). In comparison, 293T cells transfected with GFP-BCCV $G2_{1150-1159}$ showed diffuse expression throughout the cell, indicative of cytoplasmic expression, similar to the GFP control (Figure 18: constructs 4A and 1A, respectively).

Membrane fractionation was performed on transfected 293T cells to determine if the fusion proteins were membrane associated or found in the cytosol. Transfected cells were collected and separated into a supernatant fraction, representing cytosolic proteins and a membranous fraction, representing membrane associated proteins. Fusion proteins were detected by immunoblot using an anti-GFP antibody (1:2000) followed by a HRP-conjugated goat anti-rabbit antibody (1:30 000). GFP-BCCV $G1_{540-671}$ was detected in the pellet fraction, while GFP-BCCV $G2_{1150-1159}$ was detected in the supernatant fraction similar to the control (Figure 18: 2B and 4B, respectively). This data demonstrated that GFP-BCCV $G1_{540-671}$, which contained the BCCV G1 cytoplasmic tail, was targeted to a membranous compartment (most likely Golgi membranes), as confirmed by UV microscopy and membrane fractionation. In contrast, GFP-BCCV $G2_{1150-1159}$ which contained the BCCV G2 cytoplasmic tail did not contain a Golgi targeting signal since the expression of the fusion protein remained cytoplasmic.

To assess whether the cytoplasmic tails of OW and NW hantaviruses behaved similarly, 293T cells were transfected with GFP-HTNV $G1_{528-661}$.

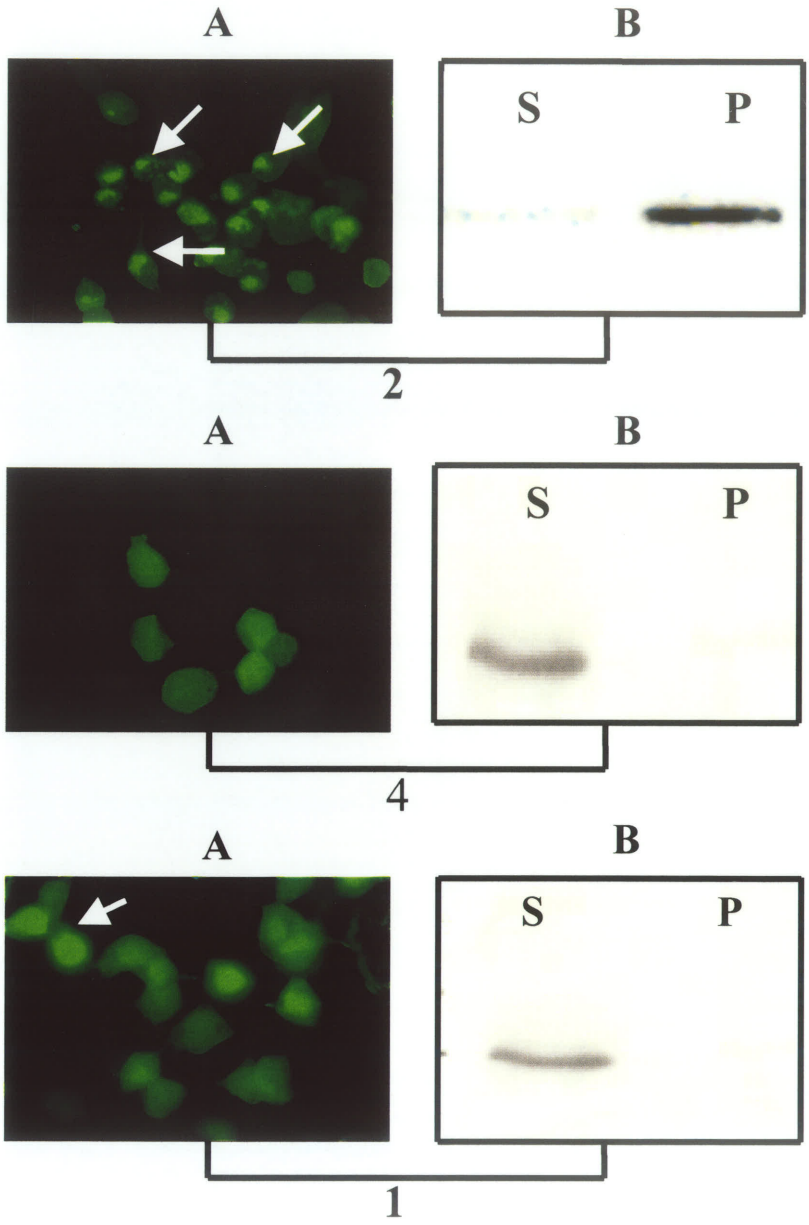

Figure 18: Intracellular localization of GFP-hantaviral glycoprotein fusion proteins by UV microscopy (100x) and membrane fractionation. 293T cells were transfected with individual constructs and viewed at 24 hours post transfection (Panel A) or membrane fractionation was performed 46 -72 hours post transfection to determine if fusion proteins were membrane associated (pellet fraction – P) or cytosolic (supernatant fraction – S) (Panel B). The number below each figure represents the construct number. 2: GFP-BCCV $G1_{540\text{-}671}$, 4: GFP-BCCV $G2_{1150\text{-}1159}$, 1: GFP. Panel 2A shows characteristic Golgi staining (bright green clumps within the cell) indicated by the arrows, which are membrane associated (2B). Panels 4A and 1A illustrate proteins with a typical cytoplasmic staining (diffuse staining throughout the cell) which are found in the supernatant fraction (4B and 1B). Some cells may appear brighter than others due to the different expression rates of GFP and due to the high sensitivity of the microscope/camera system (panel 1A, arrow).

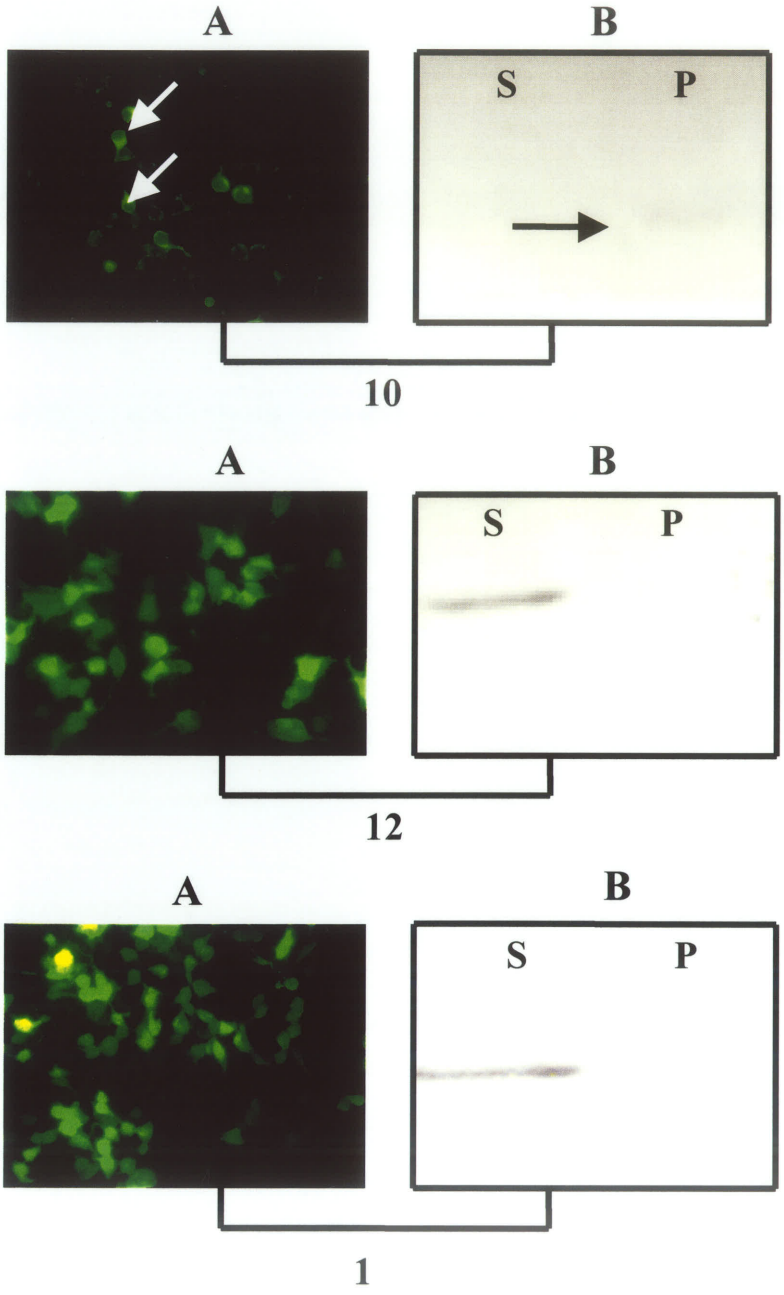

Figure 19: Intracellular localization of GFP-hantaviral glycoprotein fusion proteins by UV microscopy (40x) and membrane fractionation as described in Figure 18.
10: GFP-HTNV $G1_{528\text{-}661}$ was localized in the Golgi (10A, arrows) and GFP-HTNV $G1_{528\text{-}661}$ protein was membrane associated (arrow in 10B);
12: GFP-HTNV $G2_{1140\text{-}1148}$ showed cytoplasmic staining (12A) and was found in the supernatant fraction (12B); 1: GFP (control) showed cytoplasmic staining (1A) and was found in the supernatant fraction (1B).

Expression of GFP-HTNV $G1_{528-661}$ which contained the HTNV G1 cytoplasmic tail, resulted in clear cellular accumulations which were membrane associated (Figure 19: 10A) In comparison, GFP-HTNV $G2_{1140-1148}$ showed cytoplasmic staining (Figure 19: 12A), identical to that of GFP (Figure 19: 1A) indicating that the HTNV G2 cytoplasmic tail had no targeting signal. Thus, BCCV behaves similarly to HTNV, an OW hantaviruse.

Anheier *et al* ., (submitted) suggested that Golgi targeting of HTNV G1 was dependent on the HTNV G2 SP (23 amino acids), a hydrophobic domain after which co-translational cleavage of the GPC occurs. Knowing that GFP-BCCV $G1_{540-671}$ behaved in a similar manner to GFP-HTNV $G1_{528-661}$ (Figure 18 & 19), the BCCV G2 SP (23 amino acids) was removed from BCCV G1 cytoplasmic tail to test whether it was responsible for Golgi targeting. A construct was made which lacked the 23 aa hydrophobic BCCV G2 SP, termed GFP-BCCV $G1_{540-648}$ (truncated) (Figure 20: construct 3). Following transfection of 293T cells with this construct, a cytosolic pattern of expression was observed and the fusion protein was detected in the supernatant fraction (Figure 20: 3A & B). However, a small percentage (30%) of transfected cells showed green clumps suggesting that some Golgi targeting was still occurring despite the removal of the BCCV G2 SP (not shown in Figure 20: 3A). In comparison, removal of the HTNV G2 SP from the HTNV G1 cytoplasmic tail, termed GFP-HTNV $G1_{528-638}$ (truncated) (construct 11), resulted in complete abolishment of the Golgi targeting signal since 100% of cells showed a cytosolic pattern of expression confirmed by the presence of the fusion protein in the supernatant fraction (Figure 20: 11A & B).

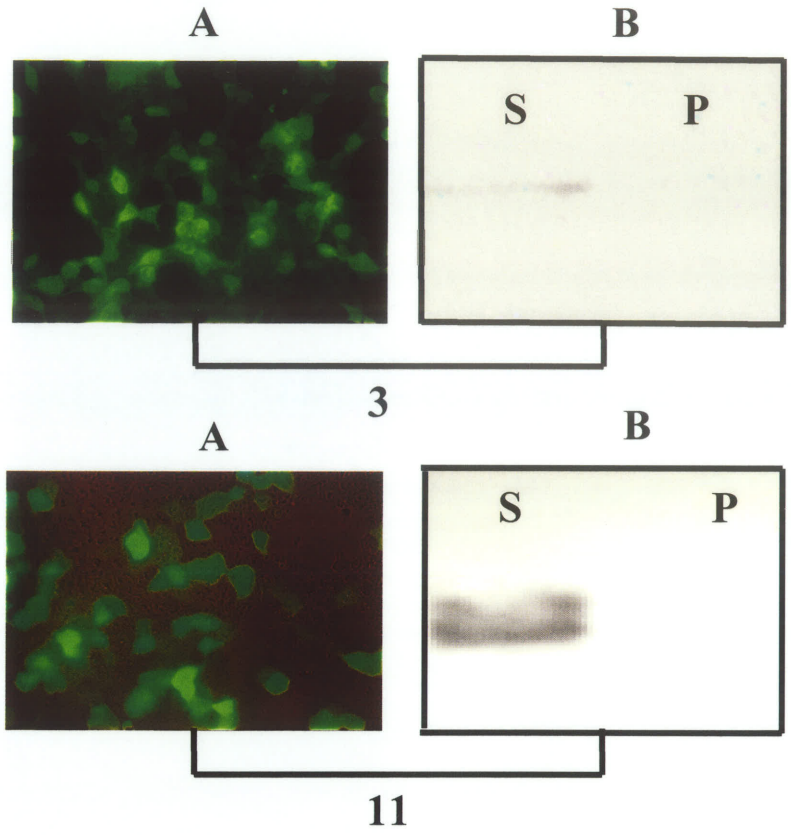

Figure 20: Intracellular localization of GFP-hantaviral glycoprotein fusion proteins by UV microscopy (40x) and membrane fractionation as described in Figure 18.
3: GFP-BCCV $G1_{540-648}$ (truncated) appeared cytoplasmic (3A) however 30% of transfected cells showed a Golgi pattern (not shown in 3A). GFP-BCCV $G1_{540-648}$ (truncated) was found in the supernatant fraction (3B); 11: GFP-HTNV $G1_{528-638}$ (truncated) appeared cytoplasmic (panel 11A) and was found in the supernatant fraction (11B). The reason for the presence of a double band in panel 11B is unknown.

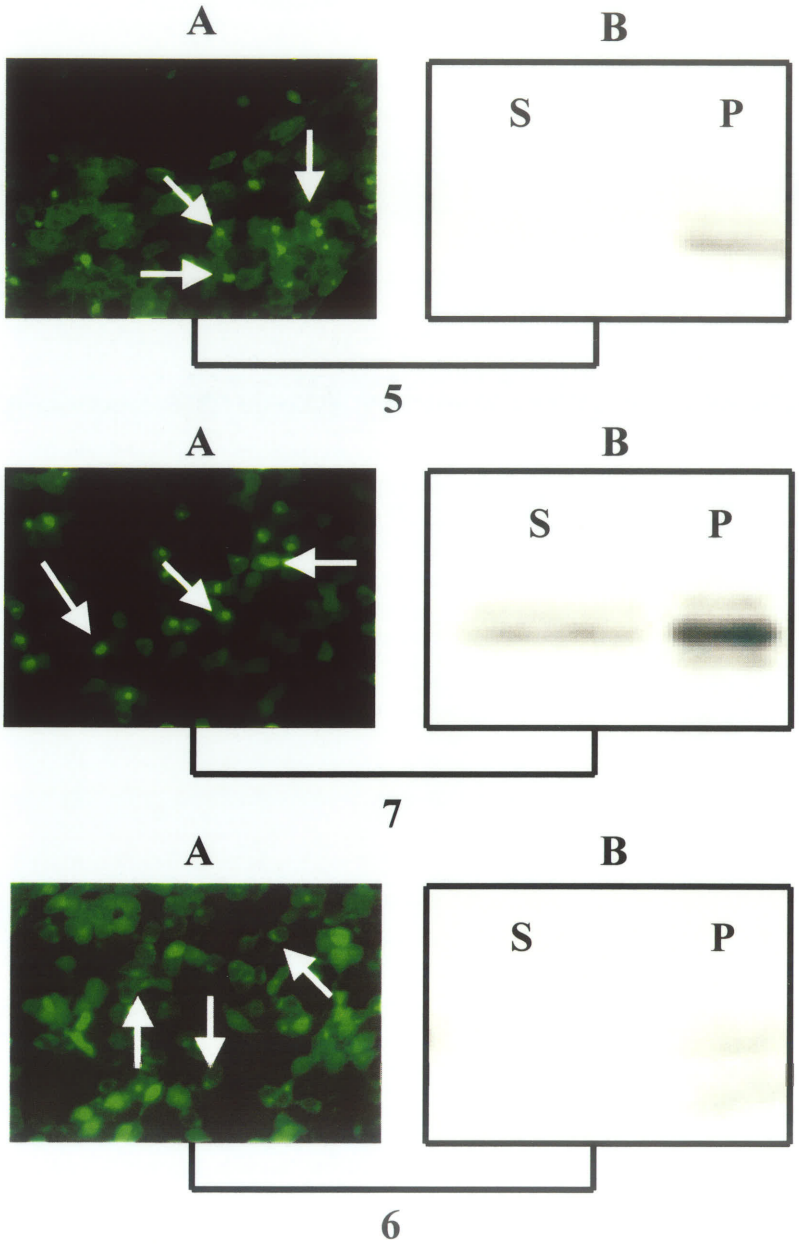

Figure 21: Intracellular localization of GFP-hantaviral glycoprotein fusion proteins by UV microscopy (40x) and membrane fractionation as described in Figure 18. 5: GFP-BCCV G2 $SP_{648-671}$ C-term protein was found in the Golgi in 50% of transfected cells (5A, arrows) and was found membrane associated (5B); 7: GFP-BCCV G2 $SP_{648-659}$ C-term (truncated) protein was found in the Golgi in 60-70% of transfected cells (7A, arrows) and was found in both the supernatant and pellet fractions (7B); 6: GFP-BCCV G2 $SP_{648-671}$ N-term protein was found in the Golgi in 50% of transfected cells (6A, arrows) but was only found in the pellet fraction (6B). The reason for the presence of a double (or triple) band in panels 5B, 7B and 6B is unknown.

To determine if the addition of BCCV G2 SP onto GFP was sufficient to confer Golgi targeting, the 23 aa hydrophobic BCCV G2 SP was cloned at the C-terminus of GFP (GFP-BCCV G2 $SP_{648-671}$ C-term) and expressed in 293T cells resulting in approximately 50% of cells showing Golgi localization (Figure 21: 5A). Although Golgi localization was only 50%, surprisingly, membrane fractionation showed the fusion protein only in the pellet fraction (Figure 21: 5B). To determine which part of the BCCV G2 SP would mediate Golgi localization, the BCCV G2 SP was truncated by removing 12 amino acids at the C terminus [GFP-BCCV G2 $SP_{648-659}$ C term (truncated)]. Addition of a truncated BCCV G2 SP (11 aa) to GFP resulted in nearly 60-70% Golgi localization (Figure 21: 7A). Membrane fractionation revealed that the majority of the fusion protein was in the pellet, while a small fraction was in the supernatant (Figure 21: 7B).

Once it was determined that the BCCV G2 SP had a Golgi targeting signal, the position of the BCCV G2 SP in relation to GFP was studied to determine if it had an effect on the localization of the fusion protein. Therefore, the 23 aa BCCV G2 SP was cloned in at the N-terminus of GFP (GFP-BCCV G2 $SP_{648-671}$ N-term) and expressed in 293T cells, resulting in Golgi localization in roughly 50% of transfected cells and the presence of the fusion protein in the pellet fraction (Figure 21: 6A & B). These results suggested that the position of the SP was not important, but rather the hydrophobicity was crucial in determining Golgi targeting.

To determine if hydrophobicity alone was sufficient to confer Golgi targeting or whether it was hantavirus sequence specific, the BCCV G2 SP was replaced with a

foreign hydrophobic sequence from influenza, specifically, the HA transmembrane domain and HA signal peptide. In addition, the sequence of the BCCV G2 SP was inverted (amino acids at the N-terminus were now at the C-terminus and vice versa) to determine if there was a specific sequence required for targeting. HA TD, HA SP and BCCV G2 SP inverted were cloned either at the C-terminus of GFP or after BCCV G1 truncated cytoplasmic tail construct. Expression of HA TD, HA SP and BCC G2 SP inverted directly on GFP (GFP-INFV HA $TD_{539\text{-}565}$, GFP-INFV HA $SP_{10\text{-}26}$, GFP-BCCV G2 $SP_{659\text{-}648}$ inverted, respectively) resulted in green clumps within the cells, characteristic of Golgi localization (Figure 22: 14A, 13A and 8A). Accordingly, the fusion proteins were found in the pellet fraction, following fractionation (Figure 22: 14B, 13B and 8B). Furthermore, addition of HA TD, HA SP and BCCV G2 SP inverted on BCCV G1 truncated cytoplasmic tail [GFP-BCCV $G1_{540\text{-}648}$ (truncated)-INFV HA $TD_{539\text{-}565}$, GFP-BCCV $G1_{540\text{-}648}$ (truncated)-INFV HA $SP_{10\text{-}26}$, GFP-BCCV $G1_{540\text{-}648}$ (truncated) – BCCV G2 $SP_{659\text{-}648}$ inverted, respectively] showed the same results (Figure 23: 16A & B, 15A & B and 9A & B), in contrast to the GFP control (Figure 18: 1A & 1B). This data suggests that hydrophobicity is the key factor in Golgi targeting for BCCV and it is not dependent on a specific sequence since a foreign sequence from influenza virus and the inverted BCCV G2 SP sequence can direct Golgi localization.

It is important to note that all studies for the GFP-hantaviral fusion proteins were carried out with and without cycloheximide (50ug/ml for 5 hours before fixation) and no difference was observed between the groups. It was hypothesized that the addition of

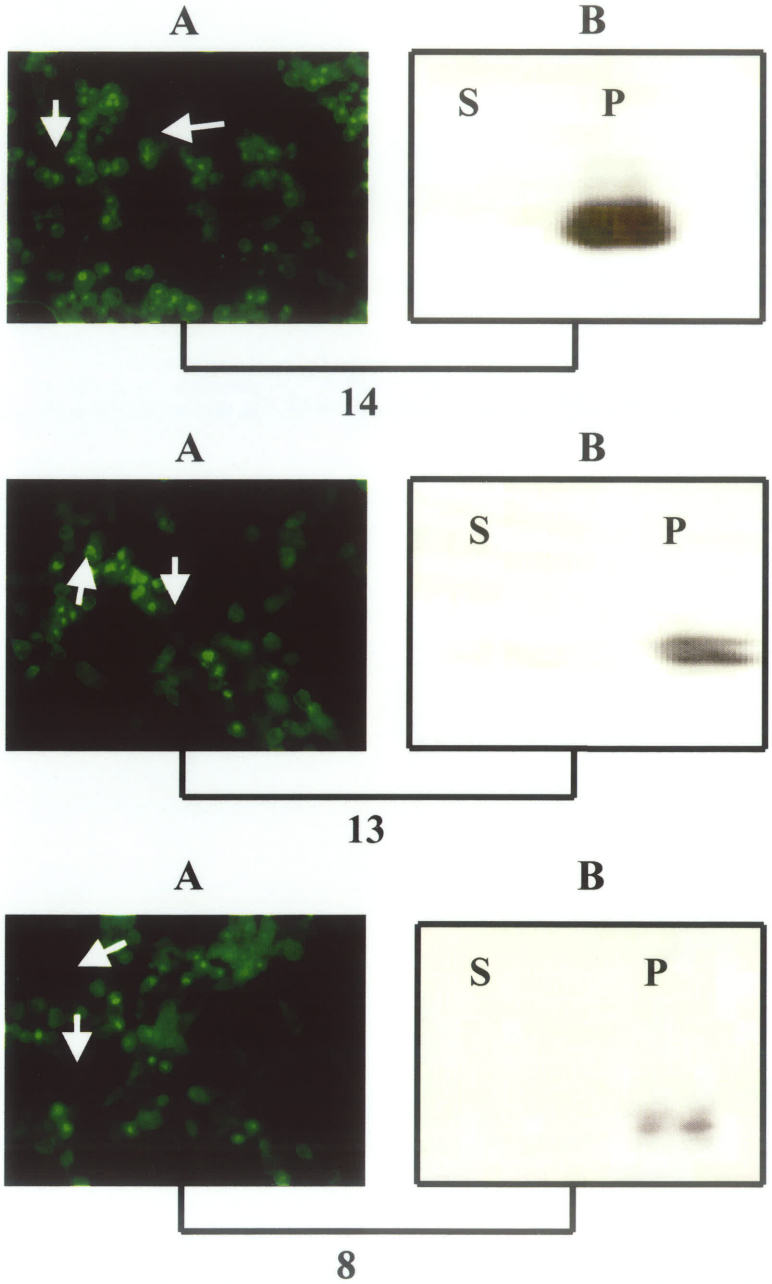

Figure 22: Intracellular localization of GFP-hantaviral glycoprotein fusion proteins by UV microscopy (40x) and membrane fractionation as described in Figure 18.
14: GFP-INFV HA $TD_{539-565}$; 13: GFP-INFV HA SP_{10-26};
8: GFP-BCCV G2 $SP_{659-648}$ inverted. Panels 14A, 13A and 8A illustrate fusion proteins which are localized in the Golgi (arrows) and that are membrane associated (14B, 13B and 8B). The reason for the presence of a double band in panel 13B is unknown.

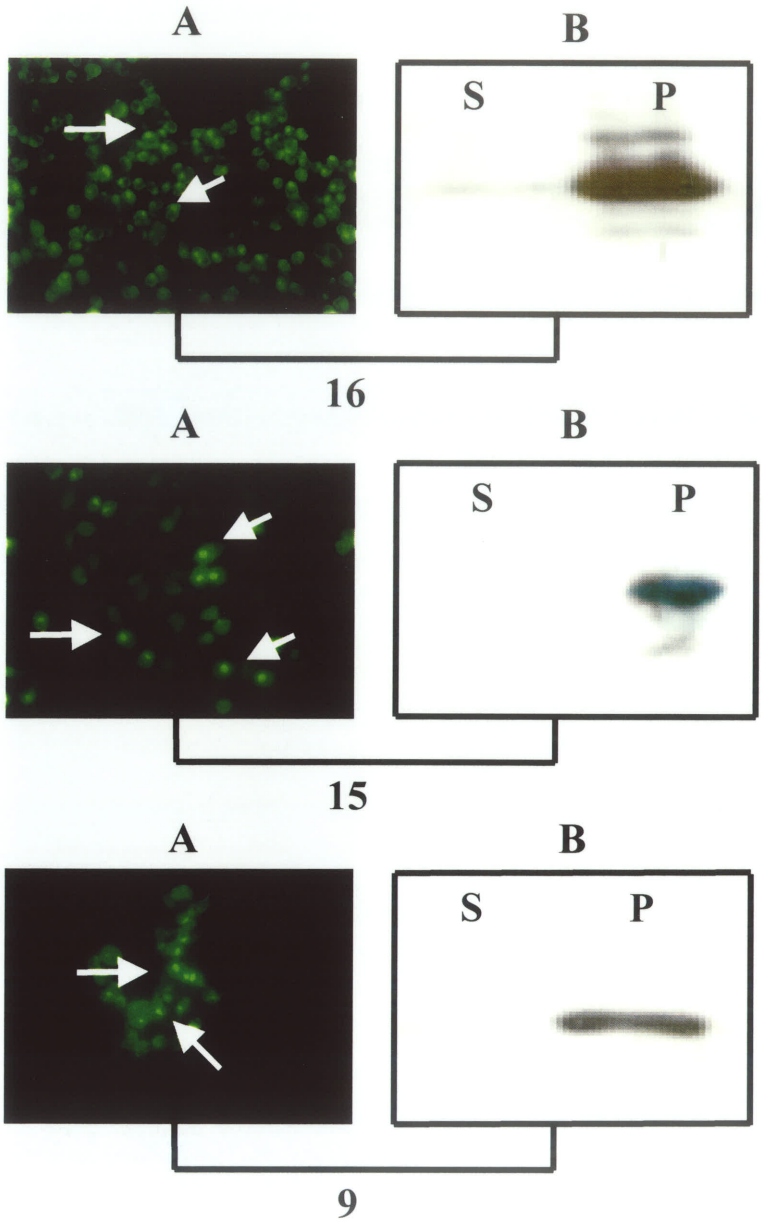

Figure 23: Intracellular localization of GFP-hantaviral glycoprotein fusion proteins by UV microscopy (40x) and membrane fractionation.
16: GFP-BCCV $G1_{540\text{-}648}$ (truncated)-INFV HA $TD_{539\text{-}565}$;
15: GFP-BCCV $G1_{540\text{-}648}$ (truncated)-INFV HA $SP_{10\text{-}26}$; 9: GFP-BCCV $G1_{540\text{-}648}$ (truncated) – BCC G2 $SP_{659\text{-}648}$ inverted. Panels 16A, 15A and 9A illustrate proteins which are localized in the Golgi (arrows) and that are membrane associated (16B, 15B and 9B). The reason for the presence of a double (triple) band in panel 16B is unknown.

cycloheximide would help generate a clearer result as to where the proteins were accumulating since protein synthesis in inhibited by this chemical.

3.3.3 Co-localization studies for GFP-hantaviral glycoprotein fusion proteins

Transfected cells were permeabilized with Triton X-100 and then incubated with either anti-giantin (1:1000). Following the incubation with the primary antibodies, a Cy3-conjugated goat anti-rabbit antibody (1:100) was added to detect anti-giantin. Co-localization of fusion proteins with the Golgi or ER markers was determined by confocal microscopy. Figure 24 shows representative co-localization data of a few GFP-hantaviral glycoprotein fusion proteins with giantin, a Golgi marker. Weak co-localization was seen for some, but not all fusion proteins where co-localization was expected. This may be attributed to the fact that the targeting of the GFP-fusion proteins occurred from the cytosolic side rather than the luminal side of the Golgi, since the proteins did not have a signal peptide to direct their entry into the secretory pathway. Since the fusion proteins were directed from the cytosolic side of the Golgi, it is likely that they would not be in the exact spatial location where the Golgi markers are commonly localized. Therefore, co-localization may not be spatially possible.

Although co-localization was demonstrated for| GFP-BCCV $G1_{540\text{-}671}$ and giantin (Figure 24), no co-localization was observed between giantin and the GFP-hantaviral glycoprotein fusion proteins which were soluble (GFP-BCCV $G2_{1150\text{-}1159}$ and GFP, Figure 24).

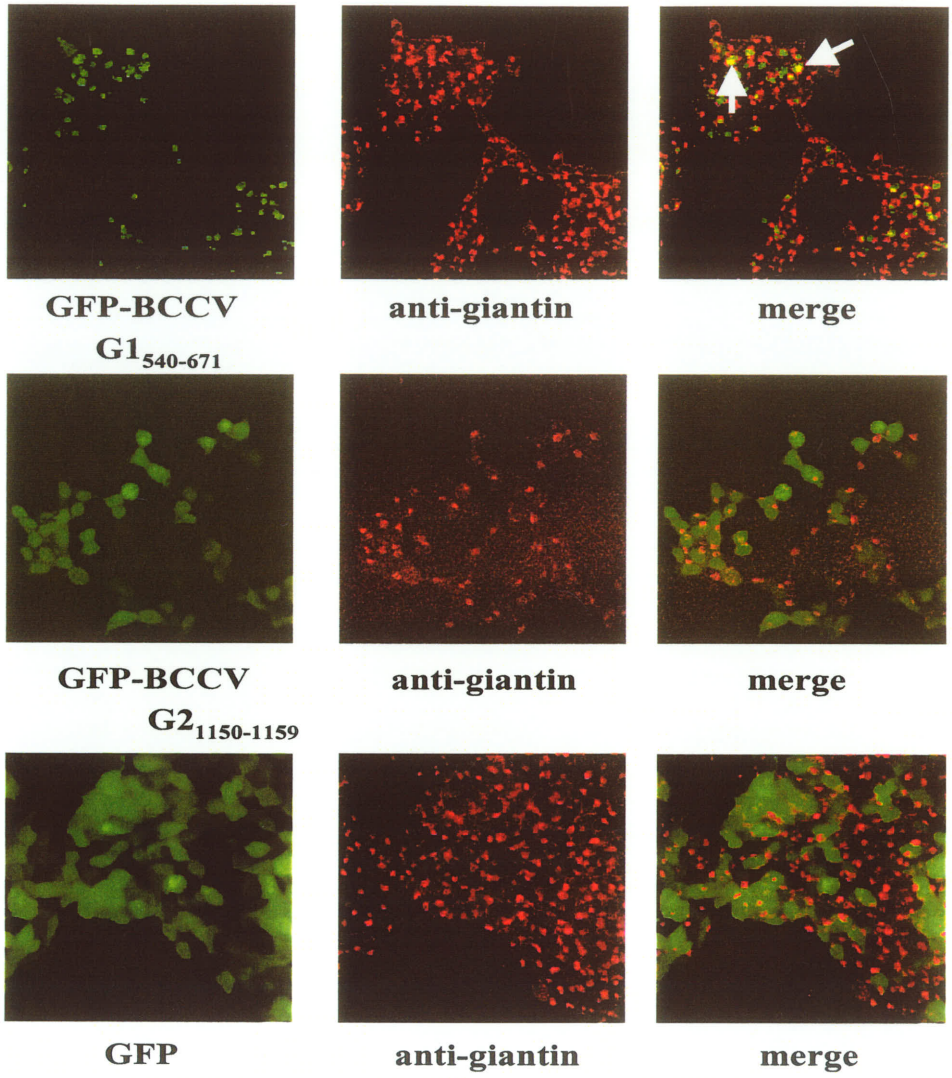

Figure 24: Co-localization studies of GFP-hantaviral glycoprotein fusion proteins with giantin. 293T cells transfected with construct were fixed with 2% paraformaldehyde at 24 hours post transfection, then permeabilized with Triton X-100. Single immunofluorescence was performed by incubating the cells with anti-giantin (1:1000). Anti-giantin was detected with goat anti-rabbit Cy3 (1:100). Co-localization was determined using confocal microscopy (40x). Expected co-localization is shown with arrows for GFP-BCCV $G1_{540-671}$ with giantin. Co-localization was not observed for either GFP-BCCV $G2_{1150-1159}$ or GFP with giantin which was expected since both fusion proteins are soluble.

4 DISCUSSION

4.1 Understanding Hantavirus Glycoprotein Expression and Targeting

The present study was established to develop an expression system for the glycoproteins of BCCV, a NW hantavirus, and to determine which subcellular compartment the glycoproteins of BCCV are targeted. The aims of this study were two-fold: first to determine if NW hantaviruses have an unique method of budding at the plasma membrane thereby verifying previous findings by Ravkov *et al.*, (1997) and secondly, to gain crucial information about the virus life cycle which could be used for the development of therapeutic strategies.

To understand NW hantavirus glycoprotein expression and targeting, two strategies were elaborated: (1) expression of BCCV G1 and G2 by transfection of recombinant plasmid DNA and by infection with recombinant SFV and (2) generation of GFP-hantaviral glycoprotein fusion proteins.

The first strategy involved using two different expression systems for the expression of the BCCV glycoproteins. BCCV G1 and G2 were cloned into a mammalian expression vector pDisplay and into a recombinant SFV expression system. Cellular localization of BCCV glycoproteins was monitored microscopically, immunologically (IFA) and biochemically (SDS-PAGE, carbohydrate analysis).

The second strategy involved creating GFP-hantaviral glycoprotein fusion proteins to test the hypothesis that a special motif either in the cytoplasmic tail of BCCV G1 or G2 or both, would harbour potential targeting signals, and thus alter the location of

GFP, a protein normally found in the cytoplasm. Subcellular localization of the GFP-hantaviral glycoprotein fusion proteins was monitored immunologically, microscopically and biochemically (membrane fractionation, SDS-PAGE, immunoblotting, IFA).

4.2 Challenges in Hantavirus Research

Several problems were encountered during this study. The initial setback was cloning the glycoprotein genes into appropriate expression plasmids. It is accepted in the hantavirus community that for unknown reasons, cloning of hantavirus genes is complex (Anheier, personal communication; Spiropoulou, 2001). The addition of approximately a dozen extra nucleotides of an unrelated sequence upstream from the start codon has allowed for easier cloning of some Hantaan virus genes (Hooper, personal communication). This strategy was also attempted for BCCV in this study, but without success.

Once the clones were obtained, expression became the next challenge with respect to BCCV G1. Despite the use of various cell lines, different transfection methods and various expression systems, BCCV G1 expression was only detected by infection with recombinant SFV (Figure 13). Lack of sufficient protein expression may be a reflection of the insensitivity of the antibodies used for detection. Accordingly, various antibody sources were tested to see of BCCV G1 could be detected by immunoblot and IFA. First, serum from a Sin Nombre virus (SNV) infected deer mouse, kindly provided by Michael Drebot (Canadian Science Centre for Human and Animal Health, Winnipeg, Manitoba) was screened to see if it would detect the glycoproteins in BCCV infected Vero E6 cells. This serum detected the nucleoprotein by immunoblot but not in IFA. The lack of

detection may be attributed to the fact that SNV antibodies do not broadly cross-react with BCCV glycoprotein epitopes.

Following this first attempt, polyclonal rabbit serum against BCCV, kindly provided by the Centers for Disease Control (Atlanta, Georgia), was used to detect the glycoproteins in infected and transfected cells. The rabbit anti-BCCV serum reacted similarly to the deer mouse serum.

As an alternate approach, mice were infected with BCCV and subsequently boostered twice with BCCV glycoprotein DNA constructs (DNA vaccination, 100 ug) to invoke a specific immune response against the BCCV glycoproteins. Again, the mouse sera only detected the nucleoprotein in an immunoblot assay but not by IFA. The fact that the deer mouse, rabbit and experimentally infected mouse sera, all preferentially detected the nucleoprotein may be due to the fact that the immune response during hantavirus infections is mainly directed against this protein (Simmons & Riley, 2002).

An additional strategy to generate BCCV glycoprotein antibodies, involved generating peptide specific antibodies. Based on the nucleotide sequences of BCCV G1 and G2, immunogenic epitopes were predicted and the corresponding peptides were synthesized by ResGen (custom antibody production, Invitrogen Corporation). The short peptides were mixed with an equal amount of Freund's Adjuvant and injected separately into two New Zealand white rabbits. Serum was harvested at weeks 4, 8 and 10 post inoculation. The G1 peptide specific polyclonal rabbit serum did not detect G1 in an immunoblot assay whereas the G2 peptide specific polyclonal rabbit serum detected BCCV G2.

Due to the lack of antibodies to detect BCCV G1, HA epitopes consisting of 9 amino acids were incorporated at the N-termini of G1 and G2. HA antibodies detected BCCV G2 (immunoblot and IFA) but only detected BCCV G1 by IFA (Figure 13). Although our group has had very good experience with the HA tag, in the future, alternate tags could be utilized such as *myc* or FLAG. In addition, a tag could be added to the C-terminus instead of the N-terminus, or incorporated at both termini and/or in multiple sets to enhance detection.

Since most attempts to express and detect BCCV G1 failed, it was necessary to confirm that the BCCV G1 construct had the potential to be transcribed and translated. To demonstrate transcription and expression of G1, the pDisplay BCCV G1 construct was introduced into an *in vitro* transcription/translation assay. Using this approach, transcription and expression was clearly demonstrated for BCCV G1 and G2 (Figure 10). The fact that G1 could be detected, suggests that the protein may be synthesized in small amounts. A lower amount of BCCV G1 protein would be directly related to a reduced copy number of mRNA transcripts coding for BCCV G1. Low levels of mRNA transcripts may be related to mRNA degradation or post-transcriptional processing such as mRNA splicing. To test this hypothesis, it would be necessary to verify levels of BCCV G1 mRNA transcripts by performing either Northern analysis, RT-PCR or conducting a ribonuclease protection assay.

4.3 BCCV G1 appears to be localized at the Golgi

BCCV G1 was cloned into pDisplay and the pSFV1 leader expression vector and expression was attempted in BHK-T7 cells and BHK-21 cells respectively. In the case of the pDisplay BCCV G1 clone, expression of G1 could not be detected by IFA or immunoblot. Many attempts at expressing BCCV G1 from the pDisplay clone were tried with no success. For example, a CMV driven T7 plasmid was co-transfected into BHK-T7 cells to increase the expression using the T7 promoter, thus increasing the expression of G1. In addition, the T7 plasmid was co-transfected into 293T cells, to allow for expression using both pDisplay promoters (CMV and T7) thus optimizing G1 expression. Despite the lack of expression *in vivo* using the pDisplay BCCV G1 clone, G1 could be synthesized *in vitro* (Figure 10).

In comparison, the expression of BCCV G1 was detected by IFA, but not confirmed by immunoblot (Figure 13 & 12), using the SFV expression system. BCCV G1 showed a Golgi pattern when detected by IFA in infected BHK-21 cells. This subcellular localization was supported when the expression of GFP-BCCV G1 cytoplasmic tail construct directed GFP to the Golgi, indicating that BCCV harboured a Golgi targeting signal. In this respect, BCCV G1 behaved similarly to HTNV G1 when expressed by itself [Pensiero and Hay, 1992; Anheir *et al.*, (submitted)]. This and the fact that plasma membrane expression could not be demonstrated do not support the work by Ravkov *et al.*, (1997).

Although BCCV G1 expression was achieved using the SFV expression system, it remained very difficult to obtain comprehensible results during the co-localization studies to confirm subcellular localization of this protein (Figure 14). However, all the data suggest that BCCV G1 is targeted to the Golgi complex, but may end up in a compartment that is different from the location of most commonly available Golgi marker proteins. Garcia-Mata *et al.*, (1999) suggest that a defined area, located in close proximity to the Golgi complex, may represent an aggresome of misfolded proteins. Another explanation for the lack of clear co-localization may be explained by the fact that SFV can alter the cellular morphology, thus, co-localization may be difficult to achieve (Flick, personal communication). This speculation is supported by IFA data for giantin, a cis-medial Golgi marker. Using anti-giantin antibodies, entire SFV infected recombinant cells were stained instead of a precise defined area (which is usually a round clump) as seen in non-infected cells. Based on these observations, it is suggested that SFV may cause either a rearrangement or alteration of the cellular organelles, resulting in abnormal organelle morphologies. Despite the alteration in cellular morphology, the SFV expression system was chosen as a last resort at BCCV G1 expression due to its high expression rate.

Preliminary and unpublished data on SNV G1 and G2 expression briefly discussed by Spiropoulou (2001) in a recent review article appear to support the findings of this study. When SNV G1 and G2 were expressed individually the proteins were located in a defined area in close proximity to the Golgi complex (Spiropoulou *et al.*, 2001, unpublished data), further supporting the lack of co-localization that was

demonstrated in the present study. Spiropoulou (2001) also indicates that there was no detection of the expressed SNV glycoproteins on the cell surface. While these data are preliminary, they support that SNV and BCCV (shown in the present study) are similar to OW hantaviruses and other bunyaviruses in terms of the subcellular localization of their glycoproteins and consequently support the general Golgi maturation theory.

On the basis of common knowledge about bunyavirus glycoproteins, it was not unforeseen that BCCV G1 is targeted to the Golgi, since the glycoprotein closest to the N-terminus of the GPC of bunyaviruses, in the case of hantaviruses, G1, usually possesses the signal for Golgi localization (Chen & Compans, 1991; Pettersson and Melin, 1996) (Table 4). However, bunyaviruses have developed different strategies to achieve Golgi targeting. For example, the Golgi retention signal of Punta Toro virus (*Phlebovirus* genus) has been mapped to the transmembrane domain and the first ten amino acids of the cytoplasmic tail of the G1 protein (Matsouka *et al.*, 1994). For UUK virus, the Golgi retention signal has been mapped to the last 50 amino acids of the cytoplasmic tail of the N-terminally located G1 protein (Andersson *et al.*, 1997).

Table 4 Summary of viruses belonging to the *Bunyaviridae* family and the intracellular localization of the glycoproteins when expressed as GPC, G1 or G2.

Virus	**Genus**	**Intracellular Localization of G1 and G2 when expressed as**		
		GPC	**G1**	**G2**
Uukuniemi[1]	*Phlebovirus*	G1: Golgi	Golgi	
		G2: Golgi		ER
Punta-Toro[2]	*Phlebovirus*	G1: Golgi	Golgi	
		G2: Golgi		PM
Bunyamwera[3]	*Orthobunyavirus*	G1: Golgi	ER	
		G2: Golgi		Golgi
Hantaan[4]	*Hantavirus*	G1: Golgi	ER[4.1 & 4.2]/Golgi[4.3]	
		G2: Golgi		ER

PM plasma membrane
ER endoplasmic reticulum

Persson & Pettersson, 1991[1]; Chen *et al.*, 1991[2]; Chen & Compans, 1991[2]; Lappin *et al.*, 1994[3]; Ruusala *et al.*, 1992[4.1];Shi & Elliott, 2002[4.2]; Pensiero & Hay, 1992[4.3]

Before discussing the principles of BCCV G1 retention, it is important to understand the concepts of targeting and retention. According to Munro (1998), a retention signal anchors a protein in a defined compartment. In comparison, a targeting or retrieval signal is used to capture a protein when it is in the wrong place and return it to the organelle it escaped from. Additionally, it is important to remember that targeting or signalling motifs, depending on the function, are simply binding sites made up of short consecutive stretches of amino acids (Stanley, 1996). It is not the sequence motif which achieves the function, but rather the binding of other proteins to this motif that in turn confer these properties (Stanley, 1996).

Currently, there are two well-known models for Golgi retention of integral membrane proteins: the oligomerization model and the "bilayer-thickness model" (Munro, 1998). The oligomerization model suggests that Golgi enzymes form oligomers within a compartment. These oligomers would be too large to enter the anterograde vesicles which traffic between the Golgi cisternae or onward to the plasma membrane (Nilsson *et al.*, 1991, 1993; Munro, 1998; Gomord *et al.*, 1999). The second model describes Golgi retention being based on the differential membrane thickness of the different subdomains within the Golgi apparatus and other membranes within the cell (Masibay *et al.*, 1993; Pelham & Munro, 1993). A cholesterol gradient exists in mammalian cells between the membranes of the various organelles of the secretory pathway and these membranes are therefore of different thickness. The plasma membrane, with a higher concentration of cholesterol, is thought to be thicker than that of the Golgi. The bilayer thickness model suggests that the concentration gradient of

cholesterol and glycolipids from the ER to the plasma membrane of mammalian cells may result in differential membrane thickness. Golgi proteins would be unable to progress across or beyond the Golgi stack due to their relatively short transmembrane domains (Munro, 1998; Gomord & Faye, 1999).

At this moment, it is difficult to speculate which retention model BCCV G1 follows.

4.4 BCCV and HTNV G1 cytoplasmic tails have Golgi targeting signals

Since BCCV G1 appeared to be targeted to the Golgi, further studies were aimed at determining which part of the glycoprotein was responsible for Golgi localization. Since Anheier *et al.*, (submitted) had shown that Golgi localization of HTNV G1 was dependent on the cytoplasmic domain, it was reasonable to hypothesize that the cytoplasmic tail of BCCV G1 may be responsible for Golgi targeting as well. GFP-hantaviral glycoprotein fusion proteins were constructed and expression was monitored by UV microscopy. Since UV microscopy can be very subjective, an independent method was used to further confirm the microscopy results. Membrane fractionation distinguished between proteins which were membrane associated or cytosolic. Although all membranes are pelleted during this method, it is important to note that the fractionation data should be taken together with the microscopy data to provide a complete picture. Furthermore, since the UV microscopy data clearly demonstrated Golgi localization for several of the constructs, it was not an issue if the fractionation method was detecting the glycoproteins on the cytoplasmic membrane since they were clearly localized at the Golgi membranes.

Expression of GFP-BCCV $G1_{540-671}$ in 293T cells clearly demonstrated a Golgi pattern and was membrane associated (Figure 18), thus suggesting that the cytoplasmic tail of BCCV G1 contained a Golgi targeting signal. This result supports the data showing the Golgi localization of the full length BCCV G1 expressed in the SFV expression system (Figure 13). Since the cytoplasmic tail of HTNV behaved similarly (Figure19), BCCV G1 and HTNV G1 cytoplasmic tails appear to both contain Golgi localization signals. In comparison, expression of the G2 cytoplasmic tails of BCCV and HTNV did not demonstrate ER/Golgi localization (Figure 18 & 19) indicating that the G2 glycoprotein did not have ER/Golgi targeting signals in the cytoplasmic domain.

Data from Anheier *et al.*, (submitted) suggested that Golgi targeting of HTNV G1 was dependent on the HTNV G2 SP (23 amino acids), a hydrophobic domain after which co-translational cleavage of the GPC by the signal peptidase complex occurs (Lober *et al.*, 2001). Removal of the BCCV G2 SP from the BCCV G1 cytoplasmic tail substantially reduced the Golgi localization (Figure 20). However, a small percentage of transfected cells continued to be targeted to the Golgi suggesting that there may be a secondary signal (in addition to the primary signal in the BCCV G2 SP) in the remainder of the BCCV G1 cytoplasmic tail. In comparison, removal of HTNV G2 SP from GFP-HTNV G1 cytoplasmic tail resulted in complete abolishment of the Golgi targeting signal. The HTNV G2 SP may be a stronger signal or rather the primary signal in comparison to BCCV.

It would not be a surprise if the BCCV Golgi localization was composed of two signal sequences. The Golgi retention signal of the mouse hepatitis coronavirus appears

to be composed of two regions: the 22 carboxy-terminal residues of the cytoplasmic tail and the transmembrane domain (Andersson *et al.*, 1997). Recently, Gerrard and Nichol (2002) demonstrated that the Golgi localization signal of Rift Valley Fever Virus (*Phlebovirus* genus) is contained within two regions consisting of both the transmembrane domain and the cytosolic tail of the amino-terminal glycoprotein using GFP fusion proteins.

Addition of BCCV G2 SP alone to GFP was sufficient to confer Golgi targeting; even when 12 amino acids were removed from the carboxy terminus of the G2 SP, Golgi localization was maintained (Figure 21). Therefore, not only does the BCCV G2 SP serve as a targeting signal, but as little as 11 amino acids are sufficient. Since the Golgi localization was less than 100%, this result supports the theory that a secondary targeting signal may be located in the remainder of the BCCV G1 cytoplasmic tail.

The Golgi targeting signal does not appear to be domain specific since when the BCCV G2 SP was cloned at the N-terminus of GFP or the inverted sequence cloned at the C-terminus of GFP, Golgi localization was maintained (Figure 21 & 22). Taken together with the previous data, it appears that the BCCV G2 SP serves as a hydrophobic Golgi targeting signal, and as little as 11 amino acids can serve as a Golgi targeting signal. Since Golgi localization is not 100%, this result supports the theory that an additional secondary targeting signal (located in the remainder of the BCCV G1 cytoplasmic tail) may be required for exclusive targeting. The fact that the 23 amino acid SP and as little as 11 amino acids from the SP can direct a soluble protein into the Golgi

further strengthens the conclusion that the G1 tail of BCCV is both necessary and sufficient to confer Golgi targeting.

Although it may be surprising that as few as 11 amino acids can confer Golgi localization it has been demonstrated previously that short peptides can direct a soluble protein into the Golgi. For example, Andersson & Pettersson (1998) demonstrated that a short peptide corresponding to a portion of the cytoplasmic tail of Uukuniemi virus was also able to direct GFP to the Golgi.

It appears that hydrophobicity alone is driving the Golgi targeting since replacing the BCCV G2 SP hydrophobic domain with a foreign hydrophobic sequence retains Golgi targeting. Recall, that the INFV HA TD does not contain Golgi targeting signals since the INFV glycoproteins are targeted to the plasma membrane. The addition of INFV HA TD and INFV HA SP directly on GFP and on GFP-BCCV $G1_{540\text{-}648}$ (truncated) showed Golgi localization and the fusion proteins were membrane associated (Figure 22 & 23). This data suggests that hydrophobicity is the key factor in Golgi targeting for BCCV and it is not dependent on a specific sequence since a foreign sequence from influenza could produce the same effect. These findings are consistent with previous findings which report that retention in the Golgi by glycosyltransferases and coronavirus glycoproteins is primarily mediated by the hydrophobic transmembrane domain and not a specific amino acid sequence (Machamer & Rose, 1987; Nilsson *et al.*, 1991; Colley *et al.*, 1992; Wong *et al.*, 1992).

To confirm the subcellular localization of the GFP-hantaviral glycoprotein fusion proteins, co-localization was attempted, producing ambiguous results (Figure 24). It is

important to remember that the fusion proteins are being targeted to the intracellular membranes from the cytosolic side rather than the luminal sides of the compartments. In this case, a spatial problem of the proteins may be the culprit of lack of co-localization since all ER/Golgi markers commonly available are proteins that are located on the luminal side.

4.5 BCCV G2 is localized to the ER

When BCCV G2 was expressed in BHK-T7 cells using the pDisplay BCCV G2 clone, IFA results revealed an ER pattern, and the protein was not found on the cell surface (Figure 9). This data was supported by the sensitivity to endoglycosidase H (Figure 11). These results support previous findings of HTNV, the prototype OW hantavirus. When HTNV G2 was expressed independently, it localized in the ER (Pensiero & Hay, 1992; Ruusala *et al.*, 1992; Shi & Elliott, 2002; Anheier *et al.*, submitted).

When BCCV G2 was expressed using the SFV expression system, the pattern of protein expression was difficult to analyze. While some infected cells appear to have an ER pattern, others showed a Golgi pattern (Figure 13). The observed ambiguity may be attributed to the fact that the SFV expression system can alter organelle morphology, thus, it may not be the most reliable system to study subcellular localization (Flick, personal communication).

The ER localization of BCCV G2 may be determined by sequence specific signals. For example, an amino acid analysis of the protein revealed an ER retention motif of the KKXX (K=lysine, X=any amino acid) type at the C-terminus of its short

cytoplasmic tail. According to Gomord *et al.*, (1999) the cytosolic di-lysine motif has been identified at the C-terminal end of many type I integral membrane proteins that reside in the ER of yeast and animal cells. Earlier studies on HTNV, suggested that this signal is functional when G2 is expressed alone, but during heterodimerization with G1, the signal is hidden, allowing G2 to exit the ER and enter the Golgi (Pensiero & Hay, 1992). Vincent *et al.*, (1998) demonstrated that such a signal is not functional when located within the 13 amino acids adjacent to the transmembrane domain. This is likely the case in the hantaviruses, since the KKXX signal in G2 is directly adjacent to the transmembrane domain (Spiropoulou, 2001).

4.6 A model for BCCV glycoprotein targeting

The data from the present study suggests that the glycoproteins of BCCV do not appear at the plasma membrane but are localized either in the Golgi for BCCV G1 or in the ER for BCCV G2. Since the localization of the glycoproteins determines the site of virus maturation, these results do challenge the plasma membrane budding theory established by Ravkov and colleagues (1997). A few explanations for this discrepancy include: (1) excessive accumulation of G1 and G2 in the Golgi leading to saturation and leakage to the cell surface; (2) detection of assembled virus being released at the plasma membrane by fusion of the secretory vesicles and (3) the presence of a tyrosine-based motif (YXXL) in the BCCV G1 cytoplasmic tail, which can be responsible for Golgi retention (Machamer, 1993). Tyrosine motifs have been implicated in the recycling of proteins from the plasma membrane to the *trans*-Golgi network and also in endocytosis via clathrin coated pits (Luzio & Banting, 1993). Thus, the G1 glycoprotein may be

transported to the plasma membrane and then recycled back to the Golgi complex due to its tyrosine motif. If this hypothesis is true, it would not be too surprising if some glycoproteins were found on the cell surface, therefore allowing virus maturation.

The data from the study propose that the hantavirus G2 SP consisting of 23 amino acids serves as a primary hydrophobic Golgi targeting signal for G1. The G2 SP hydrophobic sequence serves as a binding site for proteins which result in the retention of BCCV G1 in this compartment. Once in the Golgi, G1 retention is carried out either by following the oligomerization theory or the "bilayer thickness" model (Munro, 1998).

For efficient targeting, the BCCV G2 SP appears to work in conjunction with a secondary signal located in the remainder of the G1 cytoplasmic tail. This signal may be sequence specific. Only together, can Golgi targeting be 100% efficient. Therefore, when expressed individually, BCCV G1 is targeted to the Golgi, while BCCV G2 is retained in the ER. Although the present study did not address this issue, based on previous work on bunyaviruses, one can hypothesize that when co-expressed, G1 and G2 heterodimerize and G2 can then exit the ER, followed by transport to the Golgi. The heterodimer would then be retained in the Golgi until virus assembly is completed, followed by budding into the Golgi cisternae and transport to and release at the plasma membrane (Figure 25).

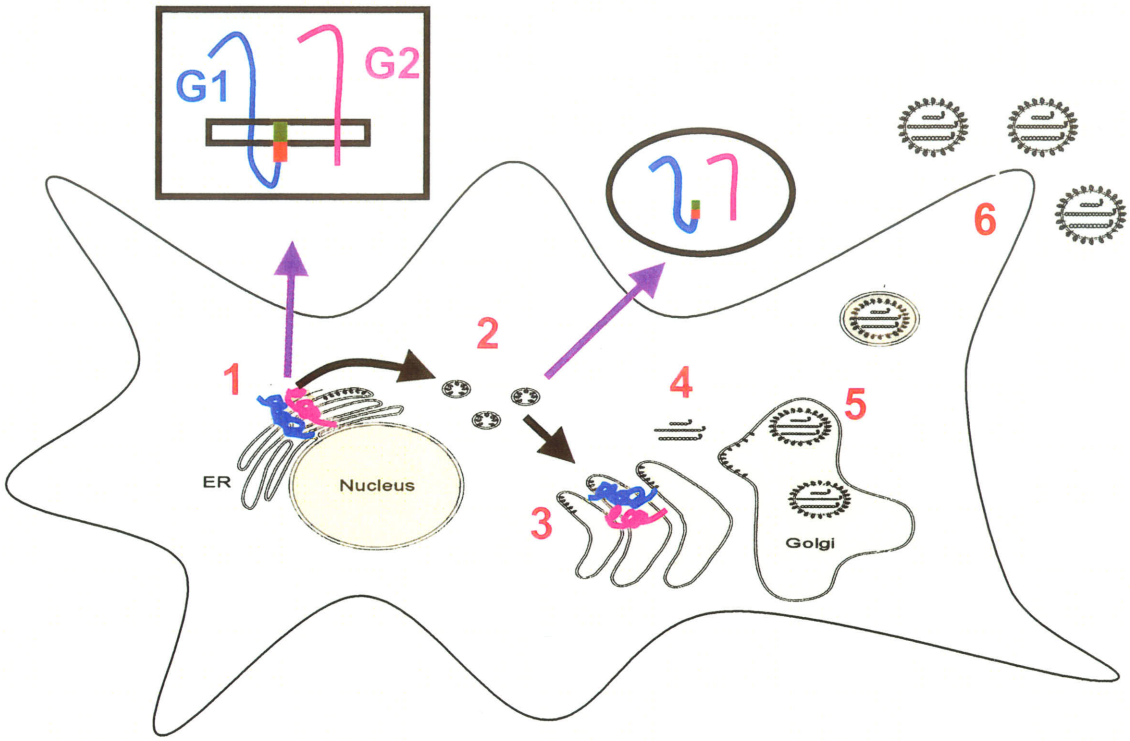

Figure 25: A model for BCCV glycoprotein targeting. (1) Following translation at the ER membrane, GPC is co-translationally cleaved into G1 and G2. The primary Golgi targeting signal of BCCV G1 is the BCCV G2 SP (shown in green) which works in conjunction with a secondary Golgi targeting signal (shown in red) located in the remainder of the G1 cytoplasmic tail. (2) Following heterodimerization in the ER, G1 and G2 are transported to the Golgi (3) The glycoprotein heterodimer accumulates at the Golgi either by following the oligomerization model or bilayer-thickness model, until (4) the replicated genome arrives. (5) The virus buds into the Golgi cisternae and is transported to the plasma membrane where (6) the viruses are released.

The results from the present study suggest that BCCV, a NW hantavirus, buds at the Golgi, similarly to OW hantaviruses. There have been speculations that the different clinical signs and symptoms of HFRS and HPS could be attributed to a difference in the budding mechanism between OW and NW hantaviruses. The present study refutes that hypothesis.

4.7 Future Work

While the expression and targeting of NW hantavirus glycoproteins remains a subject matter for debate, several avenues in this exciting area of research need to be addressed.

Firstly, if one wanted to further validate that the Golgi targeting signal of BCCV G2 SP is not sequence specific, site-directed mutagenesis could be performed. Various codons could be mutated thus changing the amino acid sequence of the BCCV G2 SP. In addition, one could randomly rearrange the nucleotide sequence, thus rearranging the amino acids of the BCCV G2 SP.

Secondly, it would be interesting to deduce the second Golgi targeting signal in the remainder of the BCCV G1 cytoplasmic tail. It would be sensible to start analyzing the amino acids directly adjacent to the BCCV G2 SP since Munro (1998) suggests that the amino acids flanking the transmembrane domain often contribute to Golgi localization. An amino acid comparison between the G1 cytoplasmic tails of BCCV and HTNV revealed a similar amino acid motif located adjacent to the hydrophobic G2 SP transmembrane domain (Figure 26). This motif (which contains within it a tyrosine-

based motif, YRTL) may be a candidate for a second targeting signal which may be sequence specific.

Thirdly, it would be interesting to try similar expression and targeting studies on other NW hantaviruses to confirm whether Golgi maturation is a common practice for other hantaviruses found in North/South America. Due to its potential for human to human transmission, the Andes virus would be an appealing agent to try.

Fourthly, in order to further understand pathogenesis, it is essential to study virion attachment and the mechanisms by which G1 and G2 interact with the host cell receptor. Likewise, it is key to identify other host cell receptors which may not have been considered yet.

Lastly, development of a reverse genetics system would be beneficial to understand the importance of each gene segment and its contribution to infectivity and pathogenesis.

The concepts outlined in this section have the potential to further strengthen the results obtained from this study and together, they can provide data to answer the question of hantavirus maturation and pathogenesis. This information will then serve as a foundation for understanding the virus life cycle and most importantly for elaboration of therapeutic interventions such as inhibitors of glycoprotein processing and/or transport.

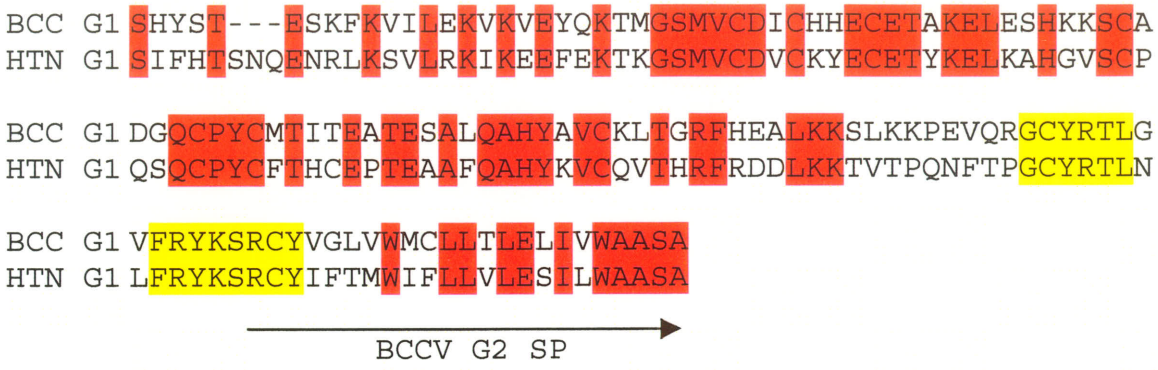

Figure 26: Amino acid comparison of the cytoplasmic tail of BCCV G1 and HTNV G1. Homologous amino acids are highlighted in red. BCCV G2 SP (23 amino acids) is denoted with an arrow. A second hypothetical Golgi targeting motif in G1 cytoplasmic tail is shown in yellow, adjacent to the BCCV G2 SP. Located within the hypothetical secondary targeting motif is a tyrosine-based motif, YRTL, which could be responsible for Golgi targeting. The BCCV G2 SP serves as a hydrophobic Golgi targeting signal which may work in conjunction with a secondary sequence specific signal in the remainder of the BCCV G1 cytoplasmic tail (yellow).

4.8 Conclusions

The following conclusions can be drawn from this study:

(1) When BCCV G1 is independently expressed it localizes in the Golgi.

(2) When BCCV G2 is independently expressed it localizes in the ER

(3) Both BCCV G1 and G2 behave in a similar fashion to HTNV, an OW hantavirus.

(4) The Golgi targeting signal for BCCV glycoproteins is located in the BCCV G1 cytoplasmic tail, specifically in the G2 SP which remains with the G1 cytoplasmic tail following cleavage.

(5) The Golgi targeting signal (G2 SP) is not sequence specific nor is the position of the SP important. The Golgi targeting function of the G2 SP is dependent on its hydrophobicity.

(6) It appears that the G2 SP works in conjunction with a second targeting signal, most likely located in the remainder of the G1 cytoplasmic tail.

5 REFERENCES

Andersson, A. M., Melin, L., Bean, A., and Pettersson, R. F. (1997). A retention signal necessary and sufficient for Golgi localization maps to the cytoplasmic tail of a Bunyaviridae (Uukuniemi virus) membrane glycoprotein. *J Virol* **71**(6), 4717-27.

Andersson, A. M., and Pettersson, R. F. (1998). Targeting of a short peptide derived from the cytoplasmic tail of the G1 membrane glycoprotein of Uukuniemi virus (Bunyaviridae) to the Golgi complex. *J Virol* **72**(12), 9585-96.

Anheier, B., Lindow, S., Schmaljoh, C., Klenk, H.D. & Feldmann, H. Subcellular targeting of Hantaan virus glycoproteins. *J. Virol* (submitted).

Antic, D., Wright, K. E., and Kang, C. Y. (1992). Maturation of Hantaan virus glycoproteins G1 and G2. *Virology* **189**(1), 324-8.

Armstrong, R. T., Kushnir, A. S., and White, J. M. (2000). The transmembrane domain of influenza hemagglutinin exhibits a stringent length requirement to support the hemifusion to fusion transition. *J Cell Biol* **151**(2), 425-37.

Beaty, B. J., and Calisher, C. H. (1991). Bunyaviridae-natural history. *Curr Top Microbiol Immunol* **169**, 27-78.

Chalfie, M. (1995). Green fluorescent protein. *Photochem Photobiol* **62**(4), 651-6.

Chen, S. Y., and Compans, R. W. (1991). Oligomerization, transport, and Golgi retention of Punta Toro virus glycoproteins. *J Virol* **65**(11), 5902-9.

Chen, S. Y., Matsouka, Y. & Compans, R. W. (1991). Golgi complex localization of the Punta Toro virus G2 protein requires its association with the G1 protein. *Virology* **183**, 351-365.

Colley, K. J., Lee, E. U., and Paulson, J. C. (1992). The signal anchor and stem regions of the beta-galactoside alpha 2,6-sialyltransferase may each act to localize the enzyme to the Golgi apparatus. *J Biol Chem* **267**(11), 7784-93.

Doms, R. W., Lamb, R. A., Rose, J. K. and Helenius, A. (1993). Folding and assembly of viral membrane proteins. *Virology* **193**, 545-562.

Drebot, M. A., Artsob, H., and Werker, D. (2000). Hantavirus pulmonary syndrome in Canada, 1989-1999. *Can Commun Dis Rep* **26**(8), 65-9.

Drebot, M. A., Gavrilovskaya, I., Mackow, E. R., Chen, Z., Lindsay, R., Sanchez, A. J., Nichol, S. T., and Artsob, H. (2001). Genetic and serotypic characterization of Sin Nombre-like viruses in Canadian Peromyscus maniculatus mice. *Virus Res* **75**(1), 75-86.

Duchin, J. S., Koster, F. T., Peters, C. J., Simpson, G. L., Tempest, B., Zaki, S. R., Ksiazek, T. G., Rollin, P. E., Nichol, S., Umland, E. T., and et al. (1994). Hantavirus pulmonary syndrome: a clinical description of 17 patients with a newly recognized disease. The Hantavirus Study Group. *N Engl J Med* **330**(14), 949-55.

Enria, D. A., Briggiler, A. M., Pini, N., and Levis, S. (2001). Clinical manifestations of New World hantaviruses. *Curr Top Microbiol Immunol* **256**, 117-34.

Feldmann, H. (2000). Hantaviruses. In: Encyclopedia of Life Sciences. London, Nature Publishing Group.

Garcia-Mata, R., Bebok, Z., Sorscher, E. J., and Sztul, E. S. (1999). Characterization and dynamics of aggresome formation by a cytosolic GFP-chimera. *J Cell Biol* **146**(6), 1239-54.

Gavrilovskaya, I. N., Shepley, M., Shaw, R., Ginsberg, M. H., and Mackow, E. R. (1998). beta3 Integrins mediate the cellular entry of hantaviruses that cause respiratory failure. *Proc Natl Acad Sci U S A* **95**(12), 7074-9.

Gerrard, S. R. and Nichol, S. T. (2002) Characterization of the Golgi retention motif of rift valley fever virus g(n) glycoprotein. *J Virol* **76**(23), 12200-10.

Gomord, V., Wee, E., and Faye, L. (1999). Protein retention and localization in the endoplasmic reticulum and the golgi apparatus. *Biochimie* **81**(6), 607-18.

Hart, C. A., and Bennett, M. (1994). Hantavirus: an increasing problem? *Ann Trop Med Parasitol* **88**(4), 347-58.

http://www.cdc.gov/ncidod/diseases/hanta/hps/noframes/caseinfo.htm
(Centers for Disease Control and Prevention)

http://www.cdc.gov/ncidod/diseases/hanta/hps
(Centers for Disease Control and Prevention)

http://www.mrw2.interscience.wiley.com/cponline
(Current Protocols Online, John Wiley & Sons)

Johnson, K. M. (2001). Hantaviruses: history and overview. *Curr Top Microbiol Immunol* **256,** 1-14.

Kyte, J., and Doolittle, R. F. (1982). A simple method for displaying the hydropathic character of a protein. *J Mol Biol* **157**(1), 105-32.

Lackie, J. M., Dow, J. A & Blackshaw, S. E. The dictionary of cell and molecular biology 3rd edition. 1999. Academic press, London.

Laemmli, U. K. (1970). Cleavage of structural proteins during the assembly of the head of bacteriophage T4. *Nature* **227**(259), 680-5.

Lappin, D. F., Nakitare, G. W., Palfreyman, J. W. & Elliott, R. M. (1994). Localization of Bunyamwera Bunavirus G1 glycoprotein to the Golgi requires association with G2 but not with NSm. *J Gen Virol* **75**, 3441-3451.

Lee, H. W., Lee, P. W., and Johnson, K. M. (1978). Isolation of the etiologic agent of Korean Hemorrhagic fever. *J Infect Dis* **137**(3), 298-308.

Liljestrom, P., and Garoff, H. (1991). A new generation of animal cell expression vectors based on the Semliki Forest virus replicon. *Biotechnology (N Y)* **9**(12), 1356-61.

Liljestrom & Garoff, technical manual 2nd edition

Lober, C., Anheier, B., Lindow, S., Klenk, H. D., and Feldmann, H. (2001). The Hantaan virus glycoprotein precursor is cleaved at the conserved pentapeptide WAASA. *Virology* **289**(2), 224-9.

Lopez, N., Padula, P., Rossi, C., Lazaro, M. E., and Franze-Fernandez, M. T. (1996). Genetic identification of a new hantavirus causing severe pulmonary syndrome in Argentina. *Virology* **220**(1), 223-6.

Lopez, N., Padula, P., Rossi, C., Miguel, S., Edelstein, A., Ramirez, E., and Franze-Fernandez, M. T. (1997). Genetic characterization and phylogeny of Andes virus and variants from Argentina and Chile. *Virus Res* **50**(1), 77-84.

Luzio, J. P., and Banting, G. (1993). Eukaryotic membrane traffic: retrieval and retention mechanisms to achieve organelle residence. *Trends Biochem Sci* **18**(10), 395-8.

Machamer, C. E., and Rose, J. K. (1987). A specific transmembrane domain of a coronavirus E1 glycoprotein is required for its retention in the Golgi region. *J Cell Biol* **105**(3), 1205-14.

Machamer, C. E. (1993). Targeting and retention of Golgi membrane proteins. *Curr Opin Cell Biol* **5**(4), 606-12.

Mackow, E. R., and Gavrilovskaya, I. N. (2001). Cellular receptors and hantavirus pathogenesis. *Curr Top Microbiol Immunol* **256**, 91-115.

Masibay, A. S., Balaji, P. V., Boeggeman, E. E., and Qasba, P. K. (1993). Mutational analysis of the Golgi retention signal of bovine beta-1,4-galactosyltransferase. *J Biol Chem* **268**(13), 9908-16.

Matsouka, Y., Chen, S. and Compans, R. W. (1994). A signal for Golgi retention in the Bunyavirus G1 glycoprotein. *The Journal of Biological Chemistry* **269**(36), 22565-22573.

McCaughey, C., and Hart, C. A. (2000). Hantaviruses. *J Med Microbiol* **49**(7), 587-99.

Mertz, G. J., Hjelle, B. L., and Bryan, R. T. (1997). Hantavirus infection. *Adv Intern Med* **42**, 369-421.

Meyer, B. J., and Schmaljohn, C. S. (2000). Persistent hantavirus infections: characteristics and mechanisms. *Trends Microbiol* **8**(2), 61-7.

Munro, S. (1998). Localization of proteins to the Golgi apparatus. *Trends Cell Biol* **8**(1), 11-5.

Nemirov, K., Vapalahti, O., Lundkvist, A., Vasilenko, V., Golovljova, I., Plyusnina, A., Niemimaa, J., Laakkonen, J., Henttonen, H., Vaheri, A., and Plyusnin, A. (1999). Isolation and characterization of Dobrava hantavirus carried by the striped field mouse (Apodemus agrarius) in Estonia. *J Gen Virol* **80** (Pt 2), 371-9.

Nichol, S. T., Spiropoulou, C. F., Morzunov, S., Rollin, P. E., Ksiazek, T. G., Feldmann, H., Sanchez, A., Childs, J., Zaki, S., and Peters, C. J. (1993). Genetic identification of a hantavirus associated with an outbreak of acute respiratory illness. *Science* **262**(5135), 914-7.

Nilsson, T., Lucocq, J. M., Mackay, D., and Warren, G. (1991). The membrane spanning domain of beta-1,4-galactosyltransferase specifies trans Golgi localization. *Embo J* **10**(12), 3567-75.

Nilsson, T., Slusarewicz, P., Hoe, M. H., and Warren, G. (1993). Kin recognition. A model for the retention of Golgi enzymes. *FEBS Lett* **330**(1), 1-4.

Pelham, H. R., and Munro, S. (1993). Sorting of membrane proteins in the secretory pathway. *Cell* **75**(4), 603-5.

Pensiero, M. N., and Hay, J. (1992). The Hantaan virus M-segment glycoproteins G1 and G2 can be expressed independently. *J Virol* **66**(4), 1907-14.

Persson, R. & Pettersson, R. F. (1991). Formation and intracellular transport of a heterodimeric viral spike protein complex. *J Cell Biol* **112**, 257-266.

Peters, C. J., and Khan, A. S. (2002). Hantavirus pulmonary syndrome: the new American hemorrhagic fever. *Clin Infect Dis* **34**(9), 1224-31.

Pettersson, R. F. and Melin, L. (1996) Synthesis, assembly and intracellular transport of *Bunyaviridae* membrane proteins In *The Bunyaviridae* edited by Richard M. Elliott, Plenum Press, New York.

Pilaski, J., Feldmann, H., Morzunov, S., Rollin, P. E., Ruo, S. L., Lauer, B., Peters, C. J., and Nichol, S. T. (1994). Genetic identification of a new Puumala virus strain causing severe hemorrhagic fever with renal syndrome in Germany. *J Infect Dis* **170**(6), 1456-62.

Plyusnin, A., Vapalahti, O., and Vaheri, A. (1996). Hantaviruses: genome structure, expression and evolution. *J Gen Virol* **77** (Pt 11), 2677-87.

Plyusnin, A., and Morzunov, S. P. (2001). Virus evolution and genetic diversity of hantaviruses and their rodent hosts. *Curr Top Microbiol Immunol* **256**, 47-75.

Plyusnin, A. (2002). Genetics of hantaviruses: implications to taxonomy. *Arch Virol* **147**(4), 665-82.

Ravkov, E. V., Nichol, S. T., and Compans, R. W. (1997). Polarized entry and release in epithelial cells of Black Creek Canal virus, a New World hantavirus. *J Virol* **71**(2), 1147-54.

Rollin, P. E., Ksiazek, T. G., Elliott, L. H., Ravkov, E. V., Martin, M. L., Morzunov, S., Livingstone, W., Monroe, M., Glass, G., Ruo, S., and et al. (1995). Isolation of black creek canal virus, a new hantavirus from Sigmodon hispidus in Florida. *J Med Virol* **46**(1), 35-9.

Ruusala, A., Persson, R., Schmaljohn, C. S., and Pettersson, R. F. (1992). Coexpression of the membrane glycoproteins G1 and G2 of Hantaan virus is required for targeting to the Golgi complex. *Virology* **186**(1), 53-64.

Sanger, F., Nicklen, S., and Coulson, A. R. (1977). DNA sequencing with chain-terminating inhibitors. *Proc Natl Acad Sci U S A* **74**(12), 5463-7.

Sacchetti, A., Ciccocioppo, R., and Alberti, S. (2000). The molecular determinants of the efficiency of green fluorescent protein mutants. *Histol Histopathol* **15**(1), 101-7.

Schlesinger, S. & Schlesinger, M. J. (2001). Togaviridae: The viruses and their replication. In: Fields BN, Knipe DM, Howley PM (eds) Virology, Lippincott-Raven Pub, Philadelphia, pp. 895-916.

Schmaljohn, C. S., Hasty, S. E., Rasmussen, L., and Dalrymple, J. M. (1986). Hantaan virus replication: effects of monensin, tunicamycin and endoglycosidases on the structural glycoproteins. *J Gen Virol* **67** (Pt 4), 707-17.

Schmaljohn, C., and Hjelle, B. (1997). Hantaviruses: a global disease problem. *Emerg Infect Dis* **3**(2), 95-104.

Schmaljohn, C. S. & Hooper, J. W. (2001). Bunyaviridae: The viruses and their replication. In: Fields BN, Knipe DM, Howley PM (eds) Virology, Lippincott-Raven Pub, Philadelphia, pp. 1581-1602.

Shi, X., and Elliott, R. M. (2002). Golgi localization of Hantaan virus glycoproteins requires coexpression of G1 and G2. *Virology* **300**(1), 31-8.

Simmons, J. H., and Riley, L. K. (2002). Hantaviruses: an overview. *Comp Med* **52**(2), 97-110.

Sjolander, K. B., Golovljova, I., Vasilenko, V., Plyusnin, A., and Lundkvist, A. (2002). Serological divergence of Dobrava and Saaremaa hantaviruses: evidence for two distinct serotypes. *Epidemiol Infect* **128**(1), 99-103.

Spiropoulou, C. F., Morzunov, S., Feldmann, H., Sanchez, A., Peters, C. J., and Nichol, S. T. (1994). Genome structure and variability of a virus causing hantavirus pulmonary syndrome. *Virology* **200**(2), 715-23.

Spiropoulou, C. F. (2001). Hantavirus maturation. *Curr Top Microbiol Immunol* **256**, 33-46.

Stanley, K. K. (1996). Regulation of targeting signals in membrane proteins. [review]. *Mol Membr Biol* **13**(1), 19-27.

Stearns, T. (1995). Green fluorescent protein. The green revolution. *Curr Biol* **5**(3), 262-264.

Van Regenmortel, M.H.V., Fauquet, C.M., Bishop, D.H.L., Carstens, E. B., Estes, M.K., Lemon, S.M., Maniloff, J., Mayo, M.A., McGeoch, D.J., Pringle, C.R., and R. B. Wickner. (2000). Virus Taxonomy. 7th report of the International Committee of Taxonomy of Viruses, 599-621.

Vincent, M. J., Martin, A. S., and Compans, R. W. (1998). Function of the KKXX motif in endoplasmic reticulum retrieval of a transmembrane protein depends on the length and structure of the cytoplasmic domain. *J Biol Chem* **273**(2), 950-6.

Wong, S. H., Low, S. H., and Hong, W. (1992). The 17-residue transmembrane domain of beta-galactoside alpha 2,6-sialyltransferase is sufficient for Golgi retention. *J Cell Biol* **117**(2), 245-58.

Young, J. C., Mills, J. N., Enria, D. A., Dolan, N. E., Khan, A. S., and Ksiazek, T. G. (1998). New World hantaviruses. *Br Med Bull* **54**(3), 659-73.

APPENDIX I

Primers and cloning strategies used for cloning into pDisplay (A), pSFV1 leader (B) and pHL2823 (C).
F = forward, R = reverse, _____ = coding sequence
1st three nucleotides of PCR & RT-PCR primers are a clamp. Restriction sites in parantheses for oligolinkers are the sticky ends that are generated after hybridization. Restriction sites in parantheses for PCR & RT-PCR primers are the sticky ends that are generated after *Bsm*BI cleavage. Oligolinkers are shown as being hybridized.

A) Primers for BCCV for pDisplay constructs

Insert	Primer Sequence (5' to 3')	Nucleotide Position	Method
BCC G1	GACCCCGGGTTCCCGCGAGTGTGCATG *Xma*I	106F	RT-PCR
	GACCTGCAGTTACTATGCACTAGCAGCCCAAACG *Pst*I STOP	2013R	
BCC G2	GACCCCGGGGATACACCCTTACTTGAACC *Xma*I	2014F	RT-PCR
	GACCTGCAGTTATTAAAGTTGCTTTTTGTGAGATC *Pst*I STOP	3477R	

APPENDIX I cont'd

B) Primers for BCCV for pSFV1 leader constructs

Insert	Primer Sequence (5' to 3')	Nucleotide Position	Method
BCC G1	AATCGTCTCTGATCCTATCCATATGATGTTCCAGATTATGCTTTCCCGCGGAGTGTGCATGAATTA *Bsm*BI (*Bam*HI) HA epitope	106F	RT-PCR
	AATCGTCTCGCCGGGTTATGCACTAGCAGCCCAAACGATC *Bsm*BI (*Xma*I) STOP	2013R	
BCC G2	AATCGTCTCTGATCCTATCCATATGATGTTCCAGATTATGCTGATACACCCTACTTGAACCTGGC *Bsm*BI (*Bam*HI) HA epitope	2014F	RT-PCR
	AATCGTCTCGCCGGGTTAAAGTTGCTTTTTGTGAGATC *Bsm*BI (*Xma*I) STOP	3477R	

APPENDIX I cont'd

C) Primers for BCCV, HTNV and INFV for GFP-hantaviral glycoprotein fusion protein constructs

Insert	Primer Sequence (5' to 3')	Nucleotide Position	Method
GFP-BCCV $G1_{540-671}$	AATCGTCTCTGATCCCACTATTCTACTGAATCAAAGTTC *Bsm*BI (*Bam*HI)	1612F	PCR
	AATCGTCTCTCTAGATTATGCACTAGCAGCCCAAACGATC *Bsm*BI (*Xba*I) STOP	2013R	
GFP-BCCV $G2_{1150-1159}$	GATCCCCCATAAGATCTCACAAAAAGCAACTTTAAT GGGGTATTCTAGAGTGTTTTTCGTTGAAATTAGATC (*Bam*HI) STOP (*Xba*I)	3448F & 3477R	Oligolinker
GFP-BCCV $G1_{540-648}$ (truncated)	AATAGATCTCACTATTCTACTGAATCAAAGTTC *Bgl*II	1612F	PCR
	AATACTAGTGAATTCGAGCGTCTCATTAACTCTTATAACGGAAAAC *Spe*I *Eco*RI STOP	1944R	
GFP-HTNV $G1_{528-661}$	AATCGTCTCTGATCCATTTTTCACACAAGTAATCAAGAG *Bsm*BI (*Bam*HI)	1583F	RT-PCR
	AATCGTCTCTCTAGATTATGCACTTGCAGCCCACAGTATG *Bsm*BI *Xba*I STOP	1984R	

APPENDIX I cont'd

C) Primers for BCCV, HTNV and INFV for GFP-hantaviral glycoprotein fusion protein constructs (cont'd)

Insert	Primer Sequence (5' to 3')	Nucleotide Position	Method
GFP-HTNV $G2_{1140-1148}$	GATCCTGTCCCGTAAGGAAGCATAAAAAATCATAAT GACAGGGCATTCCTTCGTATTTTTTAGTATTAGATC (*Bam*HI) STOP (*Xba*I)	3419F & 3445R	Oligolinker
GFP-HTNV $G1_{528-638}$ (truncated)	AATGGATCCATTTTTCACACAAGTAATCAAGAG *Bam*HI	1583F	RT-PCR
	AATTCTAGATTAGCTTTTGTATCTAAATAAATTTAGTG *Xba*I STOP	1915R	
GFP-BCCV G2 $SP_{648-671}$ C term	GATCCCGTTGCTATGTGGGCTTAGTATGGATGTGTTTGTTGAC... GGCAACGATACACCCGAATCATACCTACACAAACAACTG... (*Bam*HI) ...TCTTGAGTTGATCGTTTGGGCTGCTAGTGCATAAG ...AGAACTCAACTAGCAAACCCGACGATCACGTATTCTAGA STOP(*Xba*I)	1945F & 2013R	Oligolinker
GFP-BCCV G2 $SP_{648-671}$ N term	CGGGCCCACCATGAGATGCTATGTGGGCTTAGTATGGATGTGTTT... CATGGCCCGGGTGGTACTCTACGATACACCCGAATCATACCTACACAAA... (*Kpn*I) *Apa*I START ...GTTGACTCTTGAGTTGATCGTTTGGGCTGCTAGTGCAGT ...CAACTGAGAACTCAACTAGCAAACCCGACGATCACGTCACTAG (*Bcl*I)	1945F & 2013R	Oligolinker

APPENDIX I cont'd

C) Primers for BCCV, HTNV and INFV for GFP-hantaviral glycoprotein fusion protein constructs (cont'd)

Insert	Primer Sequence (5' to 3')	Nucleotide Position	Method
pHL2823 mutate bp 49 (G → T)	CGCCACCATGGTGATCAAGGGCGAGGAGC GCGGTGGTACCACTAGTTCCCGCTCCTCAG 3rd codon of GFP change but same aa	35F	PCR Mutagenesis*
GFP-INFV HA $TD_{539-565}$	GATCTTGGATCCTGTGGATTTCCTTTGCCATATCATGCTTTTTGCTTTGTGTTGTTTTGCT... AACCTAGGACACCTAAAGGAAACGGTATAGTACGAAAAACGAAACACAACAAAACGA (*Bam*HI) ...GGGGTTCATCATGTGGGCCTGCCAGTGAGAT ...CCCCAAGTAGTACACCCGGACGGTCACTCTAGATC STOP (*Xba*I)	1616F & 1696R	Oligolinker

APPENDIX I cont'd

C) Primers for BCCV, HTNV and INFV for GFP-hantaviral glycoprotein fusion protein constructs (cont'd)

Insert	Primer Sequence (5' to 3')	Nucleotide Position	Method
GFP-INFV HA SP_{10-26}	GATCCATGAAGACCATCATTGCTTTGAGCTACATTTTCTGTCTGCCTC... GTACTTCTGGTAGTAACGAAACTCGATGTAAAAGACAGACGGAG... *(Bam*HI) ...TCGGCCAATAAGAT ...AGCCGGTTATTCTAGATC STOP (*Xba*I)	29F & 79R	Oligolinker
GFP-BCCV G2 $SP_{659-648}$ inverted	GATCCGCAAGTGCTGCTTGGGTTATCTTGGAGCTTACTTTGTTGTGTATGT... GCGTTCACGACGAACCCAATAGAACCTCGAATGAAACAACACATACA... *(Bam*HI) GGGTATTAGGCGTGTATTGCCGTTAAGAT CCCATAATCCGCACATAACGGCAATTCTAGATC STOP (*Xba*I)	1945F & 2013R	Oligolinker

APPENDIX I cont'd

C) Primers for BCCV, HTNV and INFV for GFP-hantaviral glycoprotein fusion protein constructs (cont'd)

Insert	Primer Sequence	Nucleotide Position	Method
GFP-BCCV $G1_{540-648}$ (truncated)-INFV HA $TD_{539-565}$	GAGTTGGATCCTGTGGATTTCCTTTGCCATATCATGCTTTTTGCTTTGTGTTTTGCT... ACCTAGGACACCTAAAGGAAACGGTATAGTACGAAAAACGAAACACAAAACGA... (*Bsm*BI) GGGGTTCATCATGTGGGCCTGCCAGT CCCCAAGTAGTACACCCGGACGGTCATTAA (*Eco*RI)	1616F & 1696R	Oligolinker
GFP-BCCV $G1_{540-648}$ (truncated)-INFV HA SP_{10-26}	GAGTATGAAGACCATCATTGCTTTGAGCTACATTTTCTGTCTGCCTCTCGGCCAAT TACTTCTGGTAGTAACGAAACTCGATGTAAAAGACAGACGGAGAGCCGGTTATTAA (*Bsm*BI) (*Eco*RI)	29F & 79R	Oligolinker
GFP-BCCV $G1_{540-648}$ (truncated) – BCC G2 $SP_{659-648}$inverted	GAGTGCAAGTGCTGCTTGGGTTATCTTGGAGCTTACTTTGTTGTGTATGTGGGTATTA ... CGTTCACGACGAACCCAATAGAACCTCGAATGAAACAACACATACACCCATAAT... (*Bsm*BI) ...GTGTATTGCCGTT ...CACATAACGGCAATTAA (*Eco*RI)	1945F & 2013R	Oligolinker

APPENDIX II

Nucleotide sequence of Black Creek Canal virus M segment (L39950, 3668 bps) cRNA. Glycoprotein G1 is coloured in red, while glycoprotein G2 is in blue (non-coding region is in black). Start (ATG) and stop (TAA) codons are highlighted in yellow.

TAGTAGTAGACTCCGCAAGAAGAAGCAAGACAAAAAAAGACTGAGAGCAAT
ATGGGCAGGTTATACCTGATTGTGCTTGGGGTCCTGATTACTGCTACAGCTGG
TTTCCCGCGGAGTGTGCATGAATTAAAAATTGAATGCCCGCATACTGTCGTAT
TAGGGCAAGGATATGTCACAGGTTCTGTTGAGCTTGGCTTTATTGCTCTTGAT
CAAGTAACAGATTTAAAGATTGAGAGCTCCTGTAGCTTTGATCATCATGCAG
CACCTACAACAACACAGAACTTCACACAGCTCAAATGGGCAAAAACAGCAA
GCACAACTGACACCACAAATGCAGCCGAGACTACATTTGAAAGCAAGTCCAC
GGAAGTGCACTTAAAAGGAGTATGTACAATTCCCAGCAATGTGCTCGACGGA
CCATCTCGCCCTGTAACAGGGAGAAAAACAGTTGTCTGTTATGATTTAGCATG
CAATCAAACTCATTGTCAGCCAACTGTTCATTTGCTAGCACCAATACAAACAT
GCATGTCTGTTCGGAGCTGTATGATAAGCTTATTGGCAAGTAGGATTCAGGTG
GTCTATGAGAAGACATACTGTGTTACAGGACAACTTATAGAAGGCTTGTGTTT
TAACCCTGTCCCTAACCTTGCACTGACACAACCTGGGCACACATATGACACA
TTTACATTGCCAATTACATGCTTTCTGGTGGCCAAAAAGGGTGCAAACCTGAA
AATTGCTGTTGAGCTAGAGAAACTGACAACAAAGACTGGTTGTGCAGAAAAT
GCACTTCAGGCTTACTATATATGCTTTATAGGACAGCACTCTGAGCCATTAAC
TGTCCCGATGCTCGAGGACTATAGATCAGCTGAAATTTTCACAAGAATAATG
ATGAATCCAAAAGGTGAAGATCATGATATGGAACAGTCTTCCCAAGGTGCTT
TGCGAATTGTTGGGCCTATAAAAGGTAAAGTGCCACCCACTGAGACATCAGA
CACTGTGCAGGGGATTGCTTTTGCAGGTTTGCCTATGTATAGTTCTTTTTCGA
GCCTTGTAAGGAAAGCAGAACCTGAATATCTATTTTCACCTGGTATCATTGCA
GAATCTAATCATAGCAGCTGCGATAAGAAAACATTACCCTTAACATGGAGGG
GTTTCTTATCAATGTCTGGTGAAATTGAAAGAATTACTGGCTGTAATGTCTTT
TGTACACTTGCTGGCCCAGGTGCAAGTTGTGAGGCTTACTCTGAAAATGGAA
TATTCAATATTAGTTCTCCCACATGCTTAGTCAATAAAGTCCAAAAGTTTAGG
GGCTCAGAACAGAGAATCAACTTTATCTCCCAAAGAATAGATCAAGATGTGA
TTGTCTATTGTAATGGACAAAAGAAGGTCATTCTGACAAAAACACTAGTTAT
AGGCCAATGTATTTATACATTTACAAGTATCTTTTCACTGATCCCTAGTGTTG
CACATTCCTTGGCTGTCGAGCTCTGTGTACCAGGGATCCATGGATGGGCTACA
ATTGCATTAGTAATCACATTTTGCTTTGGCTGGTTACTTATTCCTACCACAACC
ATGGTTGTGTTGAAATGCCTGAGGCTGCTAACTTACTCGTGCTCTCACTATTC
TACTGAATCAAAGTTCAAAGTCATTCTAGAAAAGGTGAAGGTTGAATACCAG
AAGACAATGGGTTCAATGGTATGTGACATTTGTCATCATGAATGTGAAACAG
CAAAAGAACTTGAAAGCCATAAAAAAAGTTGTGCTGATGGGCAGTGCCCATA
CTGTATGACTATTACCGAGGCAACTGAGAGTGCTTTACAGGCCCATTATGCTG

TATGTAAATTAACAGGGCGCTTTCATGAGGCTTTAAAAAAATCATTAAAAAA
ACCAGAGGTTCAGAGGGGTTGTTATAGAACACTTGGTGTTTTCCGTTATAAGA
GTCGTTGCTATGTGGGCTTAGTATGGATGTGTTTGTTGACTCTTGAGTTGATC
GTTTGGGCTGCTAGTGCAGATACACCCTTACTTGAACCTGGCTGGTCAGATAC
AGCTCATGGGGTAGGTGATATTCCGATGAAGACAGACCTAGAGTTAGATTTT
GCTATCCCATCATCTTCATCATATAGTTATAGAAGGCGATTAGTAAACCCTGC
TAATTCAGATGAGACTGTTCCATTTCACTTTCAGCTTGAACGACAAGTAATCC
ATGCAGAAATACAATCGCTAGGACATTGGATGGATGCCACATTTAATATAAT
TTCTGCATTTCACTGCTATGGTGAGTGCAAGAAATACTCTTACCCTTGGCAAA
CAGCAAAATGTTTTTTTGAGAAGGACTACCAGTATGAAACAAGTTGGAGCTG
TAATCCGCCAGACTGTCCAGGGGTAGGTACTGGTTGTACTGCATGTGGCATAT
ATCTGGATAAATTGAAGTCTGTTGGGAAAGCATATAAAGTAATTACCTTGAA
ATATGCAAGAAAAGTTTGCATTCAATTAGGTACGGAACAAACATGTAAGAAT
ATCGATGTTAATGACTGTCTTGTAACTTCATCAATCAAAGTTTGTATGATTGG
CACAATCTCAAAGTTTCAACCAGGAGACACTTTACTATTTTTGGGTCCACTTG
AAGAAGGTGGCCTAGTCCTCAAACAATGGTGTACAACAACATGTTCATTTGG
TGATCCAGGTGATATTATGTCTACAACTTCAGGAATGCGTTGCCCTGAACATA
CAGGCTCCTTTAGGAAGATCTGTGGGTTTGCAACAACACCTGTTTGTGAGTAT
CAAGGGAATACAGTCTCTGGTTTTAAAAGATTGATGGCTACAAAGGACTCGT
TTCAGTCATTTAATGTATCTGAAGTACACATTACAACAACCAAGCTAGAATG
GAGTGATCCTGATAGTAACATCAAAGATCATATAAATTTGATTTTAAACCGA
GATGTATCATTTCAAGACTTAAGTGACAATCCGTGCAAAGTGGACCTTTCAAC
ACAGGCAATTGATGGTGCATGGGGCTCTGGTGTAGGTTTTACATTGACATGTA
TAGTGGGATTACAGAATGCTCTAGTTTCATGACCTCTATTAAGGTATGTGACA
TGGCTATGTGTTATGGAGCCTCAGTAGTAAACCTAGTTAGAGGCTCCAATAC
AGTTAAAATTGTTGGAAAAGGTGGTCATTCTGGTTCGACATTTAGATGCTGTC
ATGATAAGGACTGTACAAGTAATGGTCTGCTTGCATCTGCACCACATCTTGAA
CGGGTTACAGGATTCAATCAGATAGATTCTGACAAGGTTTATGATGATGGAG
CTCCACCGTGTTCTATAAAATGCTGGTTTGCAAAGTCAGGTGAGTGGCTTTTG
GGGATATTAAATGGAAATTGGGTAGTTGTTGCAGTCCTTGTTATCATATTACT
AATCTCTATCTTTCTATTCAGCTTCTTCTGCCCCATAAGATCTCACAAAAAGC
AACTTTAAATAGCCTCTAACCACCCTTAATAACAATGACTATAAAGCACTAA
CAATTTGCTAAAATATTGCCAAGATAACAGCTAACCACTTTAATCTGTATGAC
AATGAATAACATCACTAAAAAAAACTAAGAATTTAATAACATATAATAGATT
TGCCTCAAACCAGGGCTTTTGTTCCTGCGGAGCAATGGGCAGGTTATACCTAC
TACTA